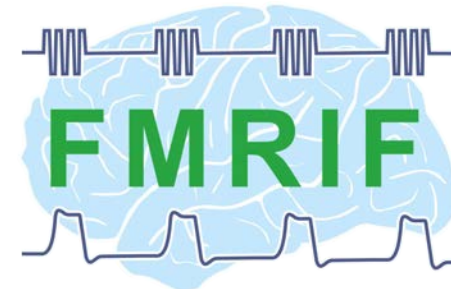
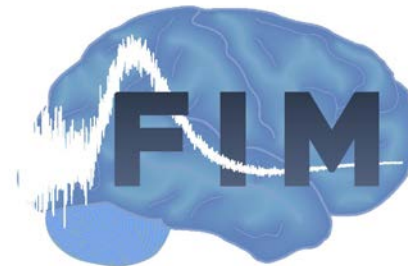
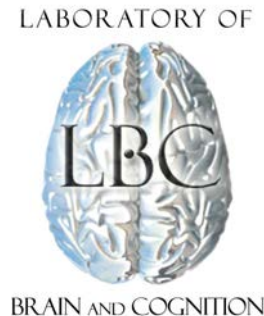


Introduction to the NIH Summer fMRI/Neuroimaging Course

Peter A. Bandettini, Ph.D.

**Section on Functional Imaging
Methods
& Functional MRI Core Facility
National Institute of Mental Health**



Lecture #	Day	Date	Time	Location	Topic	Speaker	Speaker email
1	Tuesday	5-28-24	2:00-3:00 PM	FAESB1C210	Introduction to the course & a short history of neuroimaging and fMRI	Peter Bandettini	bandettini@nih.gov
2	Thursday	5-30-24	2:00 - 3:00 PM	FAES B1C206	The basic fMRI study: all the elements to consider	Dan Handwerker	handwerkerd@mail.nih.gov
3	Tuesday	6-4-24	2:00 - 3:00 PM	FAES B1C209	MRI Acquisition Basics for the Non-Physicist	Vinai Roopchansinsh	vinai.roopchansingh@nih.gov
4	Thursday	6-6-24	2:00 - 3:00 PM	FAES B1C209	High resolution MRI and fMRI	Renzo Huber, Tyler Morgan	laurentius.huber@nih.gov, tyler.morgan@nih.gov
5	Tuesday	6-11-24	1:00 - 2:00 PM	FAES B1C207	Preprocessing Pipelines and Quality Control	Paul Taylor	paul.taylor@nih.gov
6	Thursday	6-13-24	2:00 - 3:00 PM	FAES B1C210	Physiologic Confounds in fMRI	Burak Akin	burak.akin@nih.gov
7	Tuesday	6-18-24	2:00 - 3:00 PM	FAES B1C210	Noise and Artifact in MRI and fMRI	Dan Handwerker	handwerkerd@mail.nih.gov
8	Thursday	6-20-24	2:00 - 3:00 PM	FAES B1C209	Functional contrast and processing strategies at high field and high resolution	Renzo Huber	laurentius.huber@nih.gov
9	Tuesday	6-25-24			OHBM		
10	Thursday	6-27-24			OHBM		
11	Tuesday	7-2-24	2:00 - 3:00 PM	FAES B1C210	From Line Scanning to Tensor Imaging	Tyler Morgan	tyler.morgan@nih.gov
12	Thursday	7-4-24			Holiday		
13	Tuesday	7-9-24	2:00 - 3:00 PM	FAES B1C209	The Hemodynamic Response and Acquisition, Paradigms, Processing	Peter Bandettini	bandettini@nih.gov
14	Thursday	7-11-24	2:00 - 3:00 PM	FAES B1C211	Resting state fMRI	TBD	
15	Tuesday	7-16-24	2:00 - 3:00 PM	FAES B1C206	Multi-echo fMRI	Dan Handwerker	handwerkerd@mail.nih.gov
16	Thursday	7-18-24	2:00 - 3:00 PM	FAES B1C207	Multimodal Neuroimaging Overview	Pete Molfese	peter.molfese@nih.gov
17	Tuesday	7-23-24	2:00 - 3:00 PM	FAES B1C209	Electroencephalography (EEG) with and without simultaneous fMRI	Pete Molfese	peter.molfese@nih.gov
18	Thursday	7-25-24	2:00 - 3:00 PM	FAES B1C208	Mysteries, Controversies, and Challenges of fMRI	Peter Bandettini	bandettini@nih.gov
19	Tuesday	7-30-24	2:00 - 3:00 PM	FAES B1C211	Studying Brain-Behavior correlations with fMRI	Catherine Walsh	catherine.walsh@nih.gov
20	Thursday	8-1-24	2:00 - 3:00 PM	FAES B1C209	Intersubject Correlation and Naturalistic Stimuli	Pete Molfese	peter.molfese@nih.gov
21	Tuesday	8-6-24	TBD	TBD	Connectivity and Dynamic Connectivity	Javier Gonzalez-Castillo	javier.gonzalez-castillo@nih.gov
22	Thursday	8-8-24	2:00 - 3:00 PM	FAES B1C209	Edge Analysis in fMRI	Josh Faskowitz	joshua.faskowitz@nih.gov
23	Tuesday	8-13-24	2:00 - 3:00 PM	FAES B1C209	Machine Learning in fMRI	Francisco Pereira	pereiraf2@mail.nih.gov
24	Thursday	8-15-24	2:00 - 3:00 PM	FAES B1C209	Magnetoencephalography	Allison Nugent	nugenta@mail.nih.gov
25	Tuesday	8-20-24	2:00 - 3:00 PM	FAES B1C209	Deep Scanning vs Large Populations	Peter Bandettini	bandettini@nih.gov
26	Thursday	8-22-24	2:00 - 3:00 PM	FAES B1C209	Diffusion MRI	Joelle Sarlls	sarllsjo@mail.nih.gov
27	Tuesday	8-27-24	2:00 - 3:00 PM	FAES B1C209	Representational Similarity & Multivariate Pattern Analysis	Fernando Ramirez	fernando.ramirez@nih.gov
28	Thursday	8-29-24	2:00 - 3:00 PM	FAES B1C209	Positron Emission Tomography	Robert Innis	innisr@mail.nih.gov
29	Tuesday	9-3-24	2:00 - 3:00 PM	FAES B1C209	Minimizing Information Waste	Gang Chen	gangchen@mail.nih.gov
30	Thursday	9-5-24	2:00 - 3:00 PM	FAES B1C209	Data sharing and open science	Adam Thomas	adamt@nih.gov
31	Tuesday	9-10-24	2:00 - 3:00 PM	FAES B1C210	Overview of fMRI research in the NIH intramural program	Peter Bandettini	bandettini@nih.gov
32	Thursday	9-12-24	2:00 - 3:00 PM	FAES B1C210	Future of fMRI	Peter Bandettini	bandettini@nih.gov

Brief History of Brain Imaging

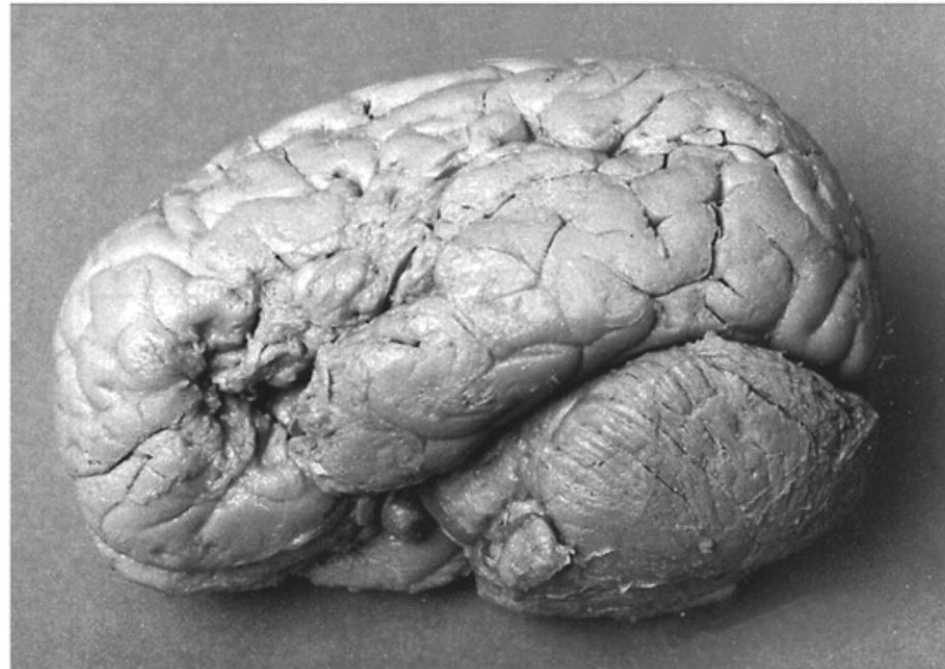
- 1. Lesion-based Mapping.**
- 2. Anatomic Imaging.**
- 3. Hemodynamic and Metabolic Imaging.**
- 4. Electrophysiologic Imaging**
- 5. Functional MRI**

Brief History of Brain Imaging

- 1. Lesion-based Mapping.**
- 2. Anatomic Imaging.**
- 3. Hemodynamic and Metabolic Imaging.**
- 4. Electrophysiologic Imaging**
- 5. Functional MRI**

1861 Paul Broca:

His patient, Leborgne, could only produce “tan.”



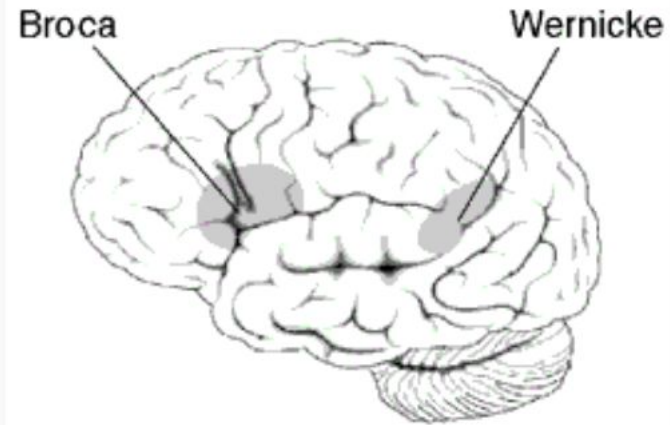
1874: Carl Wernicke

His patients could not understand or produce meaningful speech but could articulate words.

Carl Wernicke



Wernicke's area

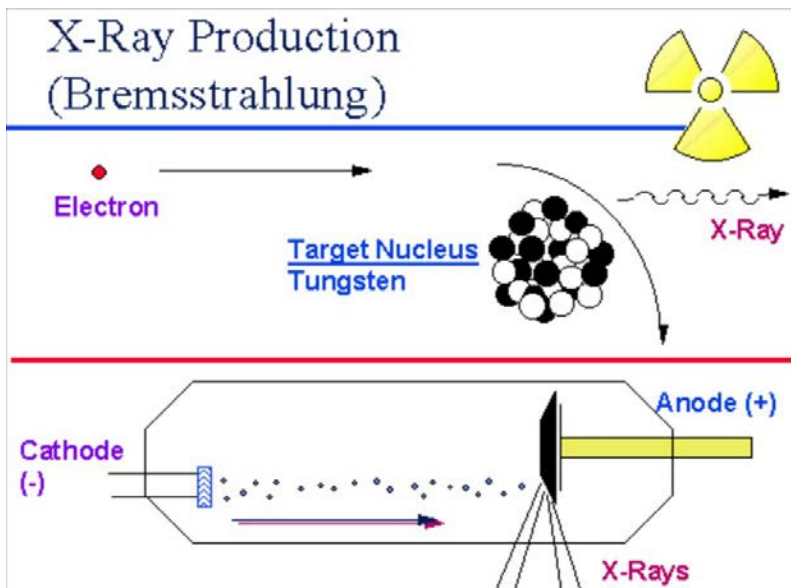


Approximate location of Wernicke's area
highlighted in grey

Brief History of Brain Imaging

- 1. Lesion-based Mapping.**
- 2. Anatomic Imaging.**
- 3. Hemodynamic and Metabolic Imaging.**
- 4. Electrophysiologic Imaging**
- 5. Functional MRI**

1895: Roentgen discovers x-rays and their utility



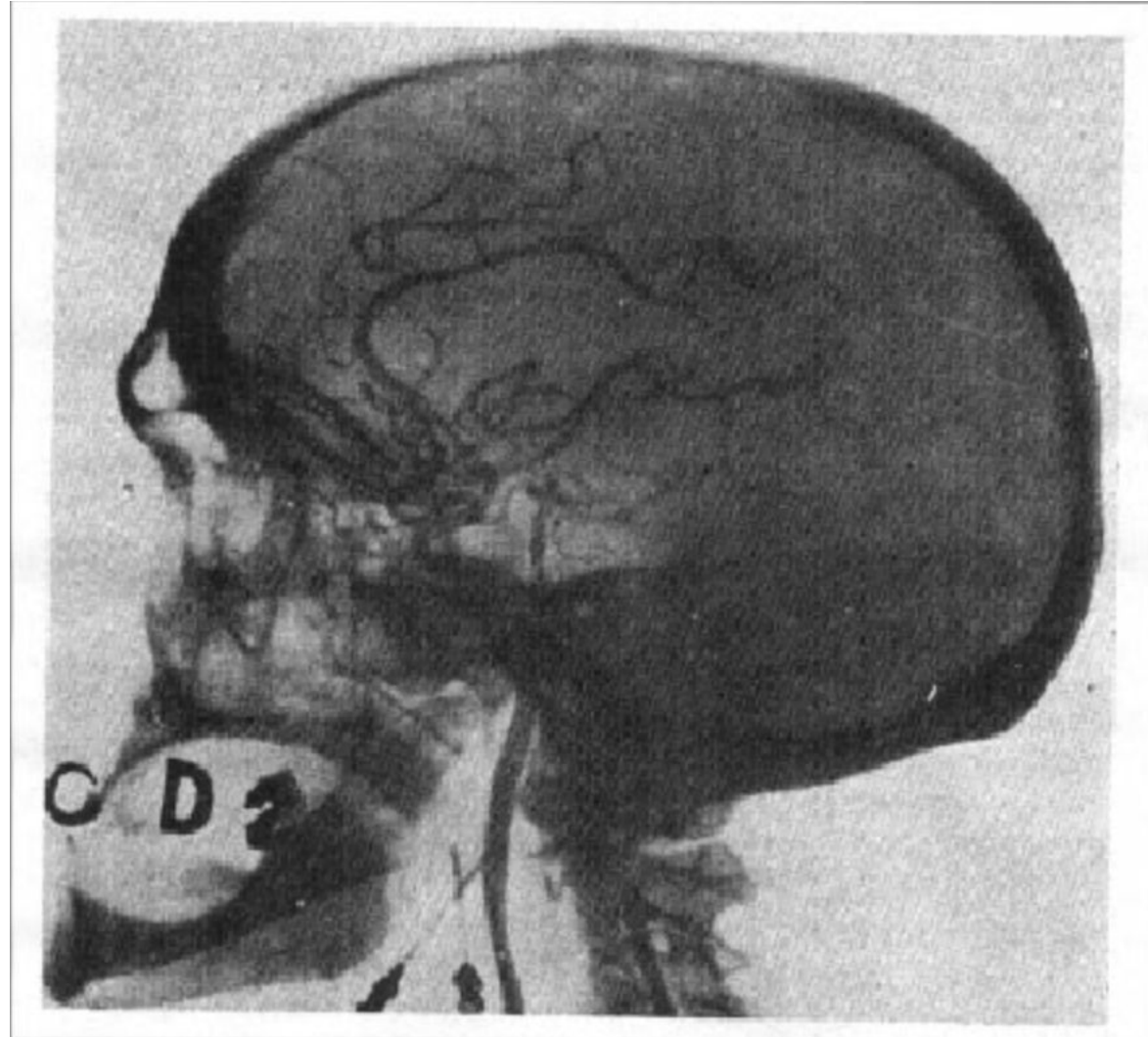
Crooke's tube

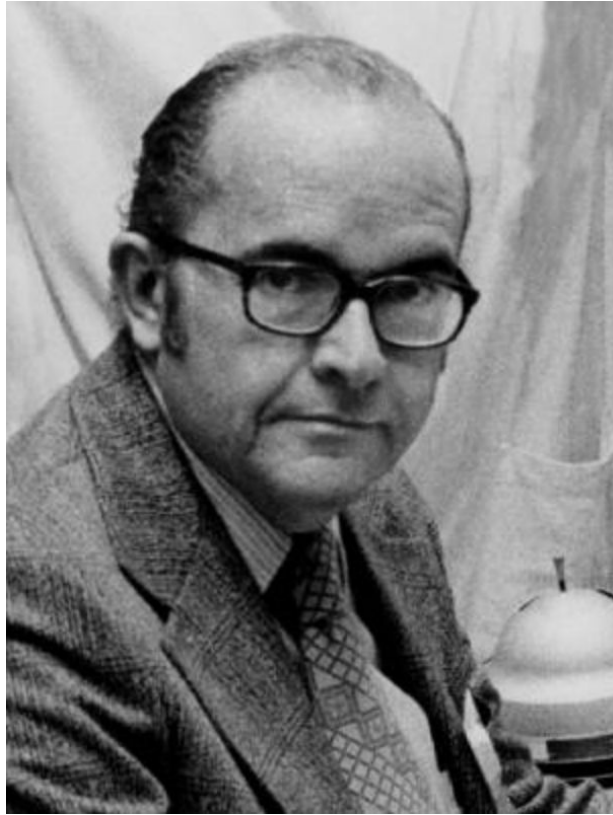
Early 1900's: Pneumoencephalography

CSF drained from the brain to enhance contrast in x-rays



1927: Antonio Egas Moniz – first Arteriogram





1960, William Oldendorf patented an electronically based device that could capture image slices continuously through a solid object – Computed Tomography



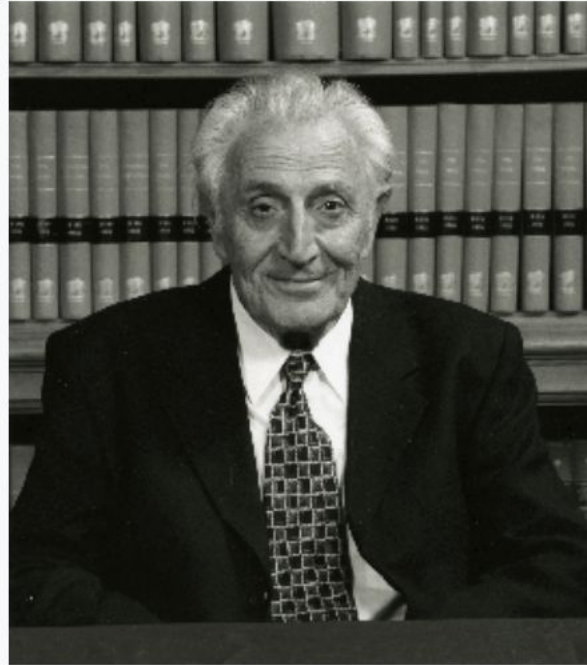
1971: Hounsfield implemented the first CT scanner



Godfrey Hounsfield received the 1979 Nobel Prize in Medicine for his work in the development of computer assisted tomography (CAT) scanning.

NMR: Nuclear Magnetic Resonance

Erwin Hahn



1950: Hahn discovered the “spin-echo” phenomenon and contributed to our understanding of T1 and T2 relaxation times.

MRI: Magnetic Resonance Imaging



Sir Peter Mansfield and Paul Lauterbur, Winners of the Nobel Prize for Medicine, 2003

Lauterbur's Contribution: Projectional NMR Tomography

Paul Lauterbur (1909-2007), a chemist working at the State University of New York at Stony Brook, published the first true MR image in *Nature* in March, 1973. His experimental setup involved two 1-mm-diameter tubes filled with water placed in an 1.4T magnet. Applying magnetic field gradients rotated successively by 45° , he was able to obtain four different 1-dimensional projections of the NMR signal. These data were then mathematically "back-projected" to form a 2-dimensional tomographic image. Because the result depended on the combined effects of two magnetic fields, Lauterbur named his technique "**zeugmatography**" after the Greek word, *zeugma*, meaning "that which is used for joining." Shortly thereafter, Lauterbur produced crude images of his first living subject: a tiny clam.

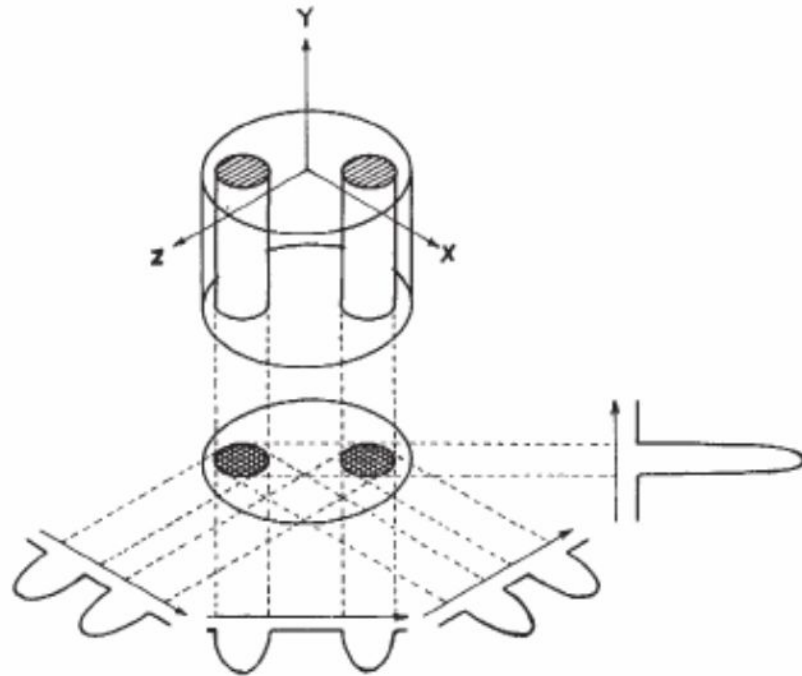
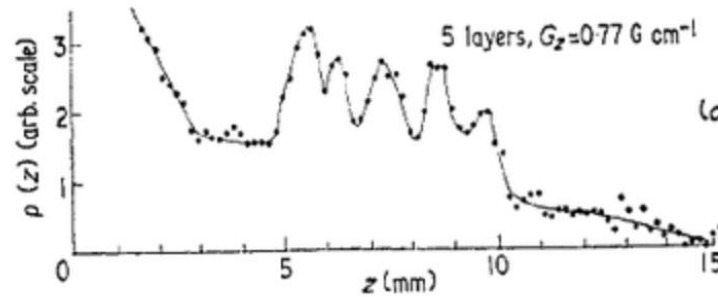


Fig. 1 Relationship between a three-dimensional object, its two-dimensional projection along the Y-axis, and four one-dimensional projections at 45° intervals in the XZ-plane. The arrows indicate the gradient directions.



Fig. 2 Proton nuclear magnetic resonance zeugmatogram of the object described in the text, using four relative orientations of object and gradients as diagrammed in Fig. 1.

Mansfield's Contribution: Use of a field gradient for slice selection



From Mansfield (1973). Five peaks corresponding to five stacked blocks of solid camphor.

Also in 1973, **Peter Mansfield** (b. 1933), a physicist working at the University of Nottingham, demonstrated how a linear field gradient could be used to localize the NMR signal on a slice-by-slice basis. Mansfield's experimental setup involved stacking multiple 1-mm-thick sheets of solid camphor into the bore of an NMR spectrometer. Applying a magnetic field gradient perpendicular to the sheets,

Mansfield measured the transient NMR signal response to an applied RF-pulse. Interference peaks similar to those seen in x-ray diffraction were observed, which when inverse Fourier transformed revealed discrete layers of the camphor sample.

Later in the decade, Mansfield and his collaborator, Andrew Maudsley, further refined this method into a line-scan technique, producing the first image of a human body part, a finger, in 1977.

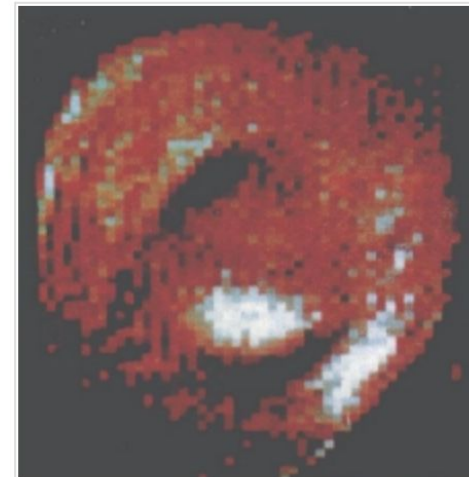
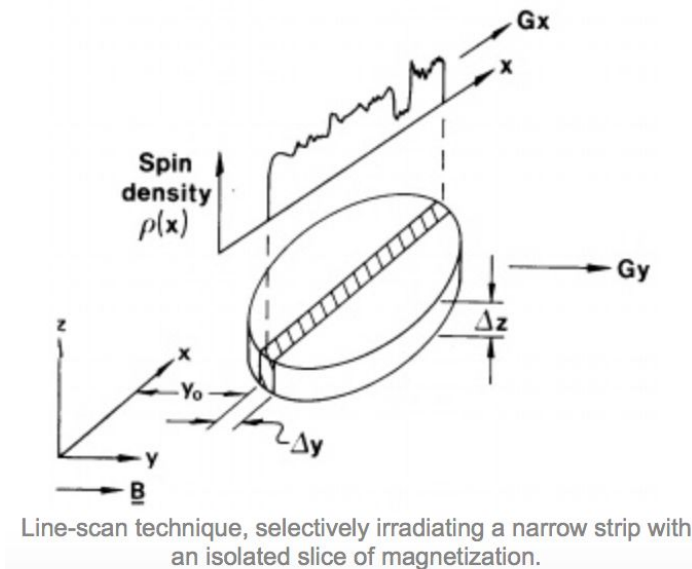


Image of human finger from Mansfield and Maudsley (1977) using line-scan technique obtained at 0.35T in 23 minutes. The white oval is marrow within the phalanx and the dark bands are tendons.

Damadian's Contribution: Vision of a human-sized scanner to detect disease

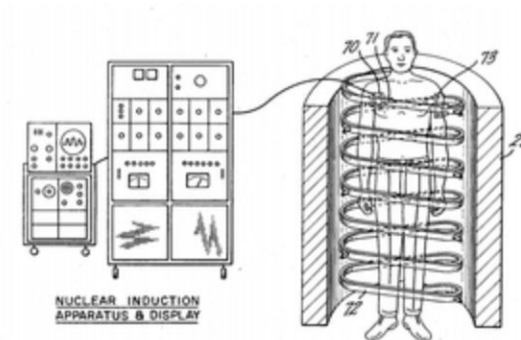


Raymond V. Damadian

While Lauterbur and Mansfield were basic scientists, **Raymond V. Damadian** (b. 1936) was a physician, an Associate Professor of Medicine at the State University of New York - Brooklyn (Downstate). He looked at NMR from a different and original perspective — as a phenomenon that might be used to probe the body and diagnose human disease. In one of his landmark early papers (*Science*, 1971) Damadian demonstrated that cancer cells had longer T1 and T2 values than normal cells. In 1972 he filed a US patent application for an apparatus and method to detect cancer in tissue. Although the details of exactly how this 'apparatus' would produce images were not included in the application, Damadian and his team set out to build such a device which was named "**Indomitable**." By mid-summer, 1977, the first whole-body MR images were being produced, including the famous one shown below of his assistant's chest.

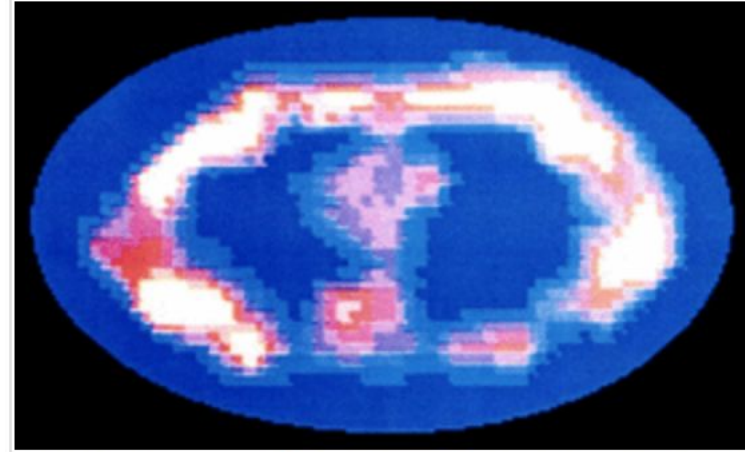


Assistant Larry Minkoff in Indomitable



Damadian's 1972 patent application

Damadian used a "sensitive point" method for spatial localization of the NMR signal. This was based on a saddle-shaped magnetic field where only a small volume at the center matched the resonance frequency of the RF pulse. The patient's body was physically moved in a rectangular pattern until signals from all pixels were obtained.



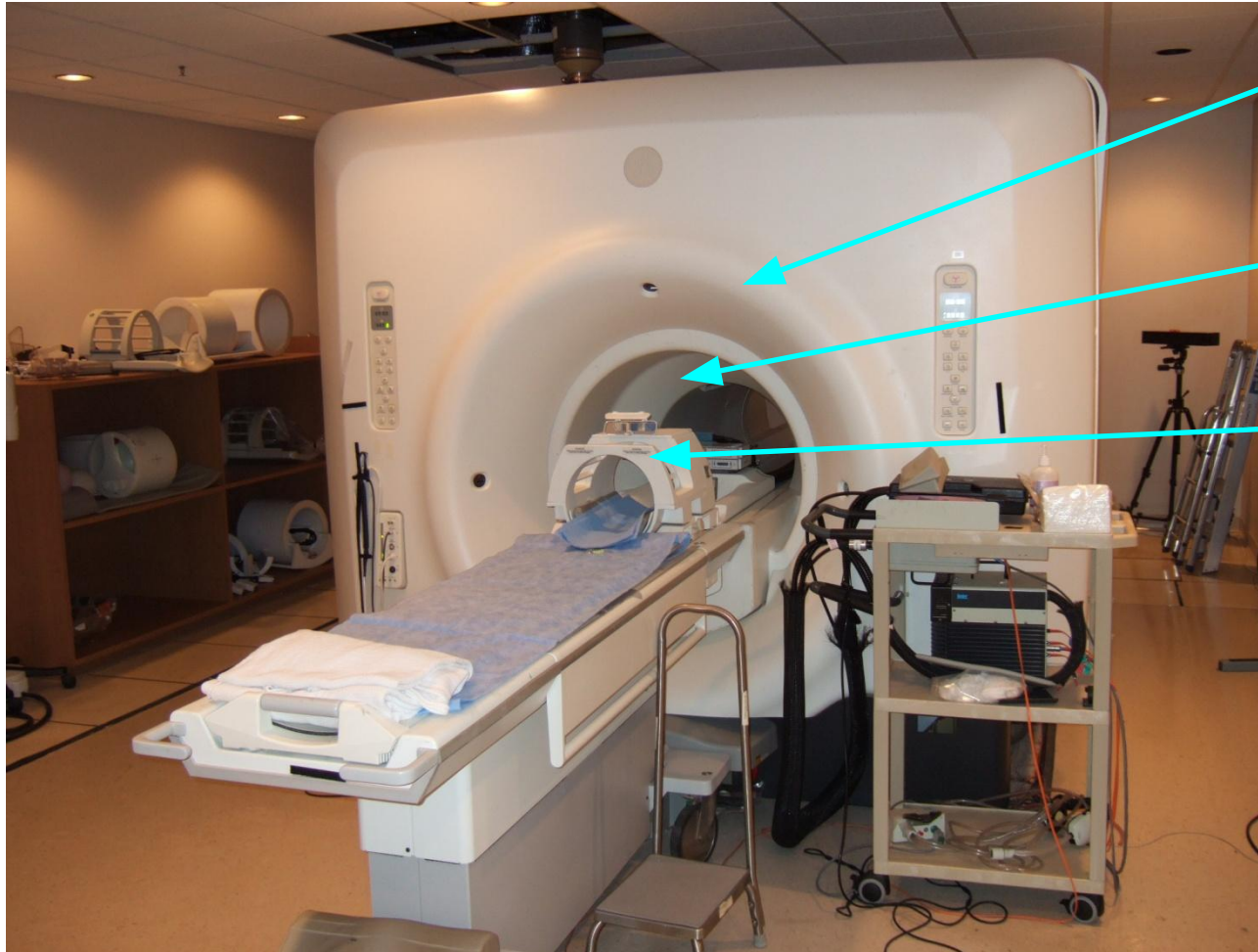
First whole body image (Minkoff's chest), obtained July, 1977. It required nearly 5 hours to produce.

Damadian called his imaging method "field-focused NMR" or FONAR. This became the name of his company, the first to manufacture clinical MR scanners commercially. It was soon recognized that the field-focused method was far too slow and clumsy for routine clinical imaging, and so it was abandoned in favor of the methods of Lauterbur and Mansfield in subsequent versions of the scanner.

When the 2003 Nobel Prizes for Medicine were announced, Damadian considered it a personal injustice that he was excluded. He placed full-page ads in several large world newspapers urging the Nobel committee to change its mind. The decision stood.

Magnetic Resonance Imaging:

Invented 1977, Introduced clinically 1984



**Magne
t**

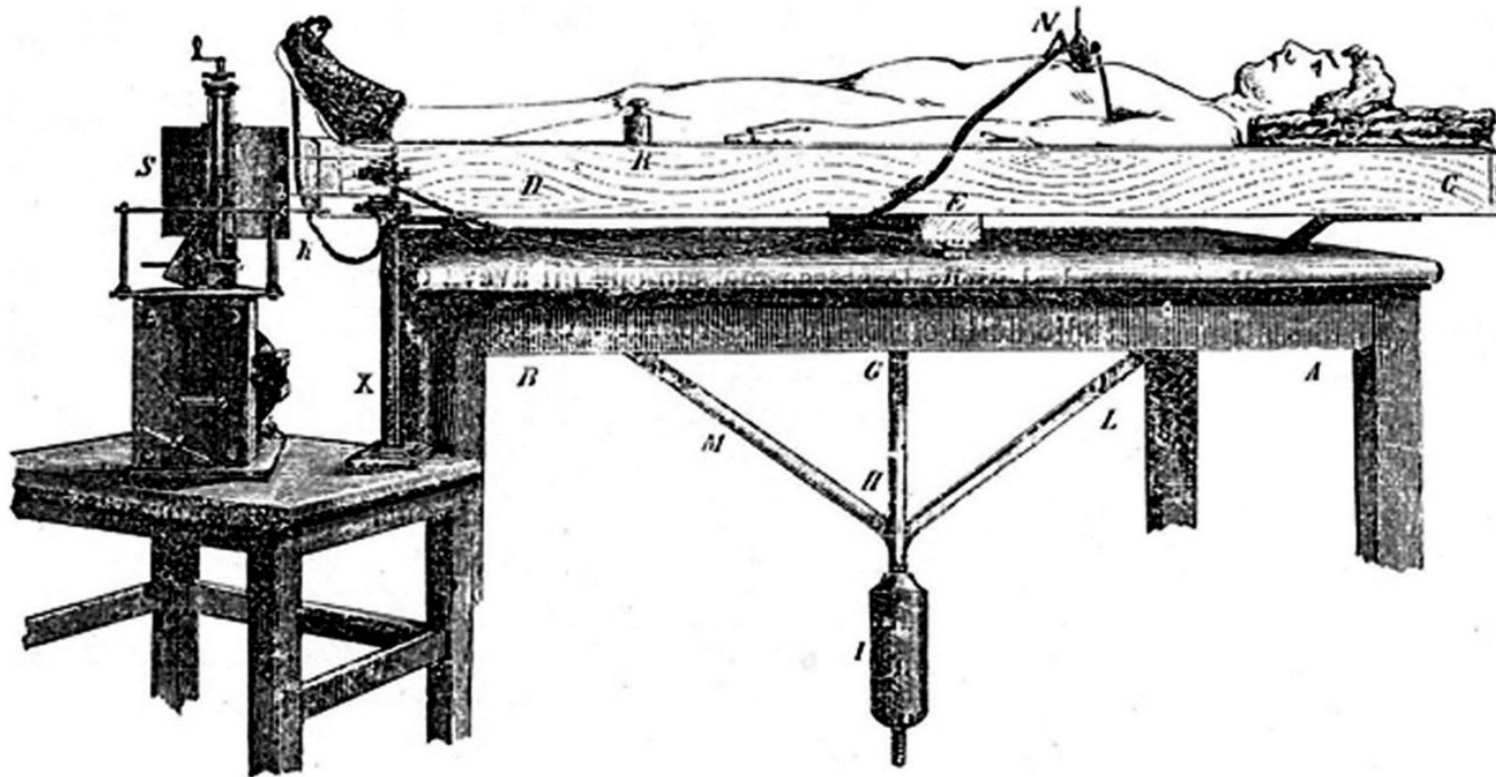
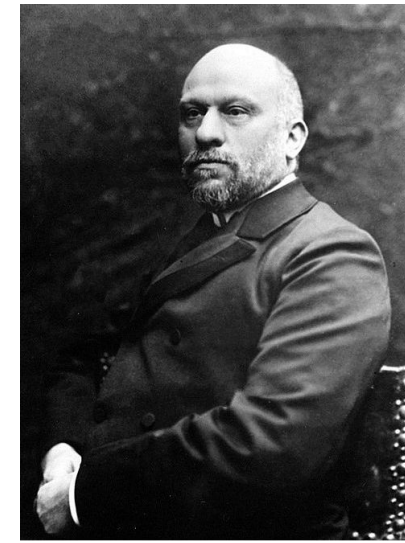
**Gradient
Coil**

**Radio-Fre
quency
Coil**

Brief History of Brain Imaging

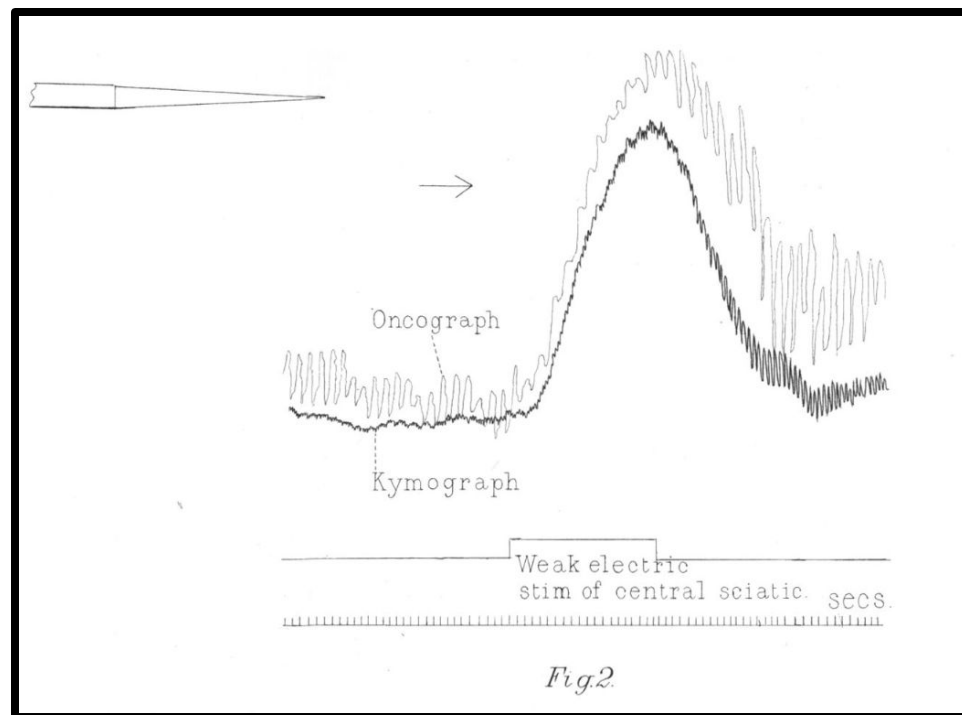
- 1. Lesion-based Mapping.**
- 2. Anatomic Imaging.**
- 3. Hemodynamic and Metabolic Imaging.**
- 4. Electrophysiologic Imaging**
- 5. Functional MRI**

1880's: Angelo Mosso's balance

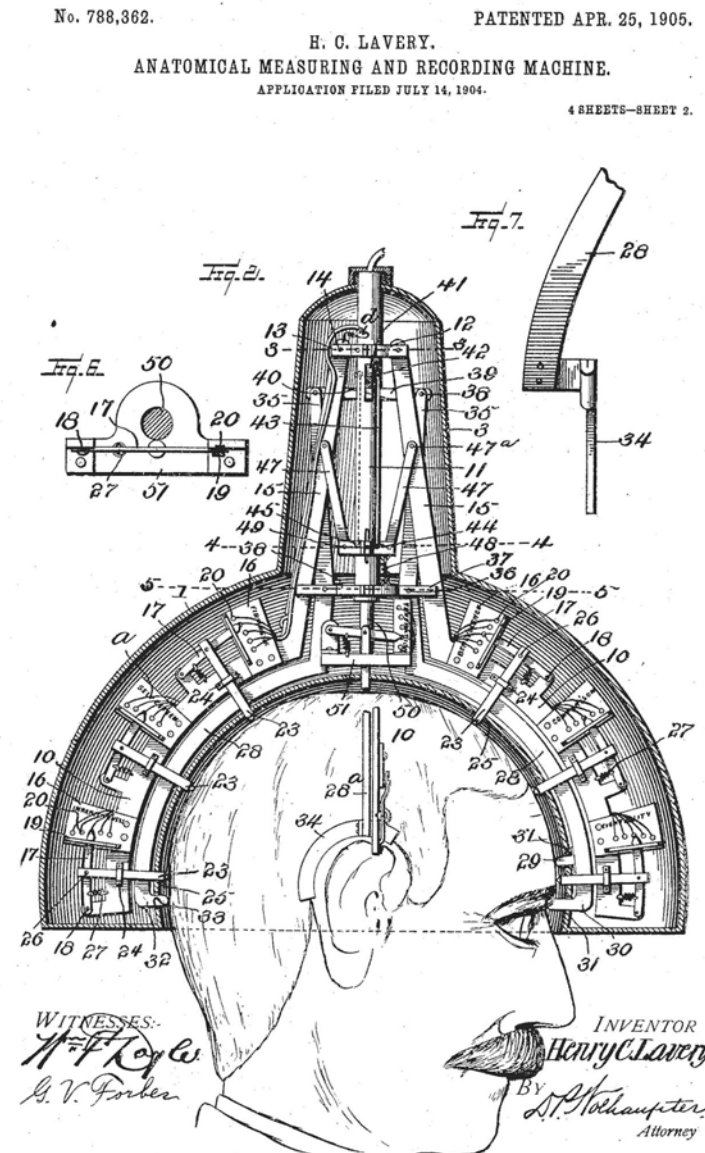


**ON THE REGULATION OF THE BLOOD-SUPPLY OF
THE BRAIN.** BY C. S. ROY, M.D., F.R.S., *Professor of
Pathology, University of Cambridge,* AND C. S. SHERRINGTON,
M.B., M.A., *Fellow of Gonville and Caius College. Lecturer on
Physiology in the School of St Thomas's Hospital, London.*
Plates II., III. and IV.

From the Cambridge Pathological Laboratory.



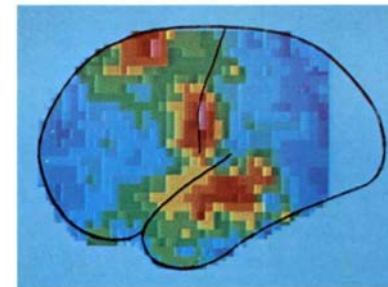
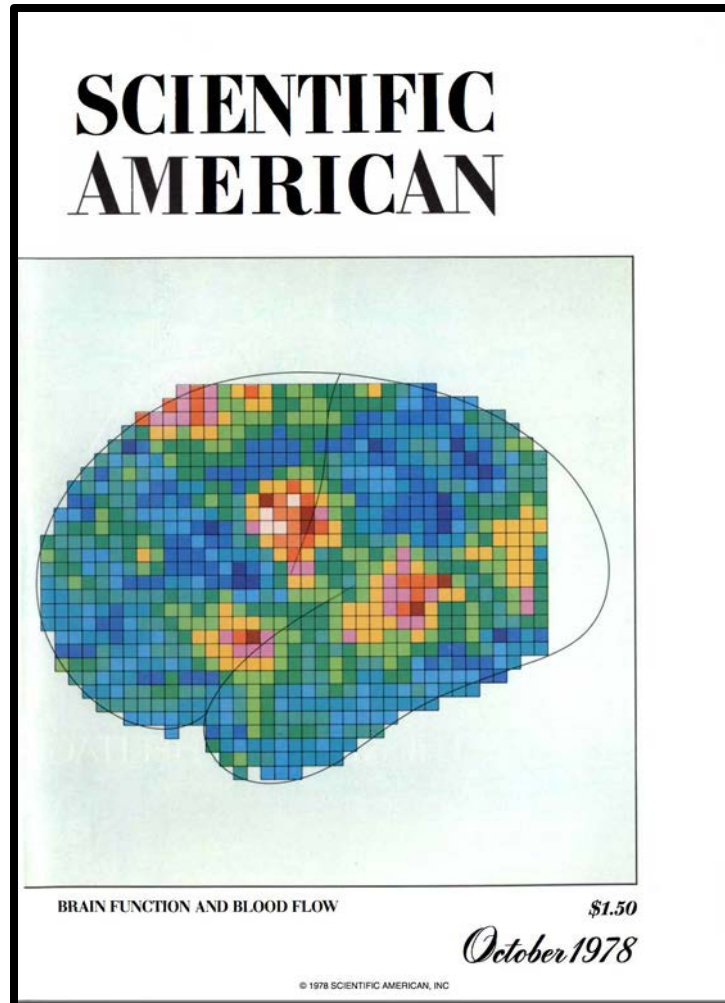
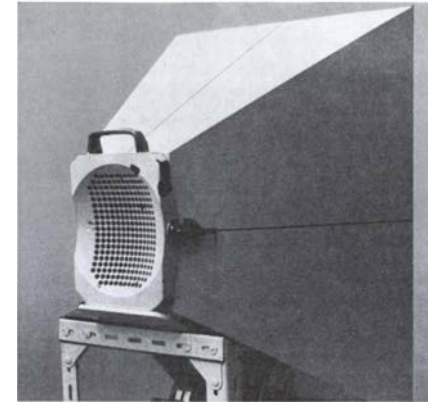
Phrenology: Brain Assessment... c. 1905



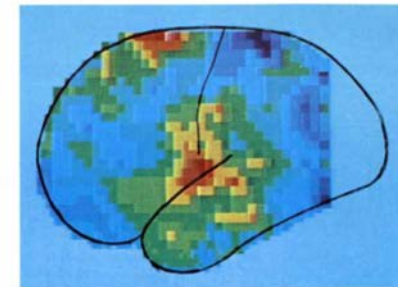
* Not

1960's to 70's: Xenon inhalation – radiation detection at the surface of brain

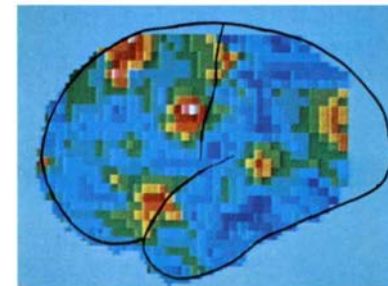
Niels A. Lassen, David H. Ingvar, Erik Skinhøj, "Brain Function and Blood Flow", Scientific American, 239(4):50-59, 1978 October



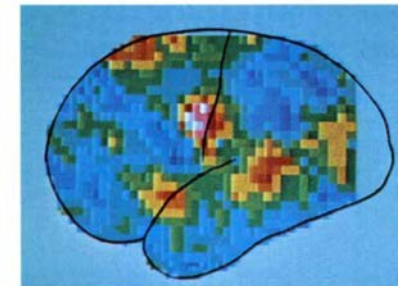
SPEAKING activates three centers in each hemisphere: the mouth-tongue-larynx area of the somatosensory and motor cortex, the supplementary motor area and the auditory cortex. Differences in activity



ty between the two hemispheres can be seen in these averaged images from nine different subjects: in the right hemisphere (right) the mouth-tongue-larynx area is less distinct and coalesces with auditory cortex.



READING SILENTLY AND READING ALOUD involve different patterns of activity in the cortex. Reading silently (left) activates four areas: the visual association area, the frontal eye field, the supplementary motor area and Broca's speech center in the lower part of the frontal lobe. Reading aloud (right) activates two more centers:



the mouth area and the auditory cortex. The left hemisphere is shown in both cases, but similar results have been obtained from the right hemisphere. Adding the primary visual cortex, which is not reached by the radioactive isotope, the act of reading aloud calls for simultaneous activity in seven discrete cortical centers in each hemisphere.

Isotope	half-life (min)	Maximum positron energy (MeV)	Positron range in water (FWHM in mm)	Production method
^{11}C	20.3	0.96	1.1	cyclotron
^{13}N	9.97	1.19	1.4	cyclotron
^{15}O	2.03	1.70	1.5	cyclotron
^{18}F	109.8	0.64	1.0	cyclotron
^{68}Ga	67.8	1.89	1.7	generator
^{82}Rb	1.26	3.15	1.7	generator

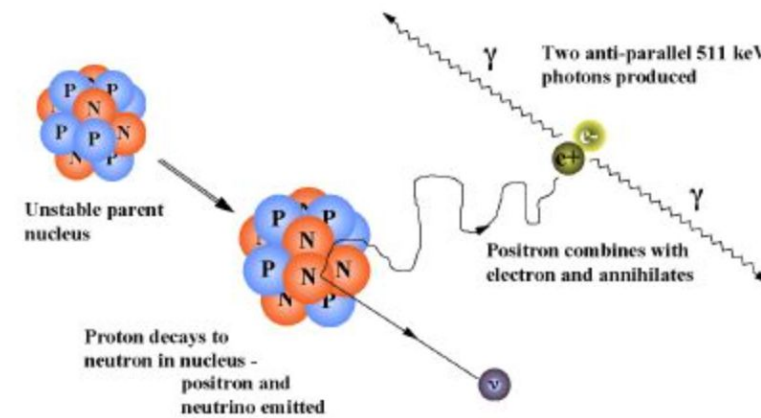


Figure 1. Positron emission and annihilation.

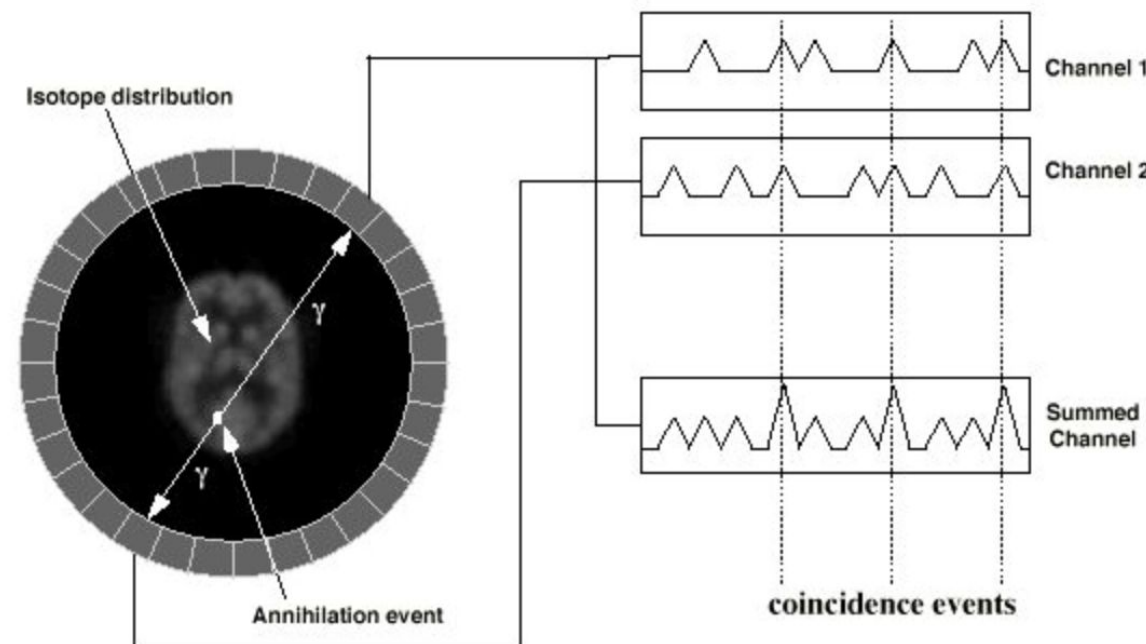
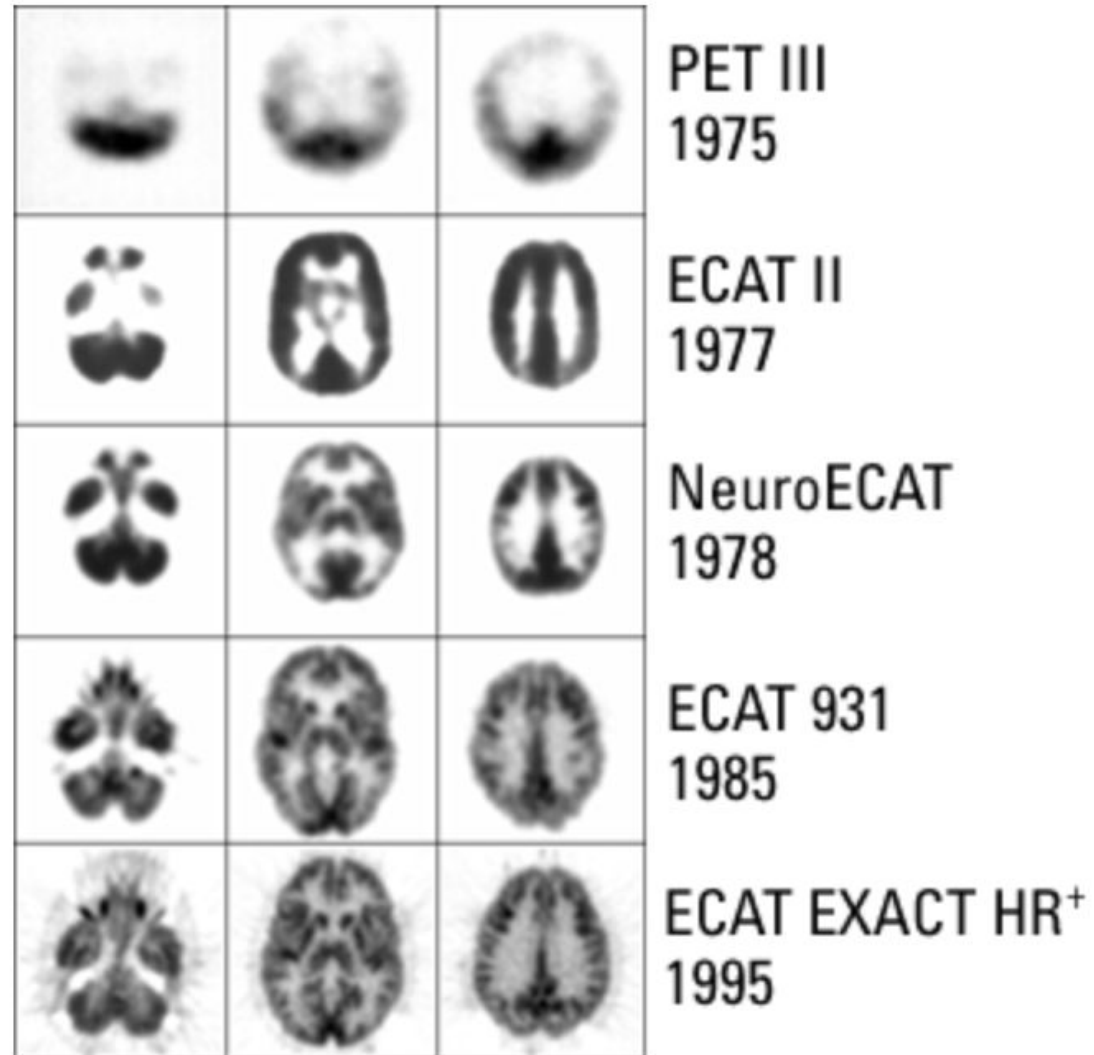
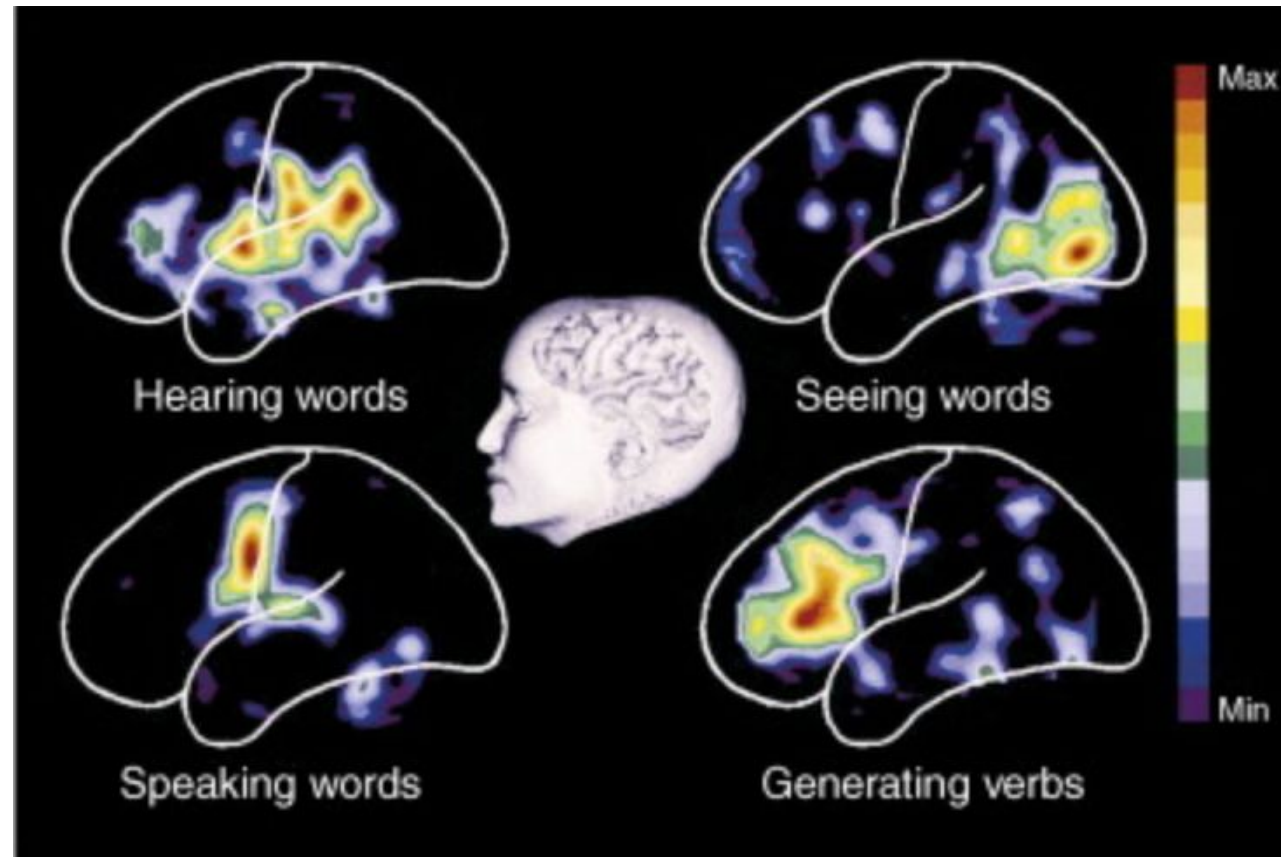


Figure 2. Coincidence detection in a PET camera.

1973: Michael Ter-Pogossian, Edward Hoffman, and Micahale Phelps - First Human PET scanner





Positron emission tomographic studies of the cortical anatomy of single-word processing. Petersen, S.E. et al. *Nature*. 1988; 331: 585–589

Brief History of Brain Imaging

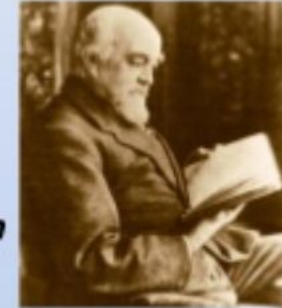
- 1. Lesion-based Mapping.**
- 2. Anatomic Imaging.**
- 3. Hemodynamic and Metabolic Imaging.**
- 4. Electrophysiologic Imaging**
- 5. Functional MRI**

EEG

From the electrical nature of brain signals ...

1875: R.C. measured currents inbetween the cortical surface and the skull, in dogs and monkeys

Richard Caton
1842 - 1926



1924: H.B. first EEG in humans, description of alpha and beta waves



Alpha activity $\sim 200 \mu V$

Hans Berger
1873 - 1941



MEG

About 50 years later ...

**Brian-
David
Josephson**



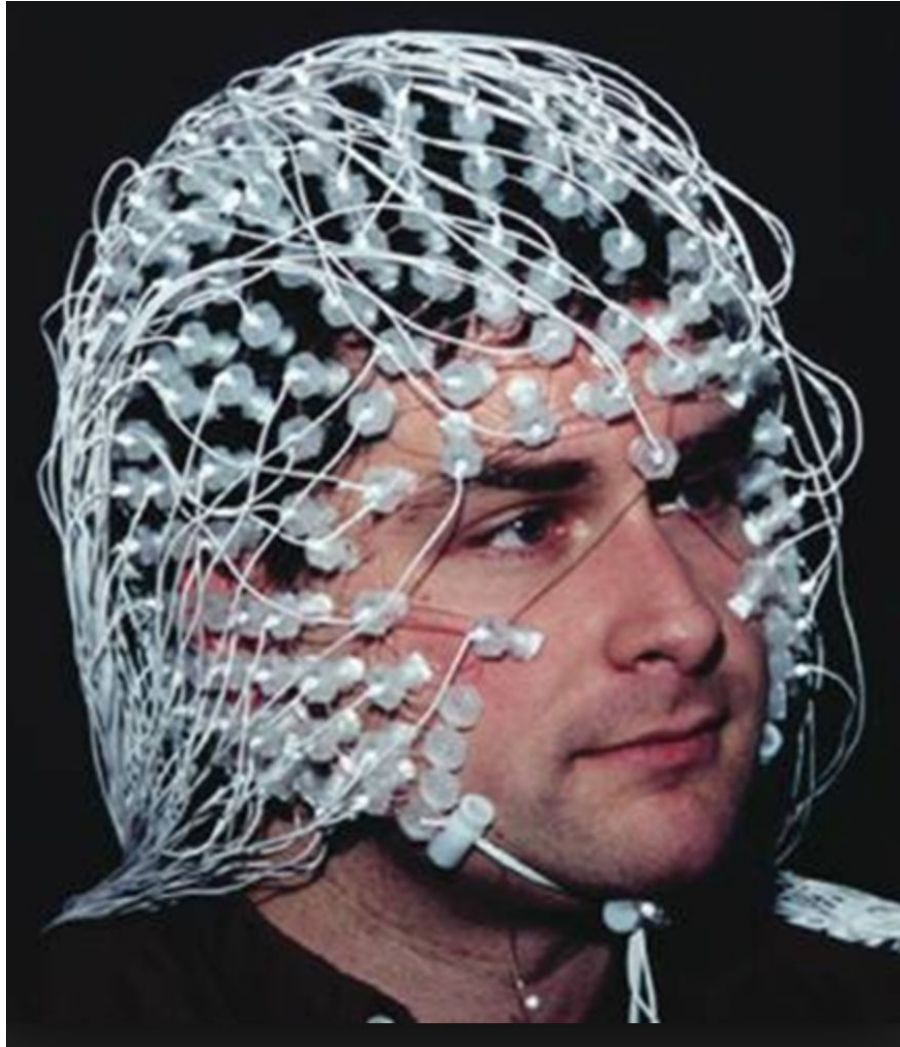
1968: first (noisy) measure of a magnetic brain signal [*Cohen, Science 68*]

1970: James Zimmerman invents the
'Superconducting quantum interference device' (SQUID)

1972: first (1 sensor) MEG recording based on SQUID

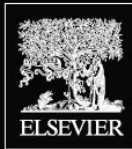
**David
Cohen**





Brief History of Brain Imaging

- 1. Lesion-based Mapping.**
- 2. Anatomic Imaging.**
- 3. Hemodynamic and Metabolic Imaging.**
- 4. Electrophysiologic Imaging**
- 5. Functional MRI**



ISSN 1053-8119
Volume 62, Issue 2, August 15, 2012

NeuroImage

Editor-in-Chief
Peter Bandettini



Special Issue
**20 Years of fMRI:
The Science
and the Stories**

Available online at www.sciencedirect.com

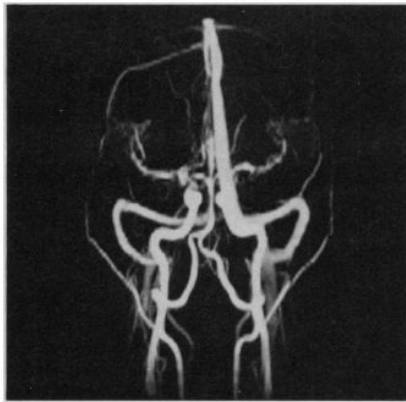
SciVerse ScienceDirect

Functional Magnetic Resonance Imaging in Medicine and Physiology

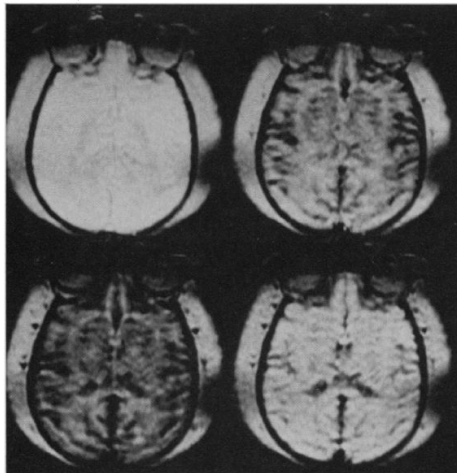
CHRIT T. W. MOONEN, PETER C. M. VAN ZIJL, JOSEPH A. FRANK,
DENIS LE BIHAN, EDWIN D. BECKER

(1990) *Science*, 250, 53-61.

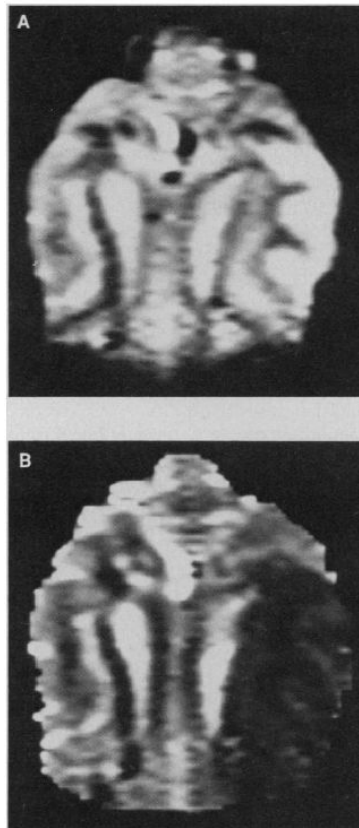
angiography



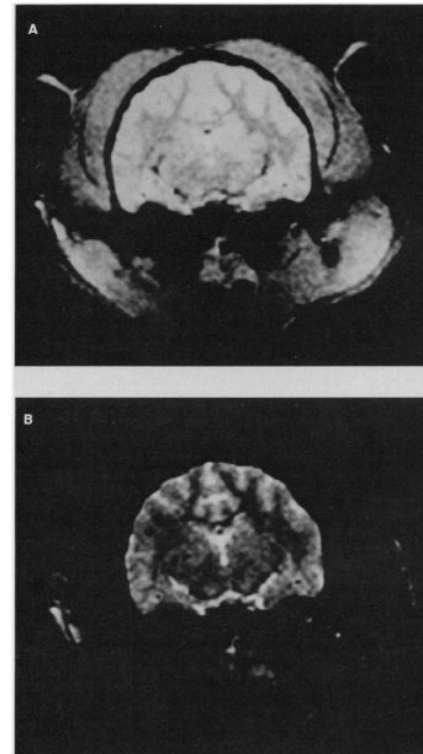
Gadolinium perfusion



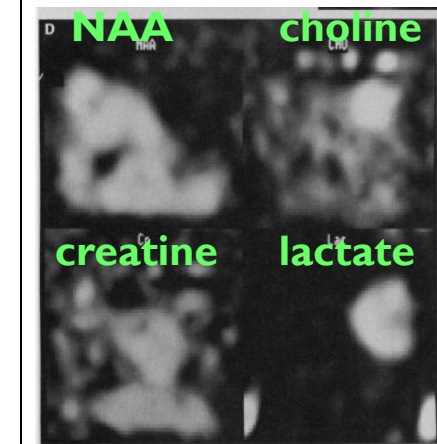
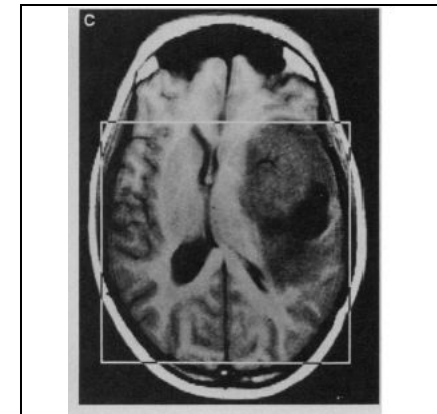
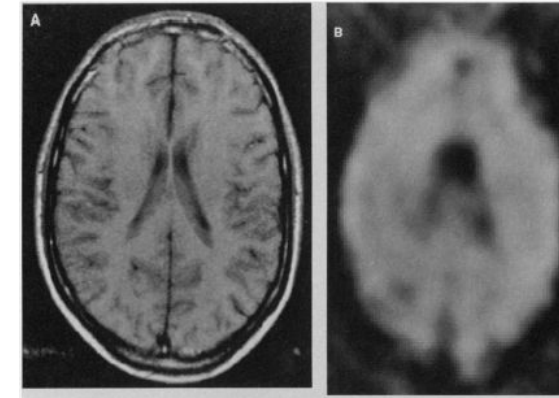
Diffusion



magnetization transfer



metabolic imaging (NAA)



How it all came together...

Five Keyt Factors For The Emergence of Functional MRI

- 1. Magnetic properties of red blood cells**
- 2. Activation related hemodynamic changes**
- 3. Spatial scale of brain activation**
- 4. Echo Planar Imaging**
- 5. Prevalence of MRI scanners**

Five Key Factors For The Emergence of Functional MRI

1. **Magnetic properties of red blood cells**
2. **Activation related hemodynamic changes**
3. **Spatial scale of brain activation**
4. **Echo Planar Imaging**
5. **Prevalence of MRI scanners**

Fundamental Work towards BOLD contrast :

L. Pauling, C. D. Coryell, *Proc.Natl. Acad. Sci. USA* 22, 210-216, 1936.

(Blood susceptibility changes with oxygenation)

K.R. Thulborn, J. C. Waterton, et al., *Biochim. Biophys. Acta.* 714: 265-270, 1982.

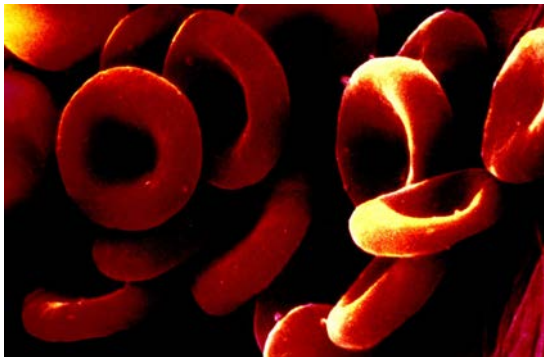
(Blood T2 is proportional to oxygenation & mechanism is bulk susceptibility)

S. Ogawa, T. M. Lee, A. R. Kay, D. W. Tank, *Proc. Natl. Acad. Sci. USA* 87, 9868-9872, 1990.

(T2 and T2 modulation in vessels in living rat brains with oxygenation changes)*

Turner, R., LeBihan, D., Moonen, C. T. W., Despres, D. & Frank, J. *MRM*, 22, 159-166, 1991

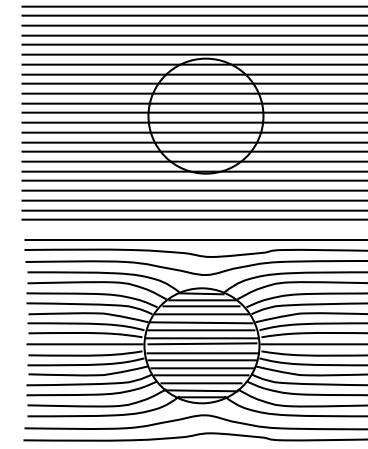
(T2 modulation with cat brain with oxygenation changes)*



red blood

oxygenate
d

deoxygenate
d



BOLD contrast investigation started in 1936...or even 1845.

210

CHEMISTRY: PAULING AND CORYELL

Proc. N. A. S.

*THE MAGNETIC PROPERTIES AND STRUCTURE OF
HEMOGLOBIN, OXYHEMOGLOBIN AND
CARBONMONOXYHEMOGLOBIN*

BY LINUS PAULING AND CHARLES D. CORYELL

GATES CHEMICAL LABORATORY, CALIFORNIA INSTITUTE OF TECHNOLOGY

Communicated March 19, 1936

Over ninety years ago, on November 8, 1845, Michael Faraday investigated the magnetic properties of dried blood and made a note "Must try recent fluid blood." If he had determined the magnetic susceptibilities of arterial and venous blood, he would have found them to differ by a large amount (as much as twenty per cent for completely oxygenated and completely deoxygenated blood); this discovery without doubt would have excited much interest and would have influenced appreciably the course of research on blood and hemoglobin.¹

Continuing our investigations of the magnetic properties and structure of hemoglobin and related substances,² we have found oxyhemoglobin and carbonmonoxyhemoglobin to contain no unpaired electrons, and ferrohemoglobin (hemoglobin itself) to contain four unpaired electrons per heme. The description of our experiments and the interpretation and discussion of the results are given below.

Biochimica et Biophysica Acta, 714 (1982) 265–270
Elsevier Biomedical Press

BBA 20122

OXYGENATION DEPENDENCE OF THE TRANSVERSE RELAXATION TIME OF WATER PROTONS IN WHOLE BLOOD AT HIGH FIELD

KEITH R. THULBORN, JOHN C. WATERTON *, PAUL M. MATTHEWS and GEORGE K. RADDA

Department of Biochemistry, University of Oxford, South Parks Road, Oxford OX1 3QU (U.K.)

(Received August 4th, 1981)

Key words: Oxygenation dependence; Transverse relaxation time; Water proton; High field NMR; (Whole blood)

At high and medium magnetic field, the transverse NMR relaxation rate (T_2^{-1}) of water protons in blood is determined predominantly by the oxygenation state of haemoglobin. T_2^{-1} depends quadratically on the field strength and on the proportion of haemoglobin that is deoxygenated. Deoxygenation increases the volume magnetic susceptibility within the erythrocytes and thus creates local field gradients around these cells. From volume susceptibility measurements and the dependence of T_2^{-1} on the pulse rate in the Carr-Purcell-Meiboom-Gill experiment, we show that the increase in T_2^{-1} with increasing blood deoxygenation arises from diffusion of water through these field gradients.



Oxygenation Changes T2

Biochimica et Biophysica Acta, 714 (1982) 265–270
Elsevier Biomedical Press

BBA 20122

OXYGENATION DEPENDENCE OF THE TRANSVERSE RELAXATION TIME OF WATER PROTONS IN WHOLE BLOOD AT HIGH FIELD

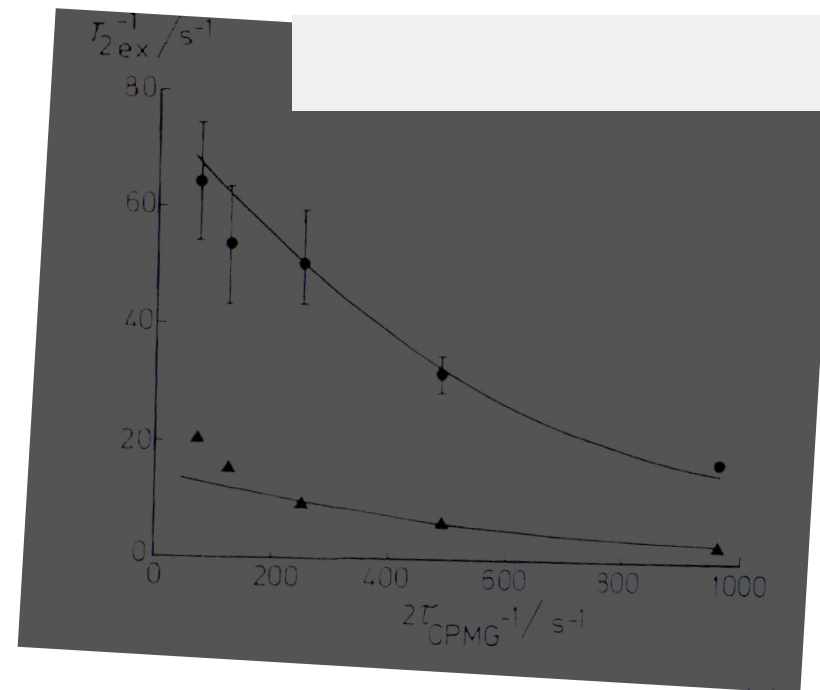
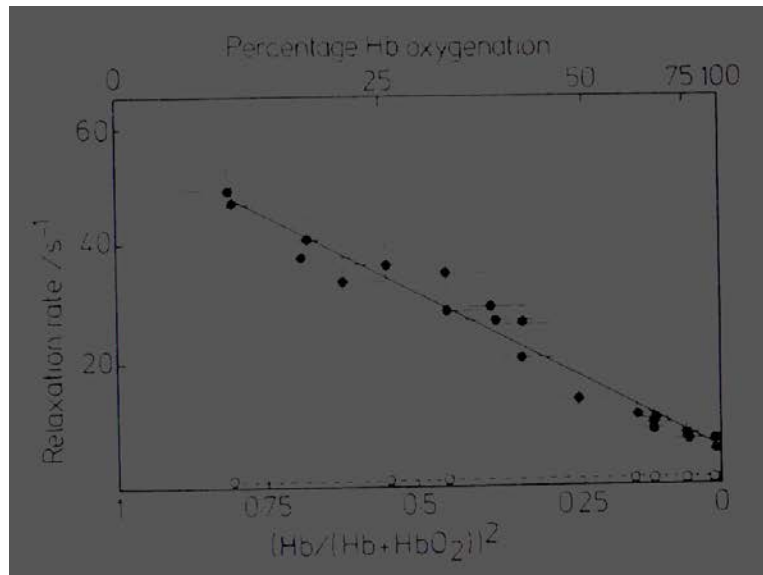
KEITH R. THULBORN, JOHN C. WATERTON *, PAUL M. MATTHEWS and GEORGE K. RADDA

Department of Biochemistry, University of Oxford, South Parks Road, Oxford OX1 3QU (U.K.)

(Received August 4th, 1981)

R2 effect is due to bulk susceptibility and not dipole-dipole interaction

Blood R2 proportional to Oxygenation



...Six years
later...

Oxygenation-Sensitive Contrast in Magnetic Resonance Image of Rodent Brain at High Magnetic Fields

SEIJI OGAWA, TSO-MING LEE, ASHA S. NAYAK,* AND PAUL GLYNN

AT&T Bell Laboratories, Murray Hill, New Jersey 07974

Received November 30, 1988; accepted June 20, 1989

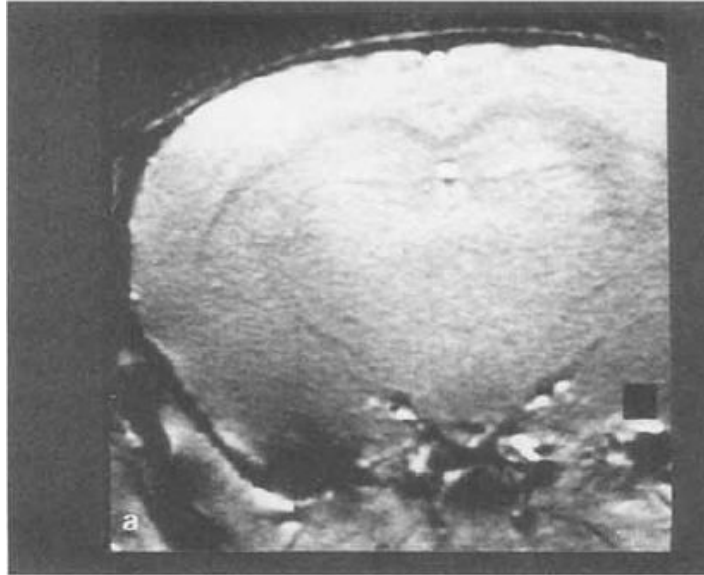
At high magnetic fields (7 and 8.4 T), water proton magnetic resonance images of brains of live mice and rats under pentobarbital anesthetization have been measured by a gradient echo pulse sequence with a spatial resolution of $65 \times 65\text{-}\mu\text{m}$ pixel size and $700\text{-}\mu\text{m}$ slice thickness. The contrast in these images depicts anatomical details of the brain by numerous dark lines of various sizes. These lines are absent in the image taken by the usual spin echo sequence. They represent the blood vessels in the image slice and appear when the deoxyhemoglobin content in the red cells increases. This contrast is most pronounced in an anoxy brain but not present in a brain with diamagnetic oxy or carbon monoxide hemoglobin. The local field induced by the magnetic susceptibility change in the blood due to the paramagnetic deoxyhemoglobin causes the intra voxel dephasing of the water signals of the blood and the surrounding tissue. This oxygenation-dependent contrast is appreciable in high field images with high spatial resolution.

© 1990 Academic Press, Inc.

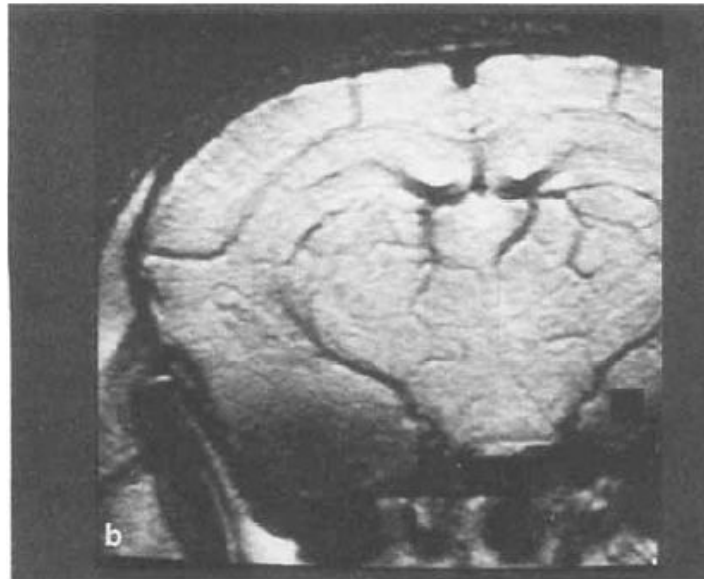


in vivo

100% O₂

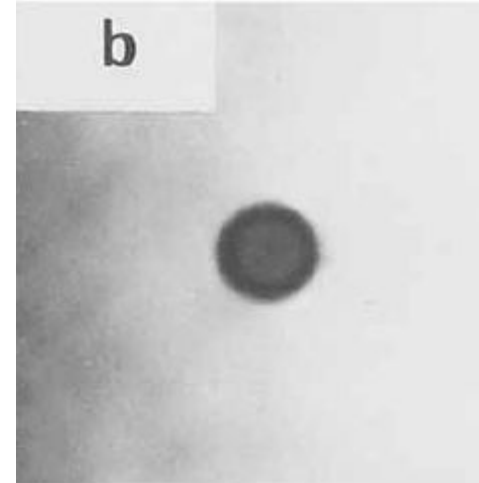


20% O₂

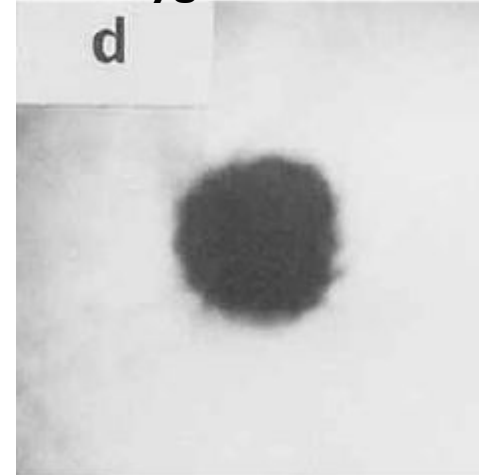


in vitro

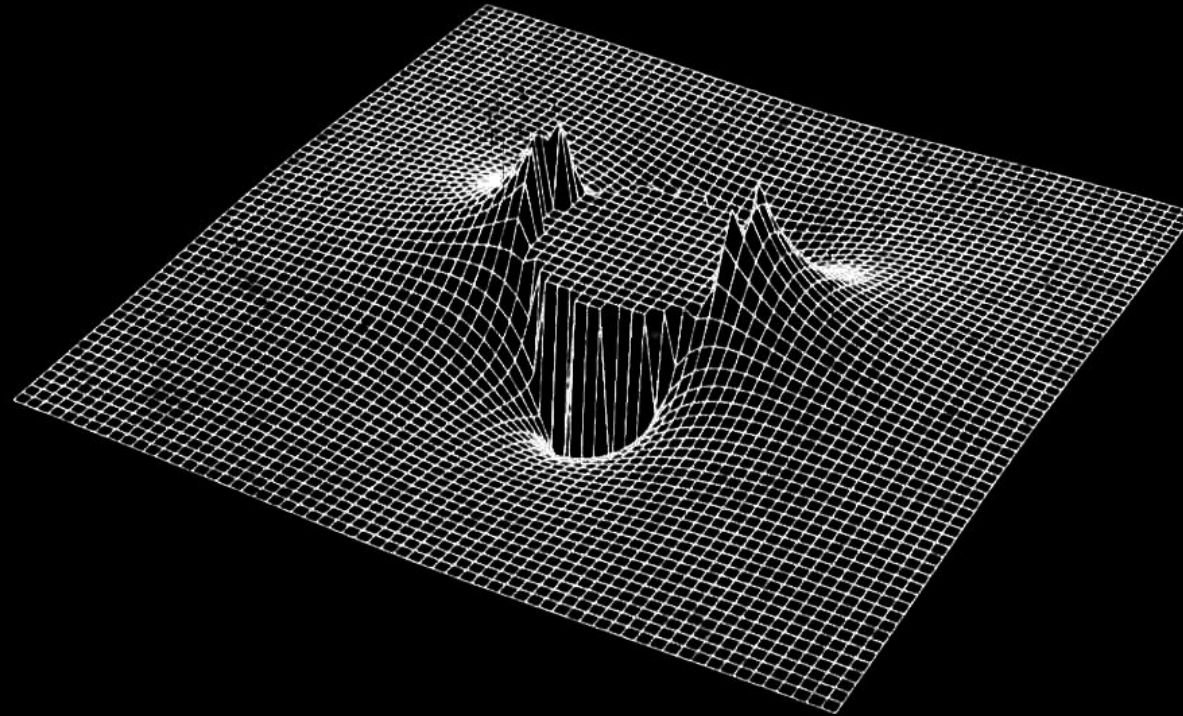
100% oxygenated blood



0% oxygenated blood



Susceptibility-Induced Field Distortion in the
Vicinity of a Microvessel \perp to B_0 .



MAGNETIC RESONANCE IN MEDICINE 22, 159–166 (1991)



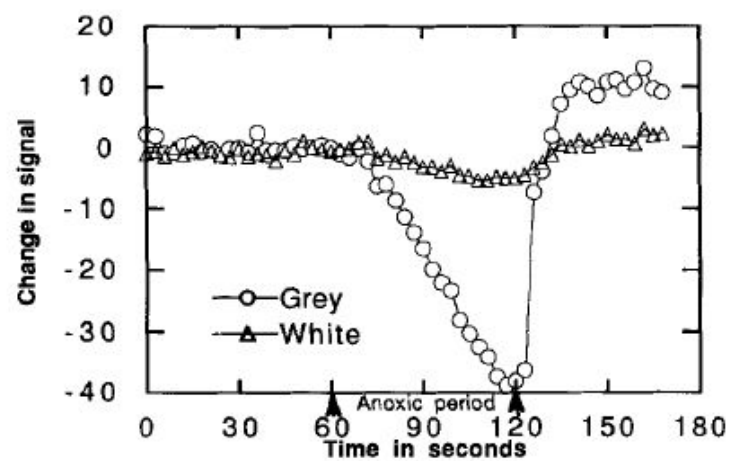
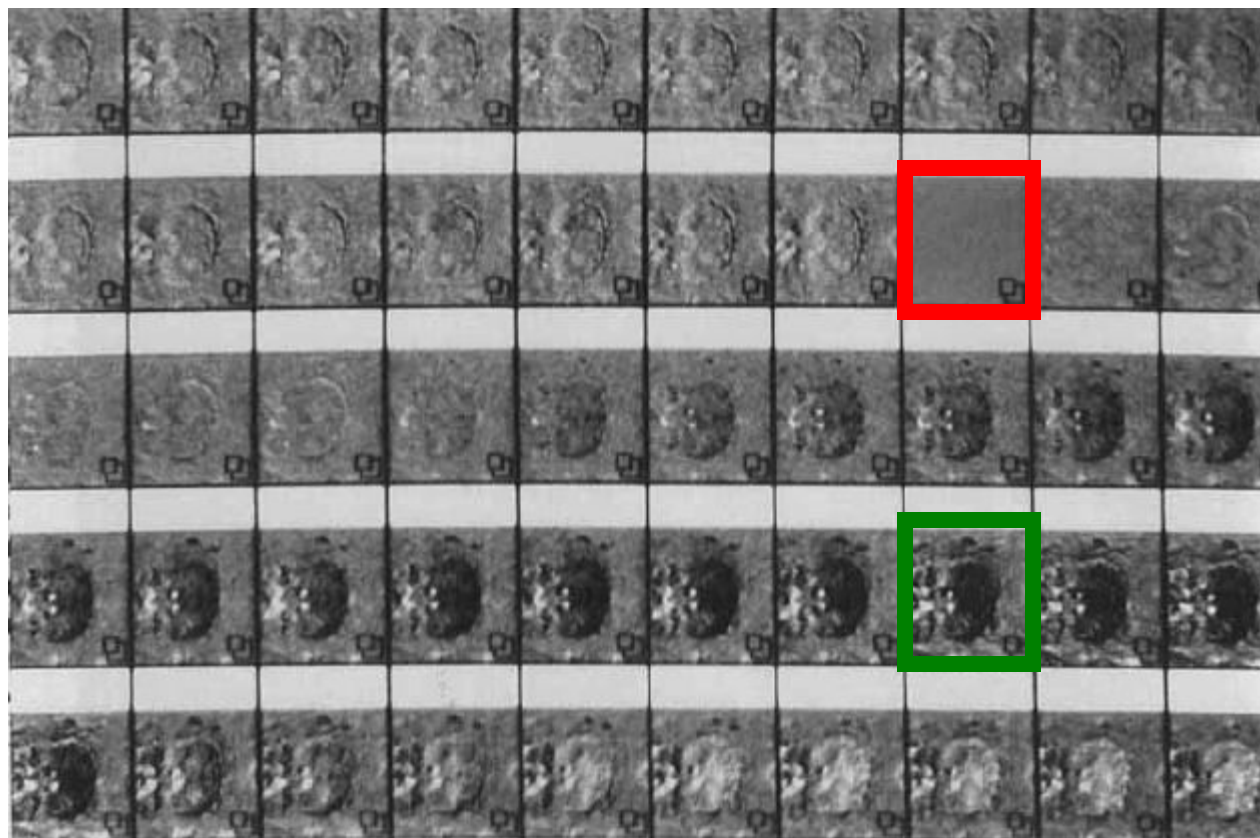
Echo-Planar Time Course MRI of Cat Brain Oxygenation Changes

ROBERT TURNER,*† DENIS LE BIHAN,‡ CHRIT T. W. MOONEN,§
DARYL DESPRES,§ AND JOSEPH FRANK‡

**Laboratory of Cardiac Energetics, ‡Diagnostic Radiology Department, and §In Vivo NMR Research Center, National Institutes of Health, Bethesda, Maryland 20892*

Received June 25, 1991; revised August 7, 1991

When deoxygenated, blood behaves as an effective susceptibility contrast agent. Changes in brain oxygenation can be monitored using gradient-echo echo-planar imaging. With this technique, difference images also demonstrate that blood oxygenation is increased during periods of recovery from respiratory challenge. © 1991 Academic Press, Inc.



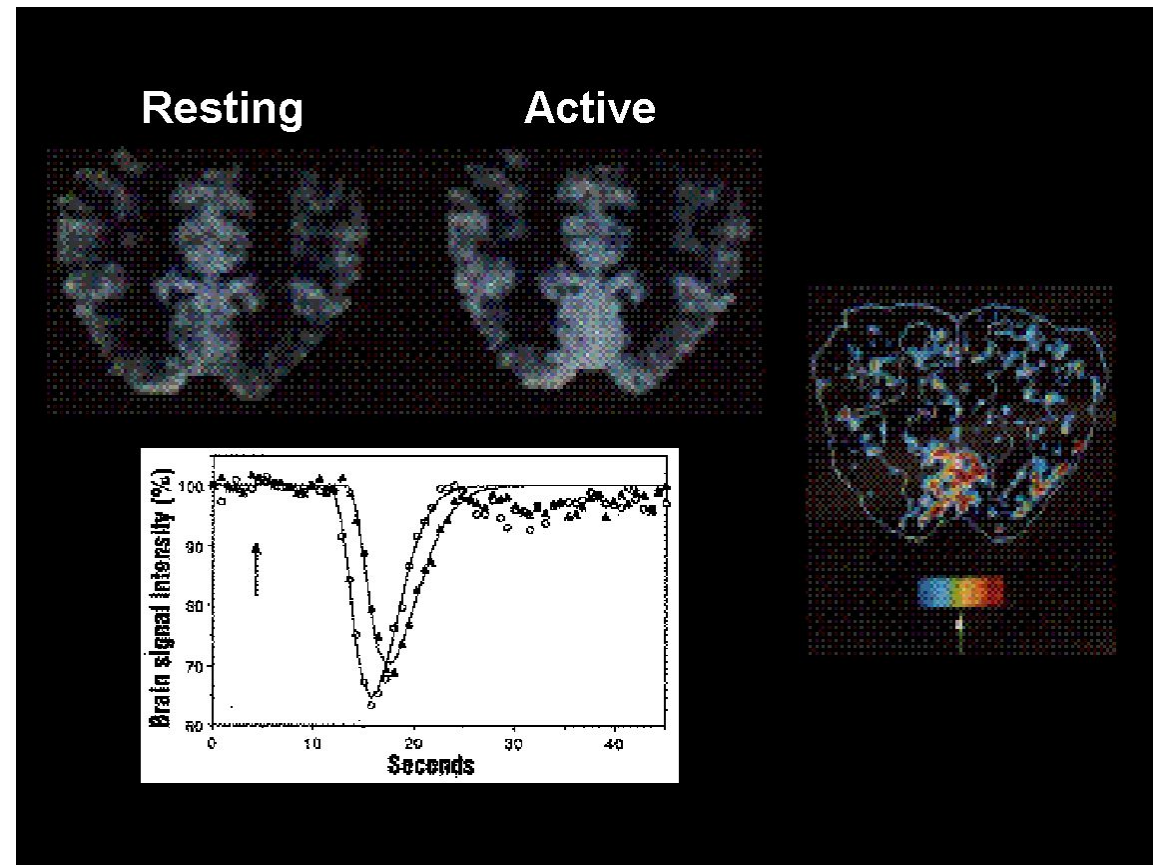
R. Turner, D. LeBihan, C.T.W. Moonen, D. Despres, J. Frank, Magn. Reson. Med, 22, 159-166 (1991)

Five Key Factors For The Emergence of Functional MRI

1. **Magnetic properties of red blood cells**
2. **Activation related hemodynamic changes**
3. **Spatial scale of brain activation**
4. **Echo Planar Imaging**
5. **Prevalence of MRI scanners**

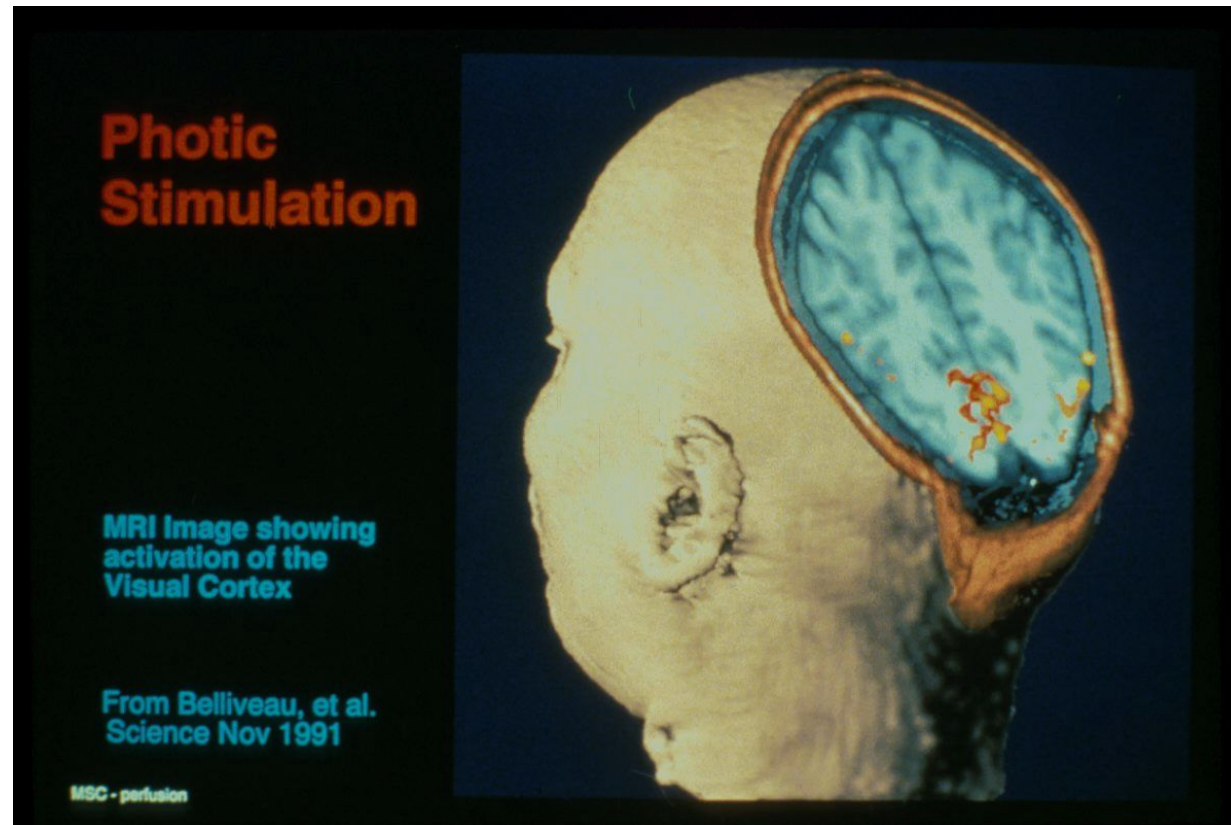
The First Functional MRI Results (MGH)

Susceptibility Contrast agent bolus injection and time series collection of T2 - weighted images



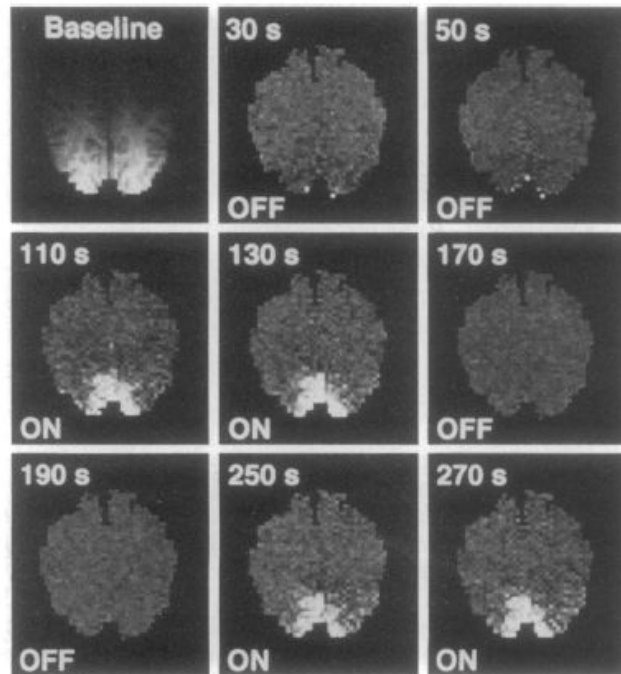
The First Functional MRI Results (MGH)

Susceptibility Contrast agent bolus injection and time series collection of T2 - weighted images



The MGH Gang





K. K. Kwong, et al, (1992) "Dynamic magnetic resonance imaging of human brain activity during primary sensory stimulation." *Proc. Natl. Acad. Sci. USA.* **89**, 5675-5679.

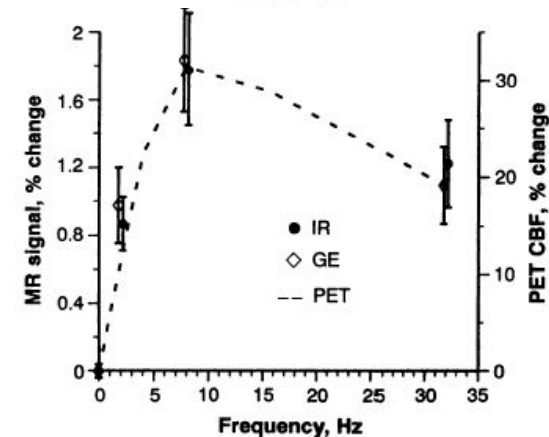
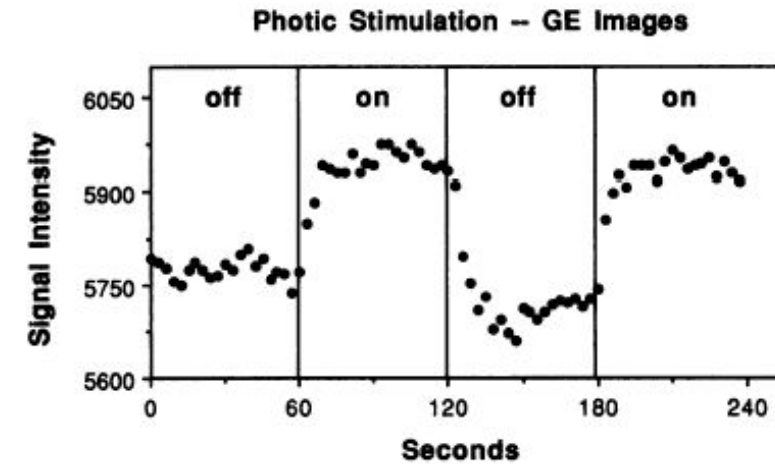
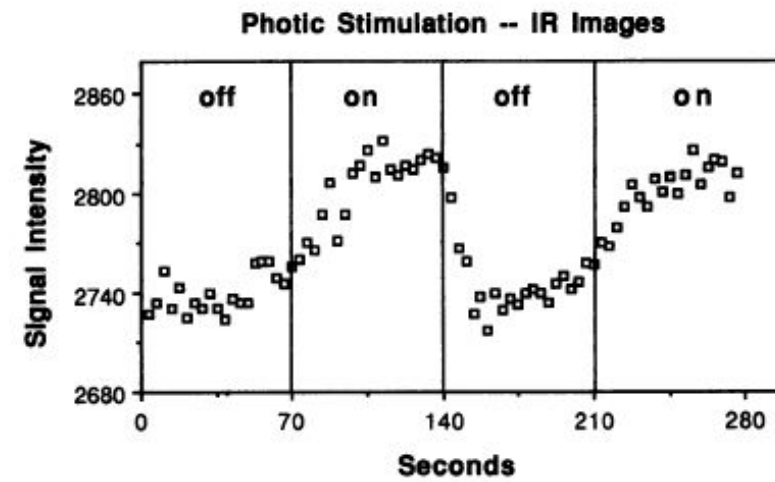
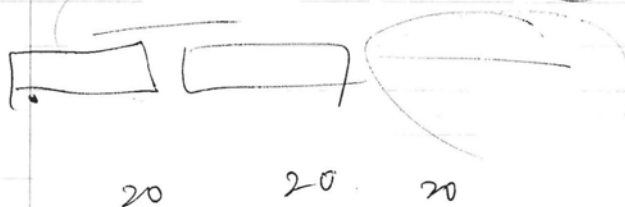
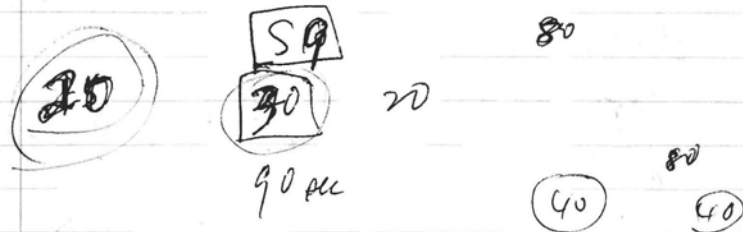


photo shi. 5 in GP
~~GR~~
 IR

GR 350
 70 sec shin
 disday = 2 30 pre 40 post

IR 3.0 TR 40 pre 40 post
 disday = 2
 TI = 1.05 s.



10 cm. slice cardiac.
 scanning
 spillover
 irstim. pre 23 5-8 13 14 16 18 19 25-29 (16 together)
 irstim. pro 34-38 40-44 49-65 67-80 (44 together)
 Avg them (with sev avg x51v)
 get mirstim. avg (save them)

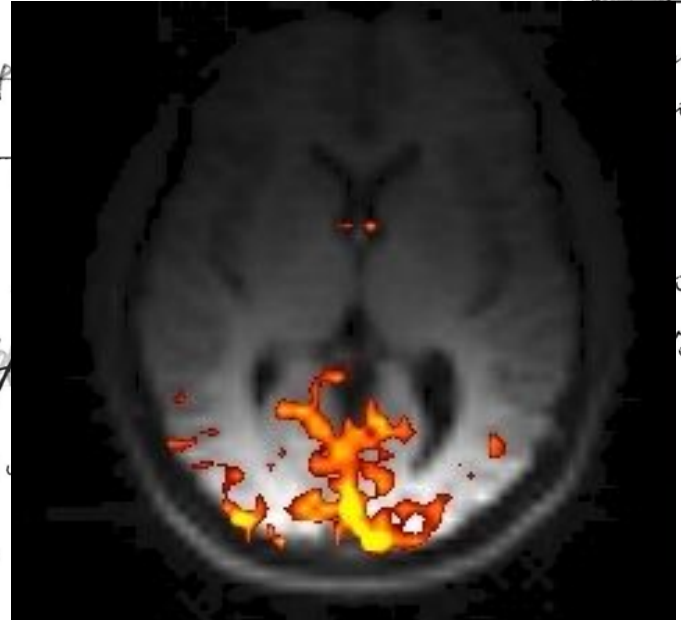
10 cm. slice cardiac
 TR = 2.55 TE = 4.0
 GR TA = 109 RA = 350 7106
 MAY 9, 91
 Michelle

3.0 on 4.0 on
 GR-stim. dat gestim. pre 3-30 (28)
 gestim. pro 33-70 (38) 30
 IR RA TA ~~gestim. avg~~ gestim. sub 20
 370 102 7106 2.3

TR = 35 TI = 1100 ms TE = 42

40 → 40
 30 50

IR Image 66
 jump up.



irstim.
 irstim.
 irstim.
 irstim.
 irstim.
 irstim. sub (45 → including 42)

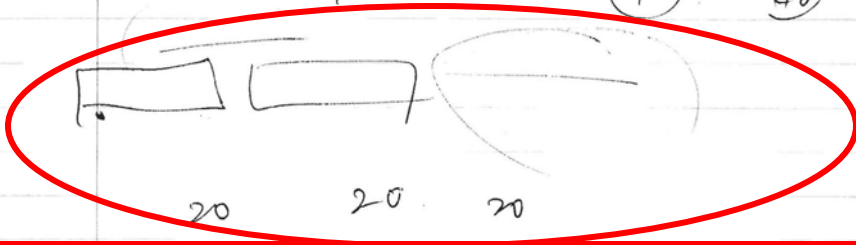
photo shi. 5 in GP

~~GR~~
IR

GR 3.50
70 sec shin
disday = 2 30 pre 40 post

IR 3.0 TR 40 pre 40 post
disday = 2
TI = 1.05 s.

20 59 20 80
30 20 80
90 sec 40 40



**The original block design
paradigm**

Spillover
irstim. pre 34-38 40-47 49-65 67-80 (44 together)
Avg them (with sev avg x51v)
get mirstim. avg (save them)

10 cm. slice carboc
TR = 2.55 TE = 4.0 MAY 9, 91

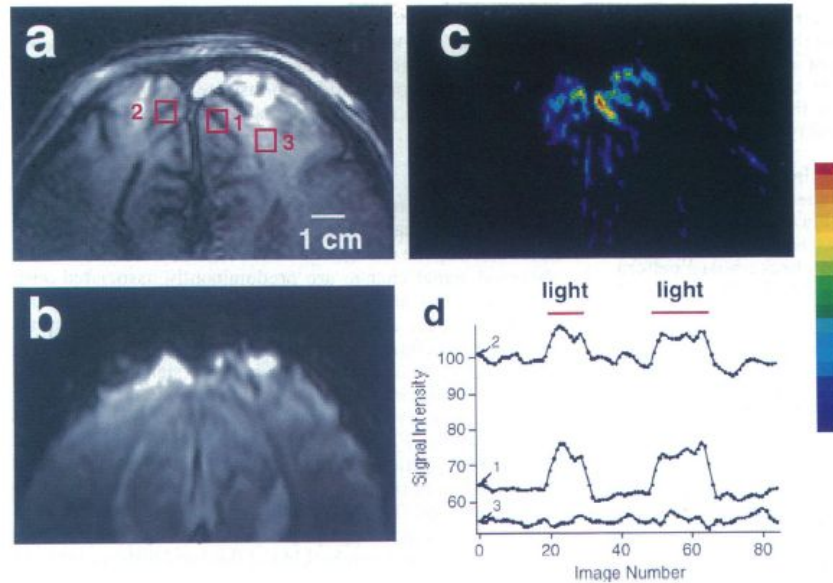
GE (BOLD) Contrast

3.0 on 4.0 on
GR-stim. dat gestim. pre 3-30 (28)
gestim. post 33-70 (38) 30
~~gestim. pre. avg~~
~~gestim. post. avg~~
IR 370 10 v 7106
gestim. sub 30
TR = 35 TI = 1100 ms TE = 4.2

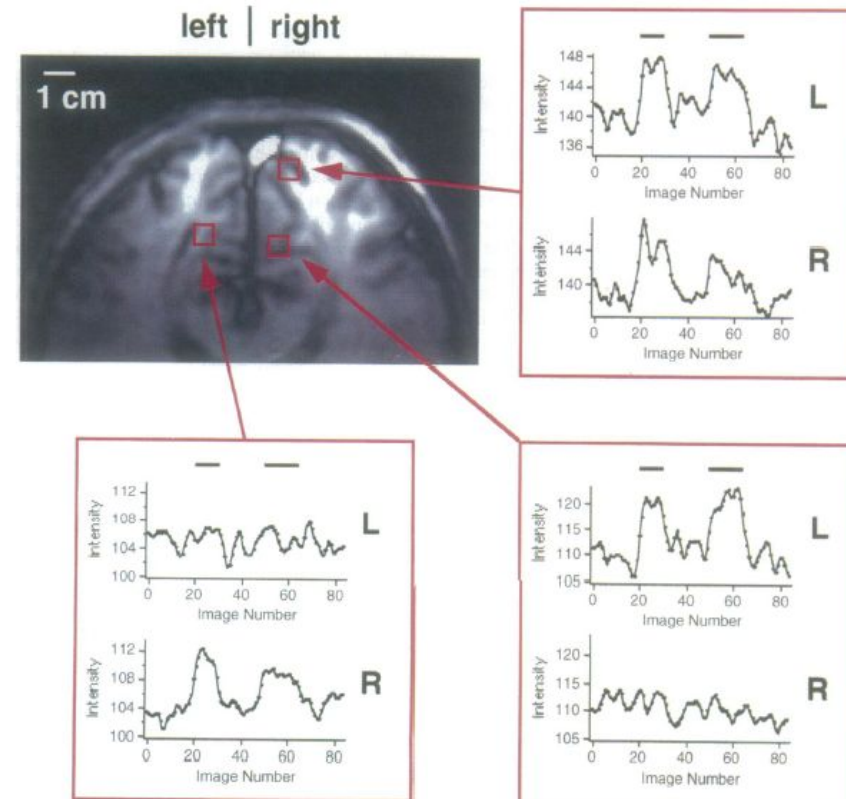
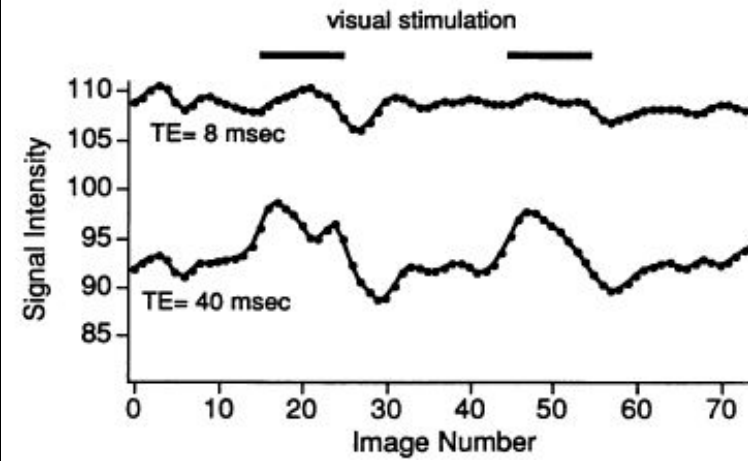
IR (CBF) Contrast

irstim. pre 3-30 (28) light off 30 in eye
light on rest.
~~irstim. pre 33-68 (44)~~
67-80 (47)
irstim. sub 1 who dived. only 2.90
change.
irstim. 74 (75) 4-30 33-65 67-80
irstim. sub (73) (subtracting from 4)
irstim. s 2-5 7 10-17 19-50
pre (28) post (28)
~~irstim. sub (45 → including 4)~~

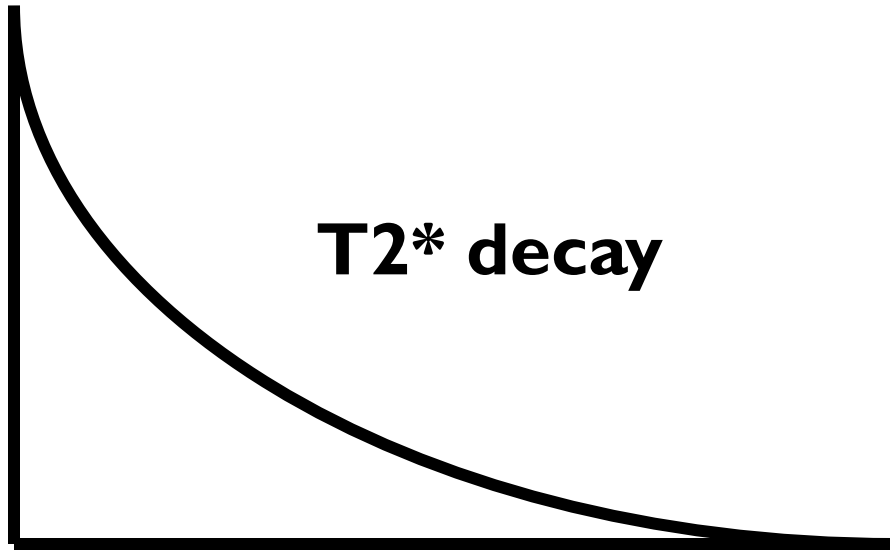
Multi-shot results at 4T, U. Minnesota.



S. Ogawa, et al., (1992) "Intrinsic signal changes accompanying sensory stimulation: functional brain mapping with magnetic resonance imaging." *Proc. Natl. Acad. Sci. USA.* **89**, 5951-5955.

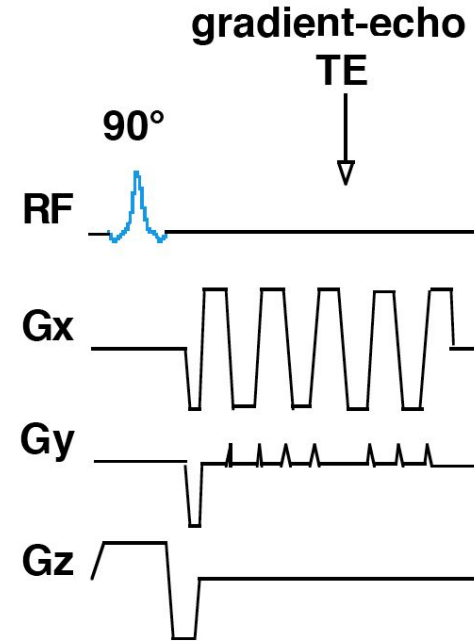


Single Shot Echo Planar Imaging (EPI)



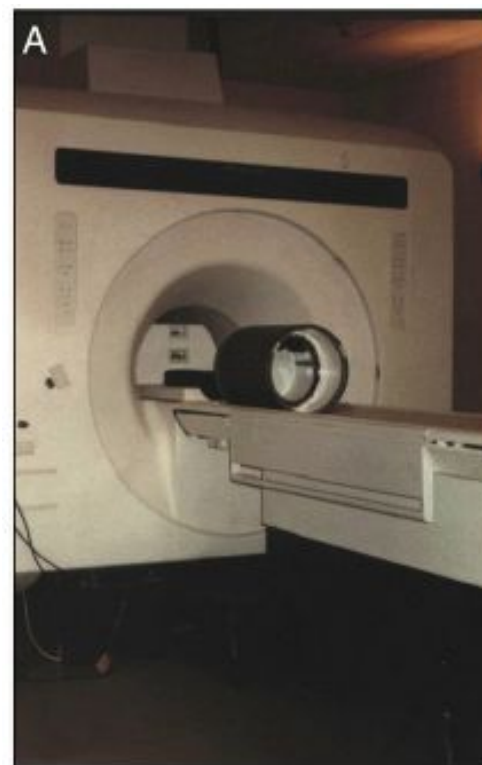
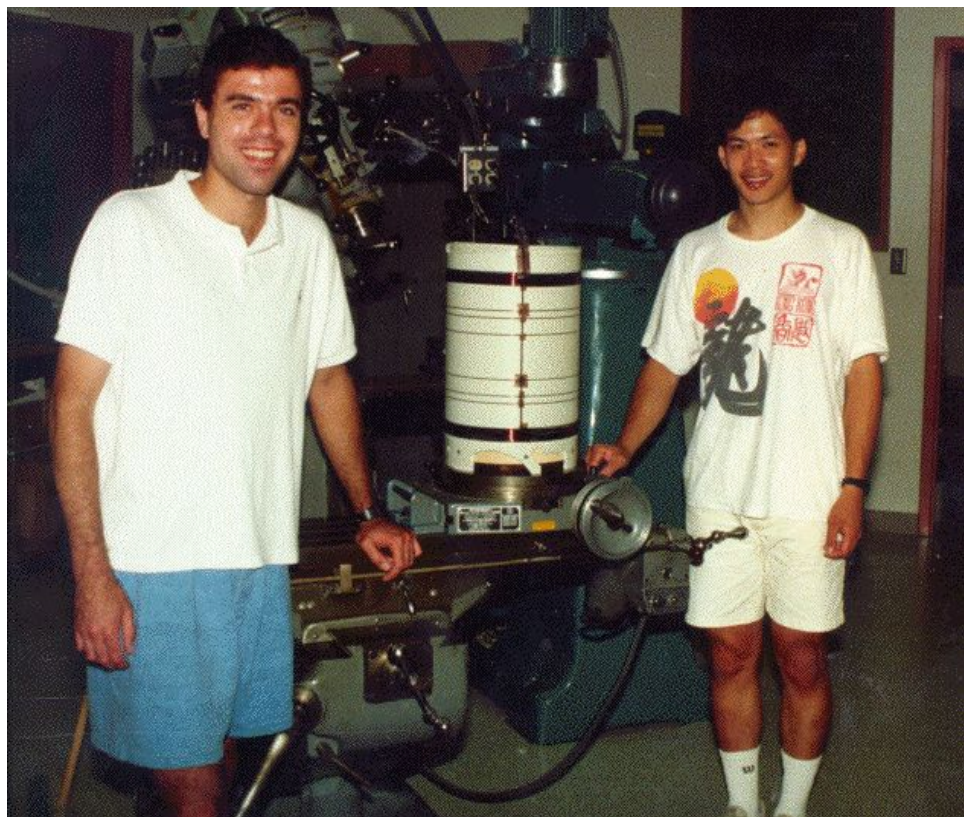
EPI Readout Window

≈ 20 to 40 ms

[illegible]

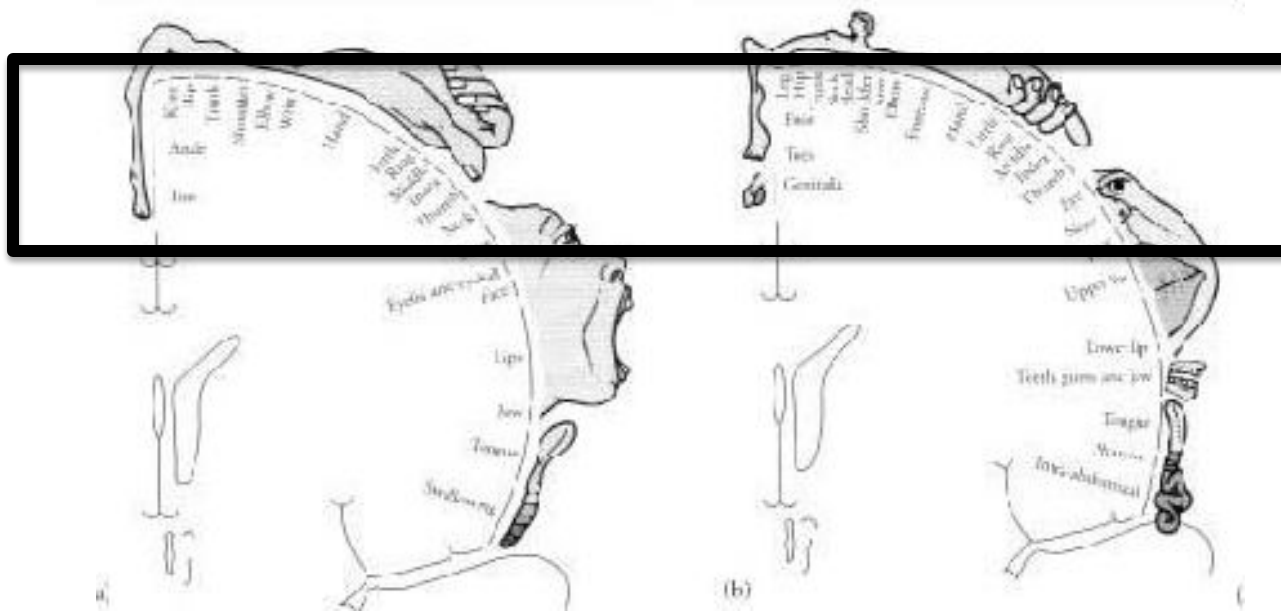
First Fast Imaging Approaches

- 1. MGH:ANMR retrofitted resonant gradient system with EPI**
- 2. Minnesota: Standard gradients with Multi-shot with navigator echoes**
- 3. MCW: local low-inductance gradient coil with EPI**



August, 1991

Initially could only do one slice...



2.5 cm !

TR = 2 sec

TE = 50 ms

One slice

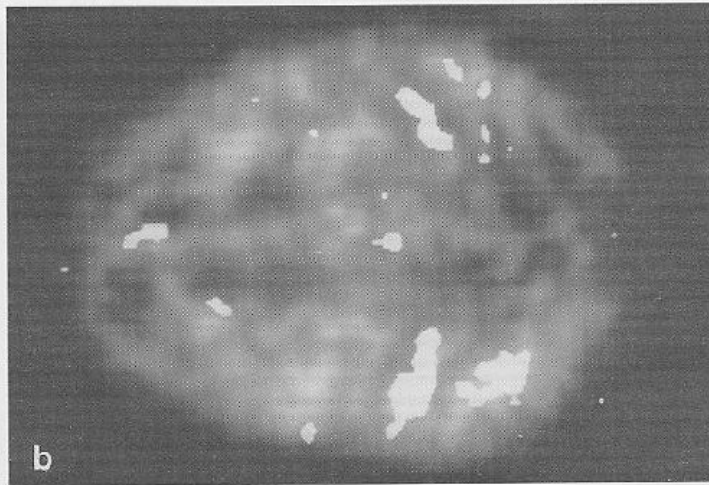
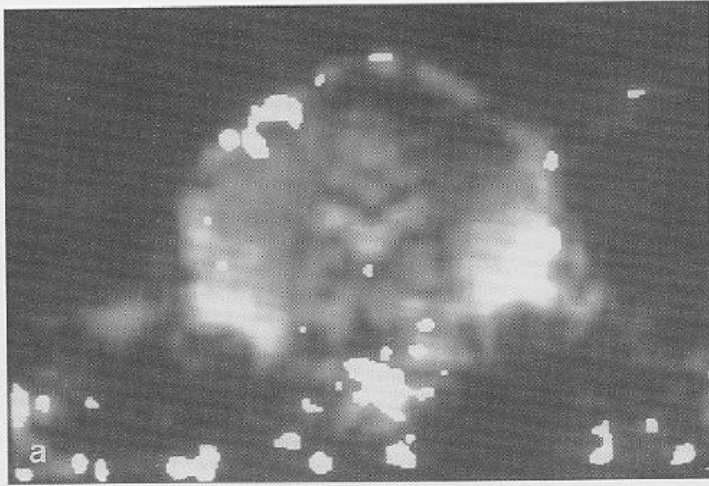
In plane 3.75 x 3.75

One little known fact...

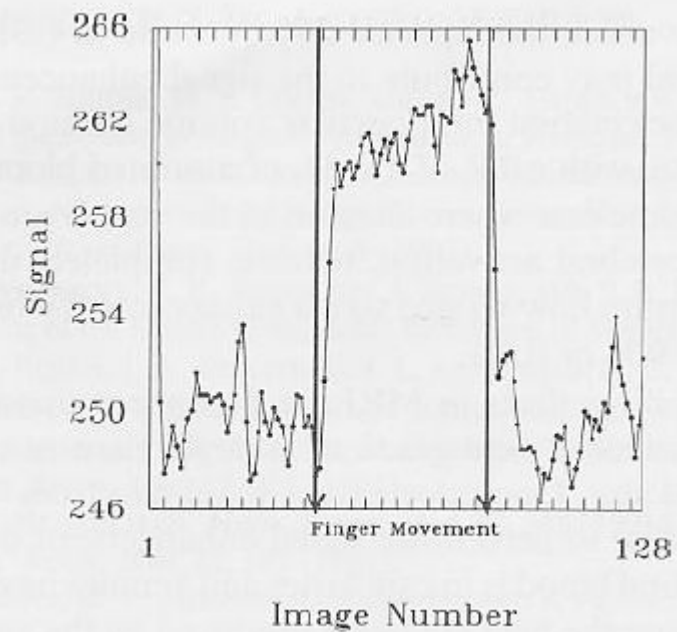
We didn't even need a gradient coil:

EPI at 5mm x 5mm x 5mm was quite possible using 100 amp gradient amplifiers and the whole body gradient coils...

Every scanner in the world in 1991 could have performed EPI-based fMRI at low resolution.



P. A. Bandettini, et al., (1992)
"Time course EPI of human brain
function during task activation."
Magn. Reson. Med 25, 390-397.



Ogawa predicted fMRI but got the sign wrong...

“...we expect this oxygenation-sensitive contrast could be used to monitor regional oxygen usages in the brain. When some region in a brain is much more active than other regions, the **active region could show darker lines in the image because of the increased level of deoxyhemoglobin resulting from higher oxygen consumption.”**

“Therefore, in addition to the anatomy of the brain, one aspect of its physiology can be studied by the MRI of water”

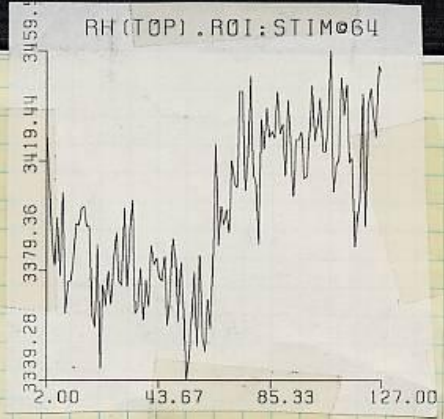
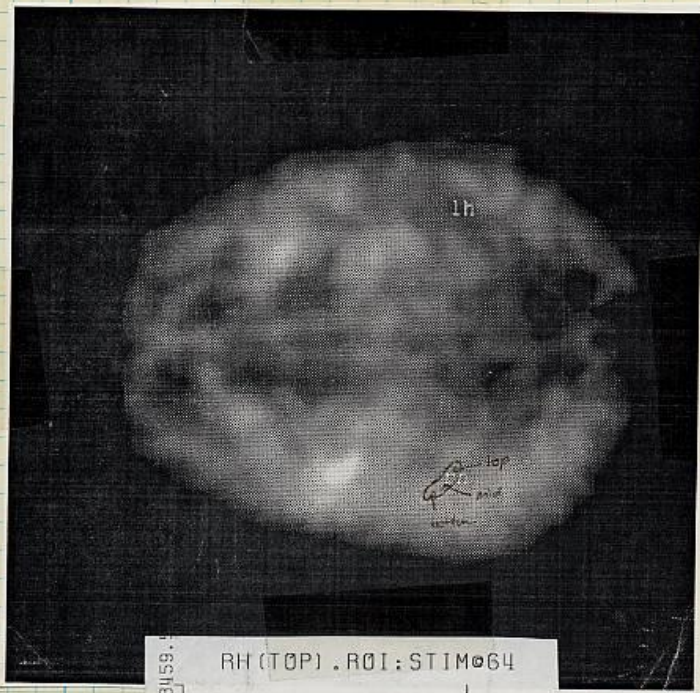
Oxygenation-Sensitive Contrast in Magnetic Resonance Image of Rodent Brain at High Magnetic Fields, Seiji Ogawa, Tso-Ming Lee, Asha S. Nayak, and Paul Glynn. **Magnetic Resonance in Medicine** 14, 68-78 (1990).

18
9-16-91

Results from dH61 (sig ↑ upon stim?!!)

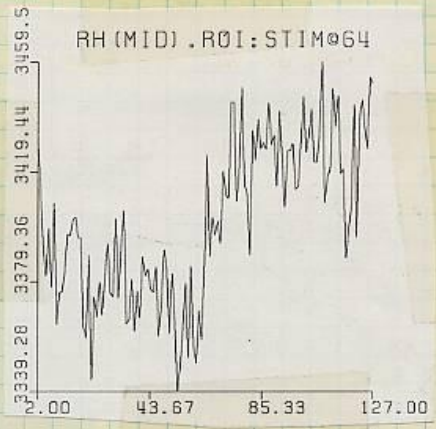
Experiment 1

Rest until 6? then move right fingers

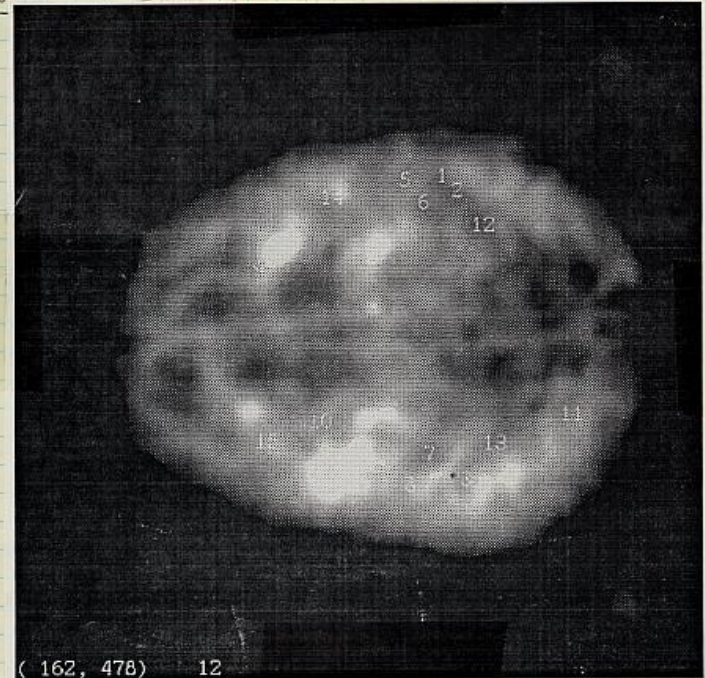


19

9-16-91



ROI's from p17





199

1

Focal physiological uncoupling of cerebral blood flow and oxidative metabolism during somatosensory stimulation in human subjects

(positron emission tomography)

PETER T. FOX^{*†‡} AND MARCUS E. RAICHLE^{*†}

^{*}Department of Neurology and Neurological Surgery (Neurology), [†]Department of Radiology (Radiation Sciences), and The McDonnell Center for Studies of Higher Brain Function, Washington University School of Medicine, St. Louis, MO 63110

Communicated by Oliver H. Lowry, October 7, 1985

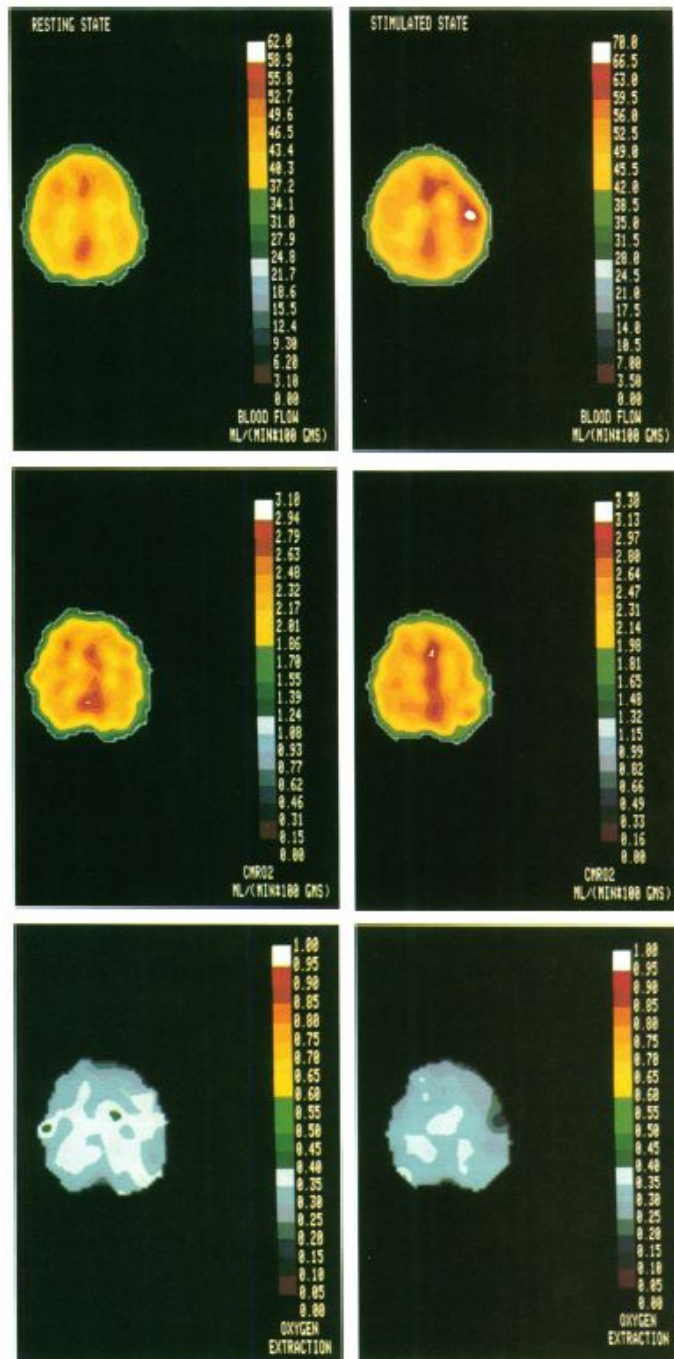
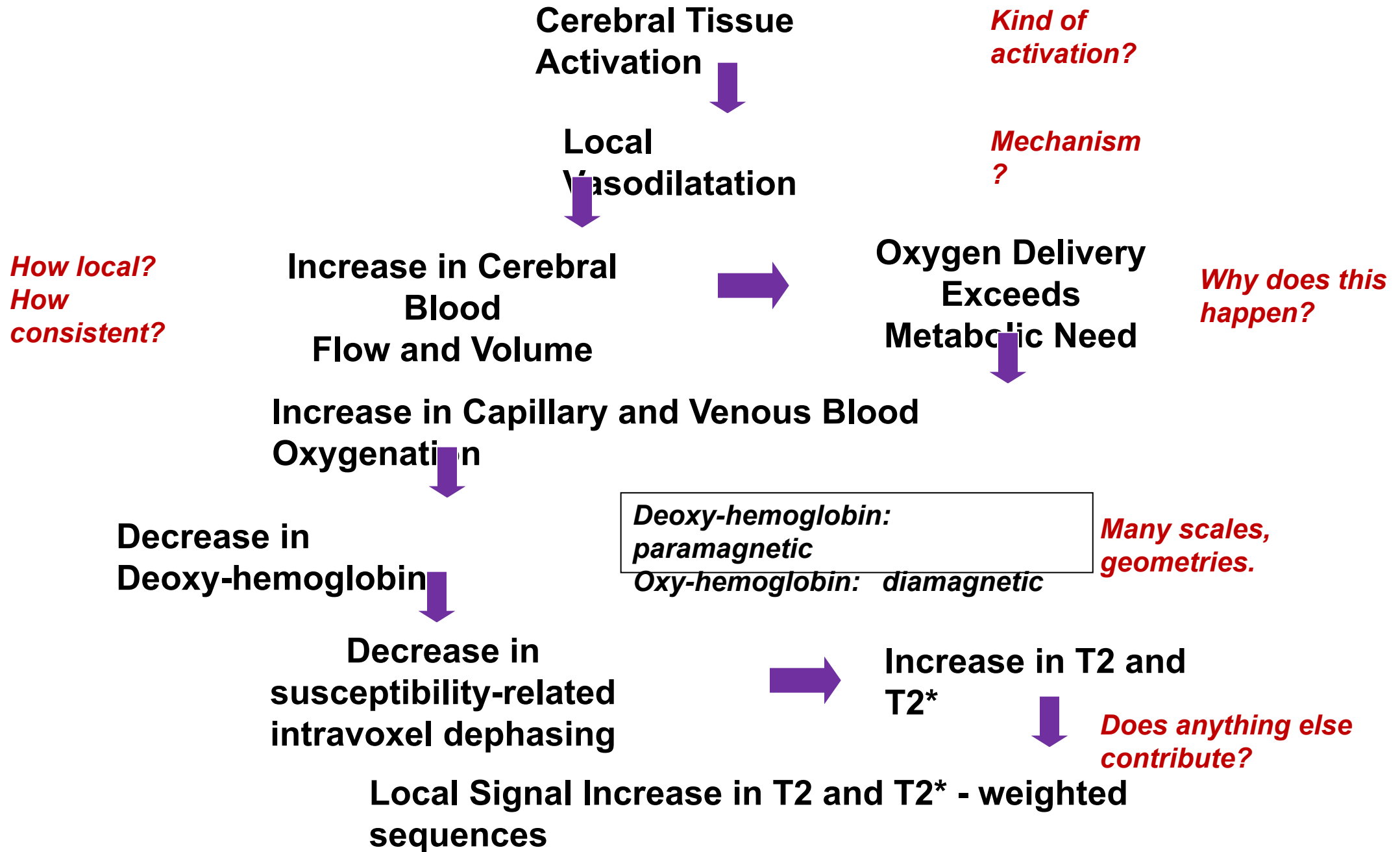
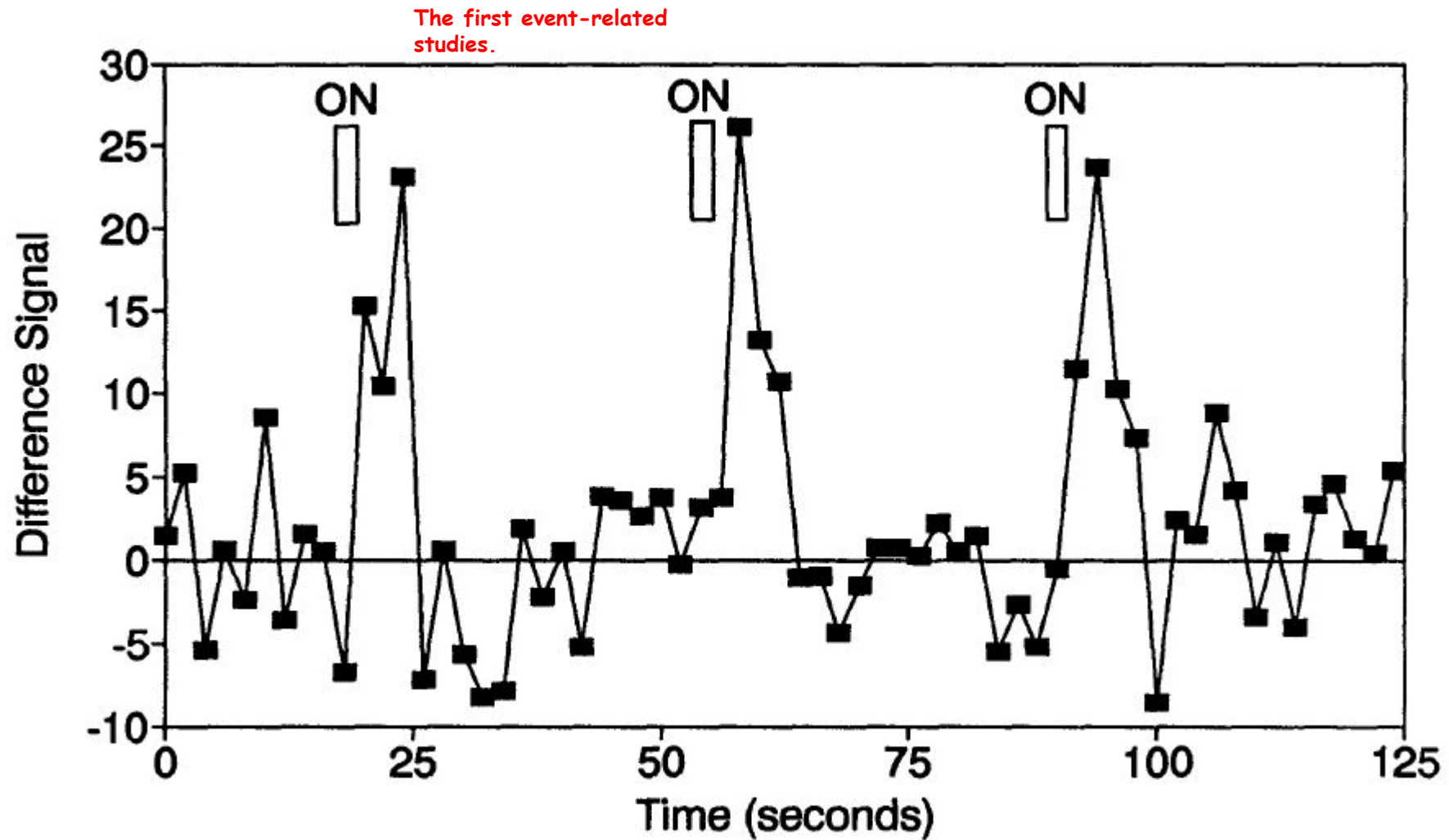


FIG. 1. Physiological uncoupling of brain blood flow and metabolism. (*Left*) Resting-state measurements. (*Right*) Stimulated-state measurements (unilateral vibrotactile stimulation of the fingers). All images are from a single subject's scanning session and pass through the same brain plane. Color scales are linear with the maxima set at a fixed multiple (1.6) of the global average, to facilitate visual comparisons (16). During specific somatosensory stimulation a marked focal increase in CBF (29% of mean, nine subjects, three trials per subject) was produced in the contralateral sensorimotor cortex. The observed increase in the CMRO₂ was much smaller (5% of mean, nine subjects, three trials per subject) and failed to attain significance. This physiological uncoupling of CBF and CMRO₂ flow produced a highly significant decrease in the local OEF (–19% of mean), indicating that tissue Po₂ (and probably pH) rose during stimulation. Note that, although the data were analyzed as contralateral/ipsilateral ratios (see text and Tables 1–4), the disparity between blood flow and metabolism was evident from the raw data and was not dependent on a particular strategy of analysis.





Blamire, A. M., et al. (1992).
"Dynamic mapping of the human
visual cortex by high-speed
magnetic resonance imaging."
Proc. Natl. Acad. Sci. USA
89: 11069-11073.

1992...Perfusion using Arterial Spin Labeling

MAGNETIC RESONANCE IN MEDICINE 23, 37-45 (1992)

Perfusion Imaging

JOHN A. DETRE,*† JOHN S. LEIGH,* DONALD S. WILLIAMS,‡
AND ALAN P. KORETSKY ‡§

**Metabolic Magnetic Resonance Research Center and Department of Biochemistry and Biophysics,
University of Pennsylvania School of Medicine, Philadelphia, Pennsylvania 19104; and*
‡*Pittsburgh NMR Center for Biomedical Research and §Department of Biological Sciences,
Carnegie Mellon University, Pittsburgh, Pennsylvania 15213*

Received July 2, 1990; revised January 3, 1991

Measurement of tissue perfusion is important for the functional assessment of organs *in vivo*. Here we report the use of ^1H NMR imaging to generate perfusion maps in the rat brain at 4.7 T. Blood water flowing to the brain is saturated in the neck region with a slice-selective saturation imaging sequence, creating an endogenous tracer in the form of proximally saturated spins. Because proton T_1 times are relatively long, particularly at high field strengths, saturated spins exchange with bulk water in the brain and a steady state is created where the regional concentration of saturated spins is determined by the regional blood flow and regional T_1 . Distal saturation applied equidistantly outside the brain serves as a control for effects of the saturation pulses. Average cerebral blood flow in normocapnic rat brain under halothane anesthesia was determined to be $105 \pm 16 \text{ cc} \cdot 100 \text{ g}^{-1} \cdot \text{min}^{-1}$ (mean \pm SEM, $n = 3$), in good agreement with values reported in the literature, and was sensitive to increases in arterial pCO_2 . This technique allows regional perfusion maps to be measured noninvasively, with the resolution of ^1H MRI, and should be readily applicable to human studies. © 1992 Academic Press, Inc.



Proc. Natl. Acad. Sci. USA
Vol. 89, pp. 212–216, January 1992
Biophysics

Magnetic resonance imaging of perfusion using spin inversion of arterial water

(cerebral blood flow/adiabatic fast passage/hypercarbia/rat brain/cold injury)

DONALD S. WILLIAMS*, JOHN A. DETRE^{†‡}, JOHN S. LEIGH[†], AND ALAN P. KORETSKY*[§]

*Pittsburgh Nuclear Magnetic Resonance Center for Biomedical Research, and [§]Department of Biological Sciences, Carnegie Mellon University, Pittsburgh, PA 15213; and [†]Metabolic Magnetic Resonance Research Center, Department of Radiology, and [‡]Department of Neurology, University of Pennsylvania School of Medicine, Philadelphia, PA 19104

Communicated by Mildred Cohn, September 19, 1991

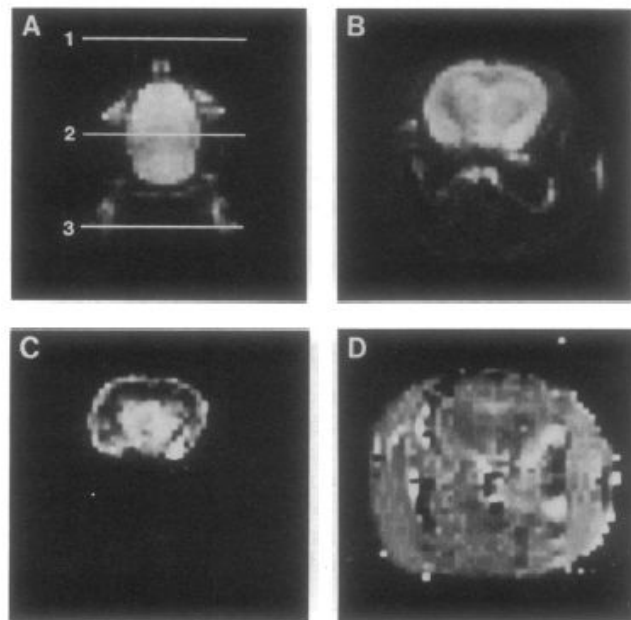


FIG. 2. (A) Coronal image of a rat head. The resonance planes for radiofrequency used for spin inversion by AFP for control and inversion images are indicated by 1 and 3, respectively, and plane 2 is the detection plane. (B) Control transverse image from the detection plane (plane 2 in A). (C) Difference image between control and inversion images. (D) T_{1app} image.

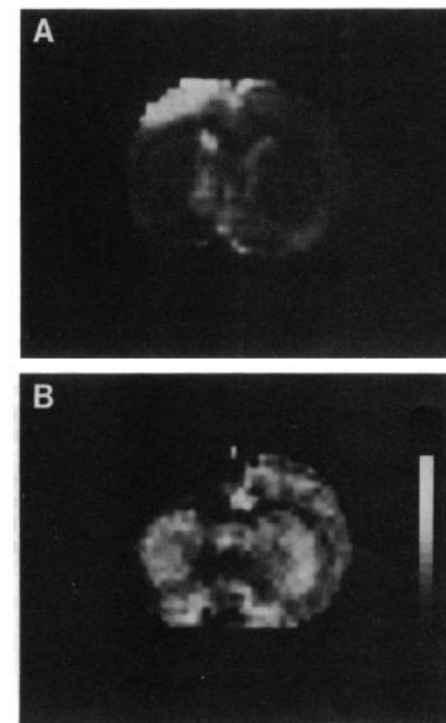
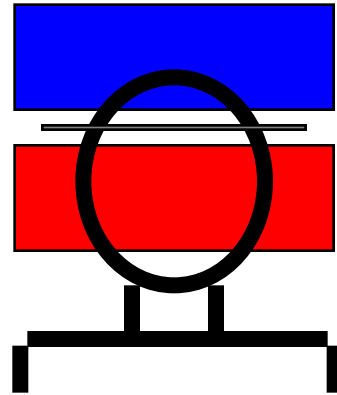


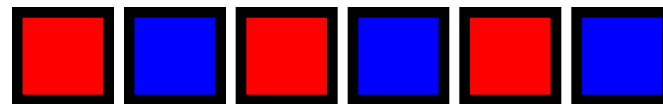
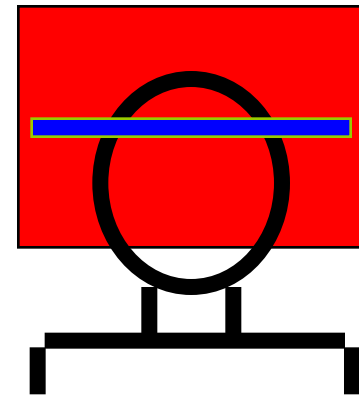
FIG. 5. Comparison of conventional MRI and perfusion imaging of a rat brain subjected to a regional cold injury. (A) Conventional T_2 -weighted image ($TE = 60$ ms, $TR = 2$ s). The injured region shows up as hyperintensity due to a longer T_2 . (B) Perfusion image of the same slice. The grey scale is from 0 to $6 \text{ ml} \cdot \text{g}^{-1} \cdot \text{min}^{-1}$. The injured region is dark due to low flow.

Perfusion Contrast

EPISTAR

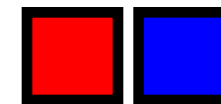


FAIR

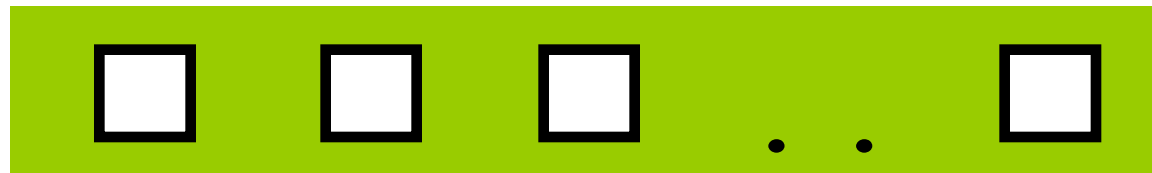


.

.



.



Perfusion
Time Series

TI (ms)

FAIR

EPISTAR

200

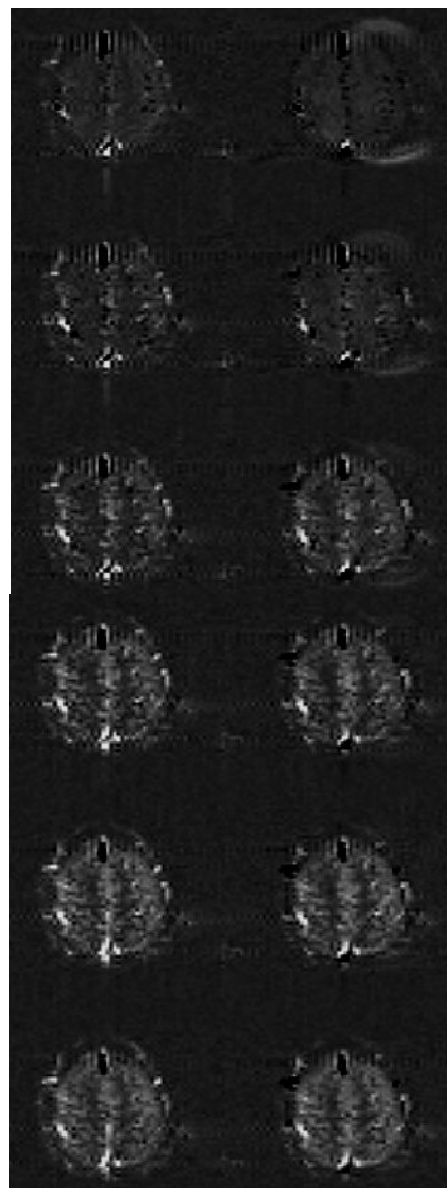
400

600

800

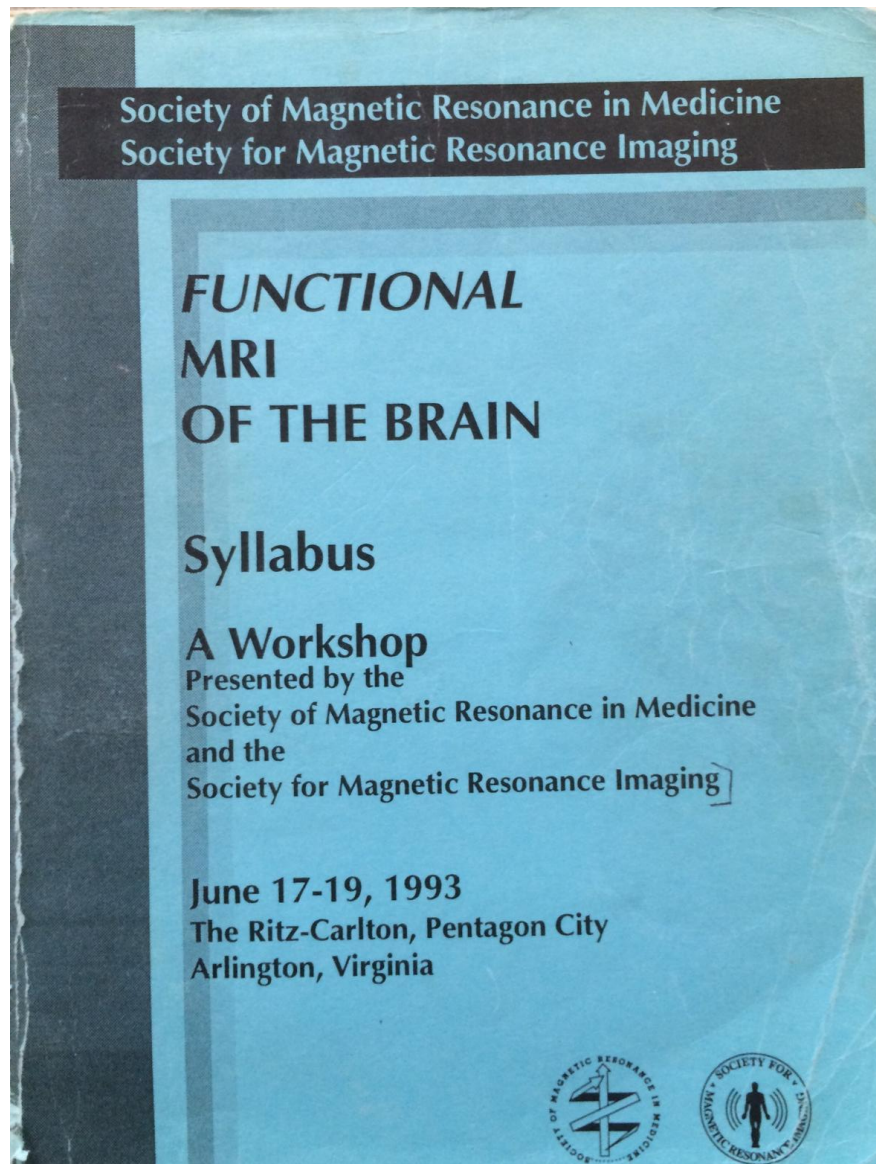
1000

1200



- **K. K. Kwong, et al, (1992)** “Dynamic magnetic resonance imaging of human brain activity during primary sensory stimulation.” **Proc. Natl.Acad. Sci. USA. 89, 5675-5679.**
- **S. Ogawa, et al., (1992)** “Intrinsic signal changes accompanying sensory stimulation: functional brain mapping with magnetic resonance imaging.” **Proc. Natl.Acad. Sci. USA. 89, 5951-5955.**
- **P.A. Bandettini, et al., (1992)** “Time course EPI of human brain function during task activation.” **Magn. Reson. Med 25, 390-397.**
- **Blamire, A. M., et al. (1992).** “Dynamic mapping of the human visual cortex by high-speed magnetic resonance imaging.” **Proc. Natl.Acad. Sci. USA 89: 11069-11073.**
- **Frahm, J., et al (1992)** “Dynamic MR Imaging of Human Brain Oxygenation During Rest and Photic-Stimulation.” **Journal of Magnetic Resonance Imaging, 2, 501-505.**

A proposed acronym...



Functional Neuroimaging with EPI: Sequence Issues

Robert Turner, Peter Jezzard, #Lucie Hertz-Pannier, #Denis Le Bihan, *David Feinberg

Laboratory of Cardiac Energetics, National Heart, Lung, and Blood Institute, and
#Diagnostic Radiology Department, Clinical Center, NIH, Bethesda, MD 20892

*Department of Radiology, NYU Medical Center, New York, NY

ABSTRACT

Freedom from motion artifact, comparatively good SNR, rapid multi-slice capability, and excellent time resolution make Echo-Planar Imaging an excellent choice for BOLD contrast MR functional neuroimaging. However, when the gradient echo version of EPI is used for this purpose, problems arise regarding image quality and interpretation. Large draining veins distant from active neural regions are the major confusing factor. At high enough static magnetic fields, spin-echo EPI can be used to obtain images showing local changes of blood oxygenation related to brain activation, in which draining veins have less effect. The ideal MRFN sequence will combine gradient-recalled echo and spin echo features, and thus be some variant of GRASE (GRAdient echo and Spin Echo).

The earliest successful magnetic resonance functional neuroimaging (MRFN) studies with BOLD contrast were based on the use of echo-planar imaging (EPI). The EPI technique, proposed by Mansfield in 1977 (4), allows the capture of a complete MR image in under 100 ms. Thus most motions in the body are frozen and motion artifact rarely appears. EPI relies on a very rapidly switched magnetic field gradient of large amplitude, and a fast data capture rate. Since these features were not considered necessary by most manufacturers of commercial MR systems until recently, the technique has been available only in a few pioneering laboratories. The technique normally uses a full 90 degree rf pulse for spin excitation, and hence provides a comparatively high single-shot signal/noise ratio (SNR), considering the large receiver bandwidth required. For brain imaging, with equal voxel size, an EPI image with 40 ms acquisition time has been found to have the same SNR as a FLASH image with optimized bandwidth taking 2 seconds to acquire. Faster FLASH images will have a poorer SNR than EPI. Low flip-angle variants of EPI (5) can of course provide much higher values of SNR/unit time, though this sacrifices SNR in each

Local Gradient Coil & 4T @NIH

FIG. 1

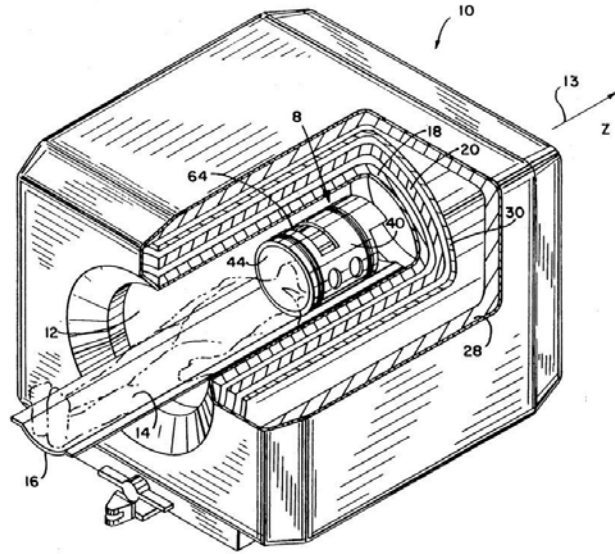
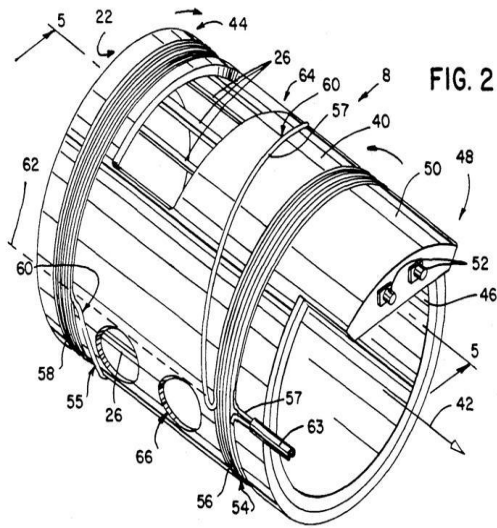


FIG. 2



Functional Mapping of the Human Visual Cortex at 4 and 1.5 Tesla Using Deoxygenation Contrast EPI

R. Turner, P. Jezzard, H. Wen, K. K. Kwong, D. Le Bihan, T. Zeffiro, R. S. Balaban

MRM 29:277-279 (1993)

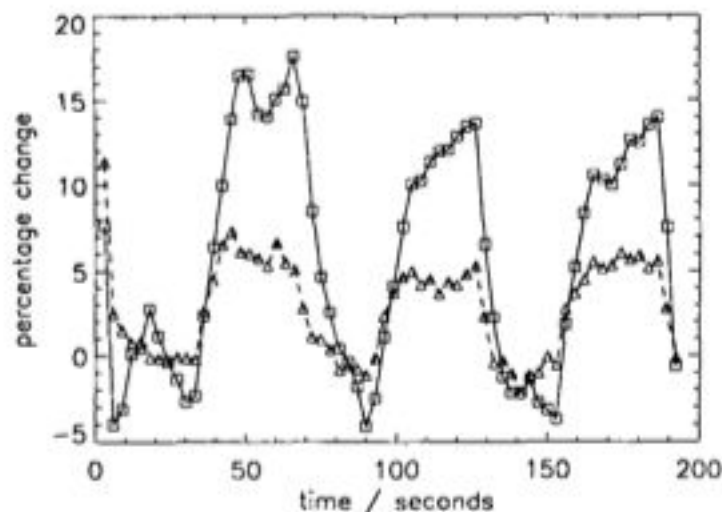
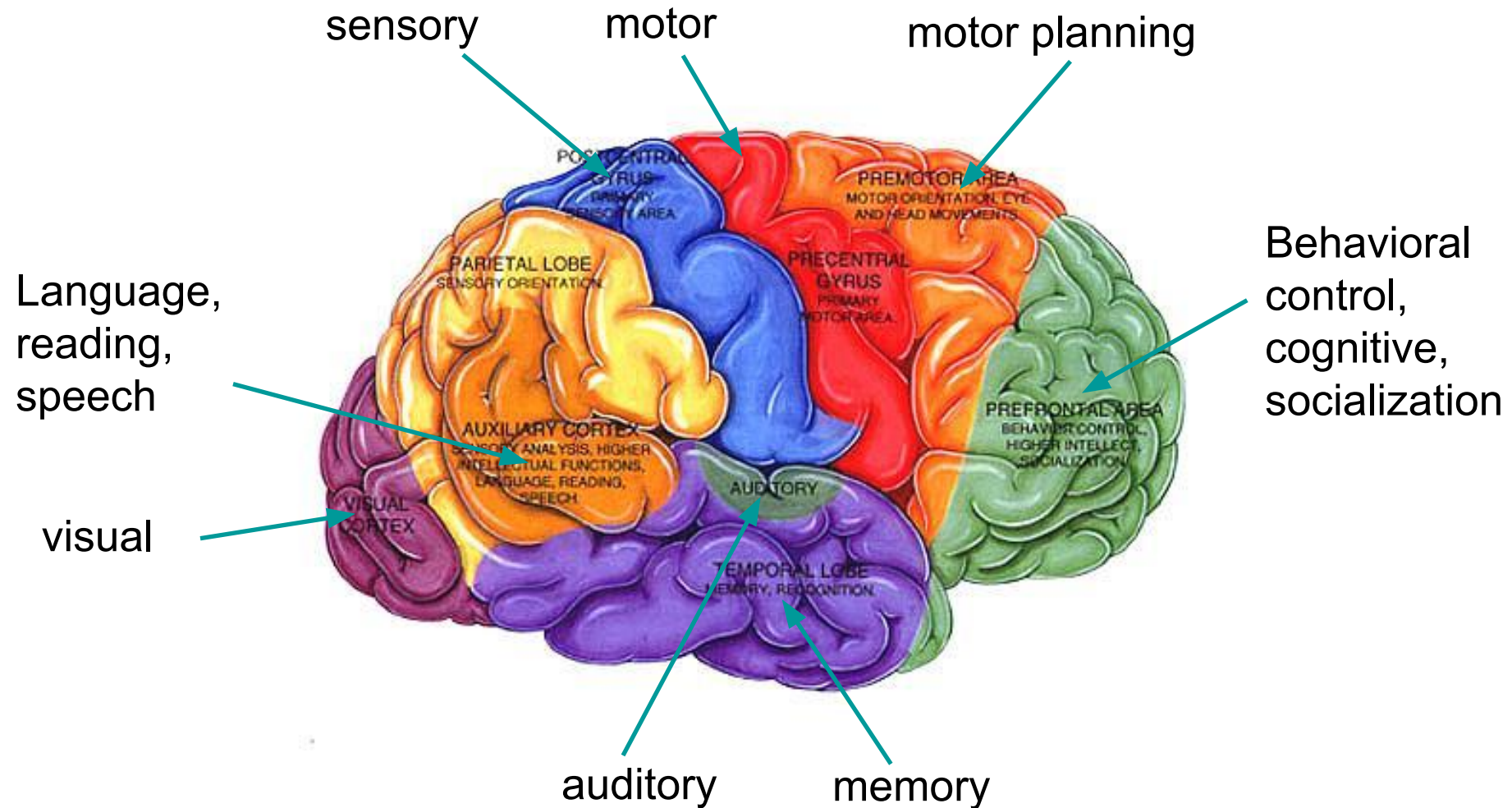


FIG. 2. Plot of fractional change in 4 T (squares) and 1.5 T (triangles) EPI image intensity versus time in the eight-voxel regions of interest in the visual cortex shown in Fig. 1, for a volunteer experiencing alternate 30-s periods of rest and photic stimulation. Details of acquisition for the 4 and 1.5 T data are described in the

Five Key Factors For The Emergence of Functional MRI

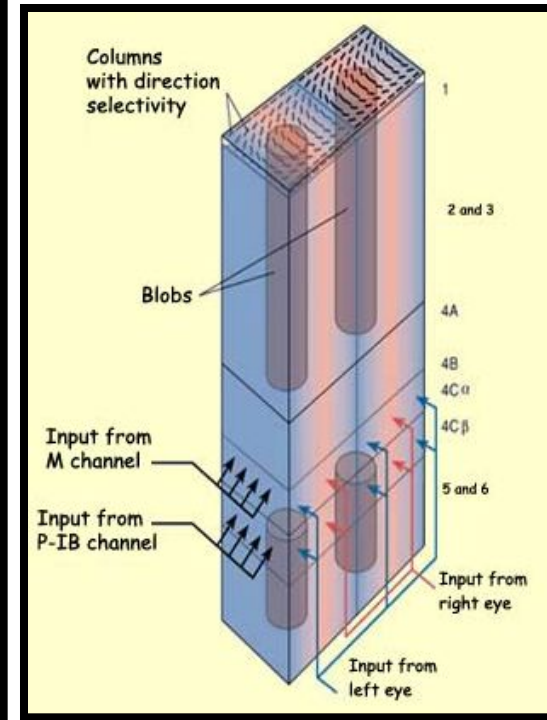
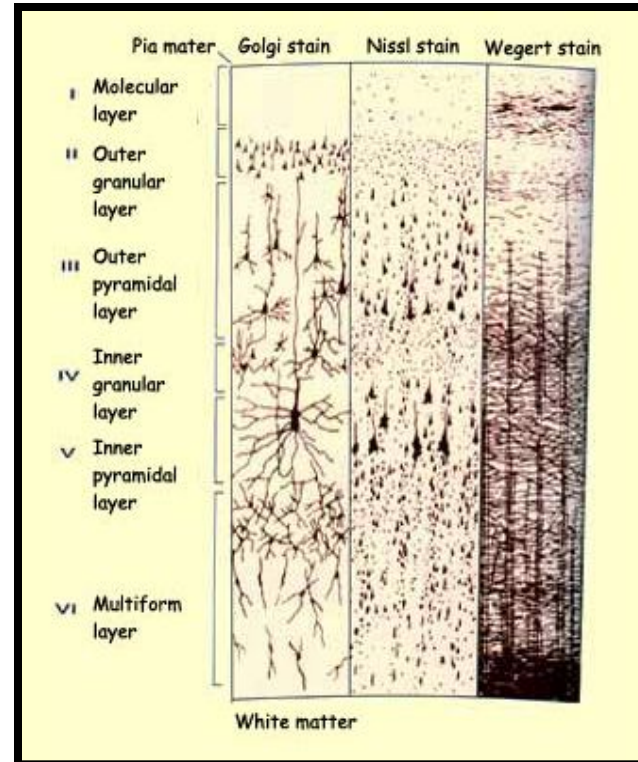
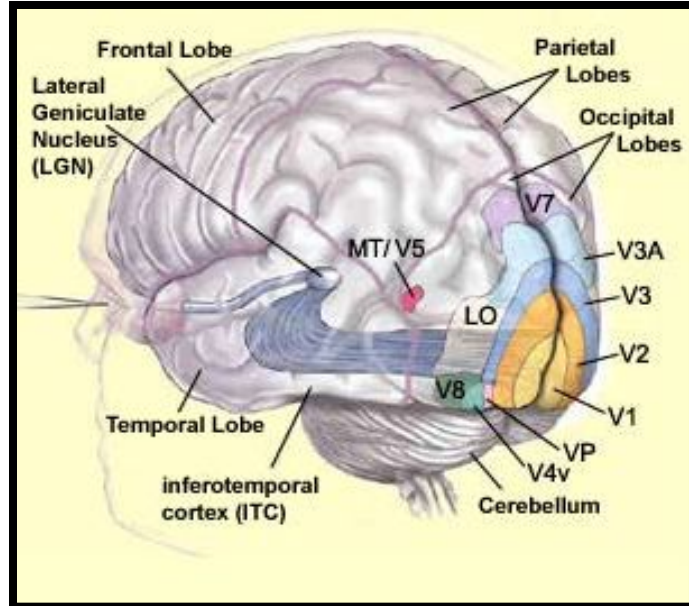
1. **Magnetic properties of red blood cells**
2. **Activation related hemodynamic changes**
3. **Spatial scale of brain activation**
4. **Echo Planar Imaging**
5. **Prevalence of MRI scanners**

Brain Function

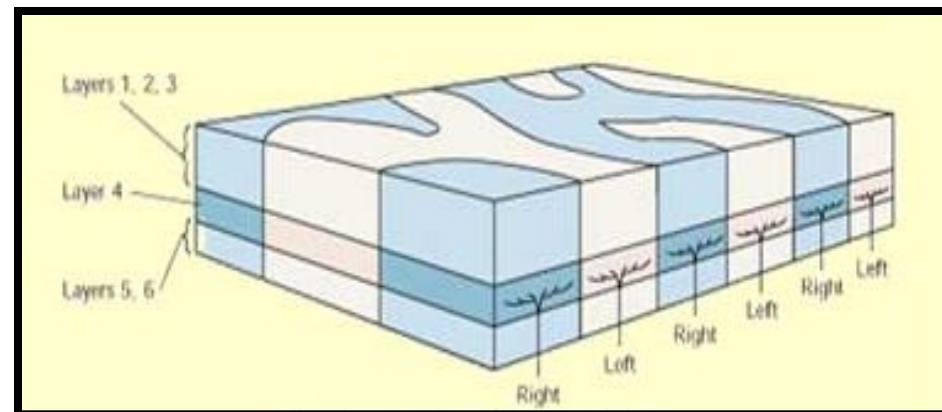




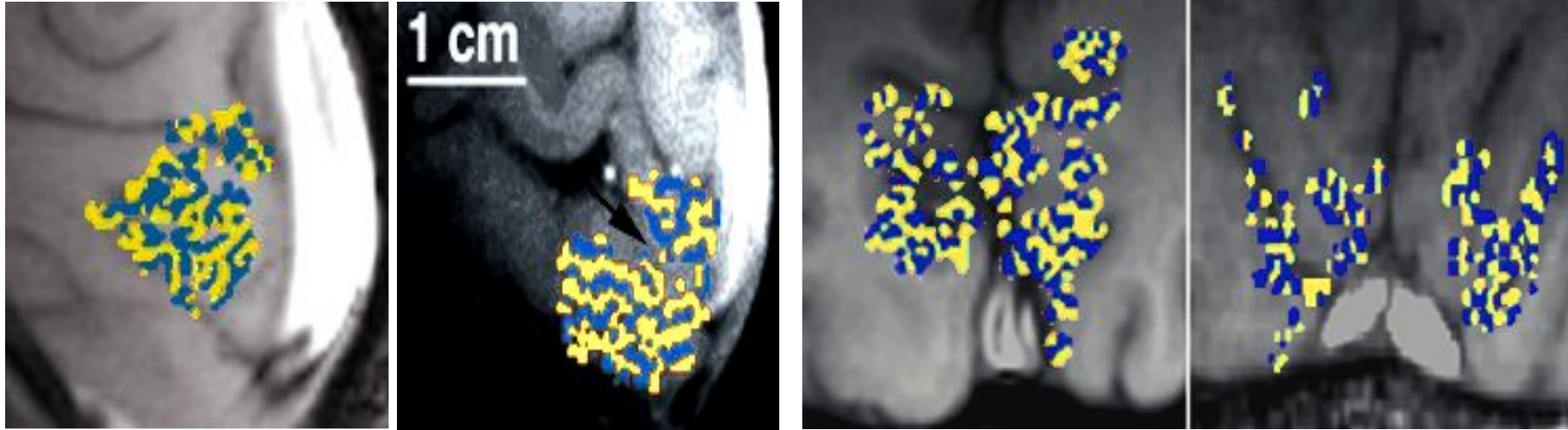
Visual Cortex Organization



<http://www.thebrain.mcgill.ca>

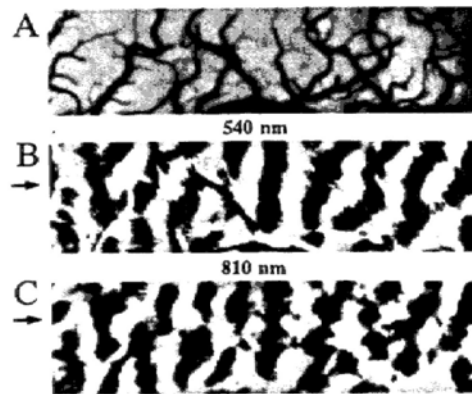


Ocular Dominance Column Mapping

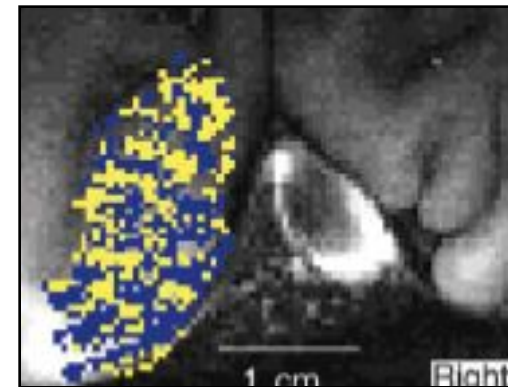


Menon, R. S., S. Ogawa, et al. (1997). *J Neurophysiol* 77(5): 2780-7.
0.54 x 0.54 in plane resolution

Optical Imaging

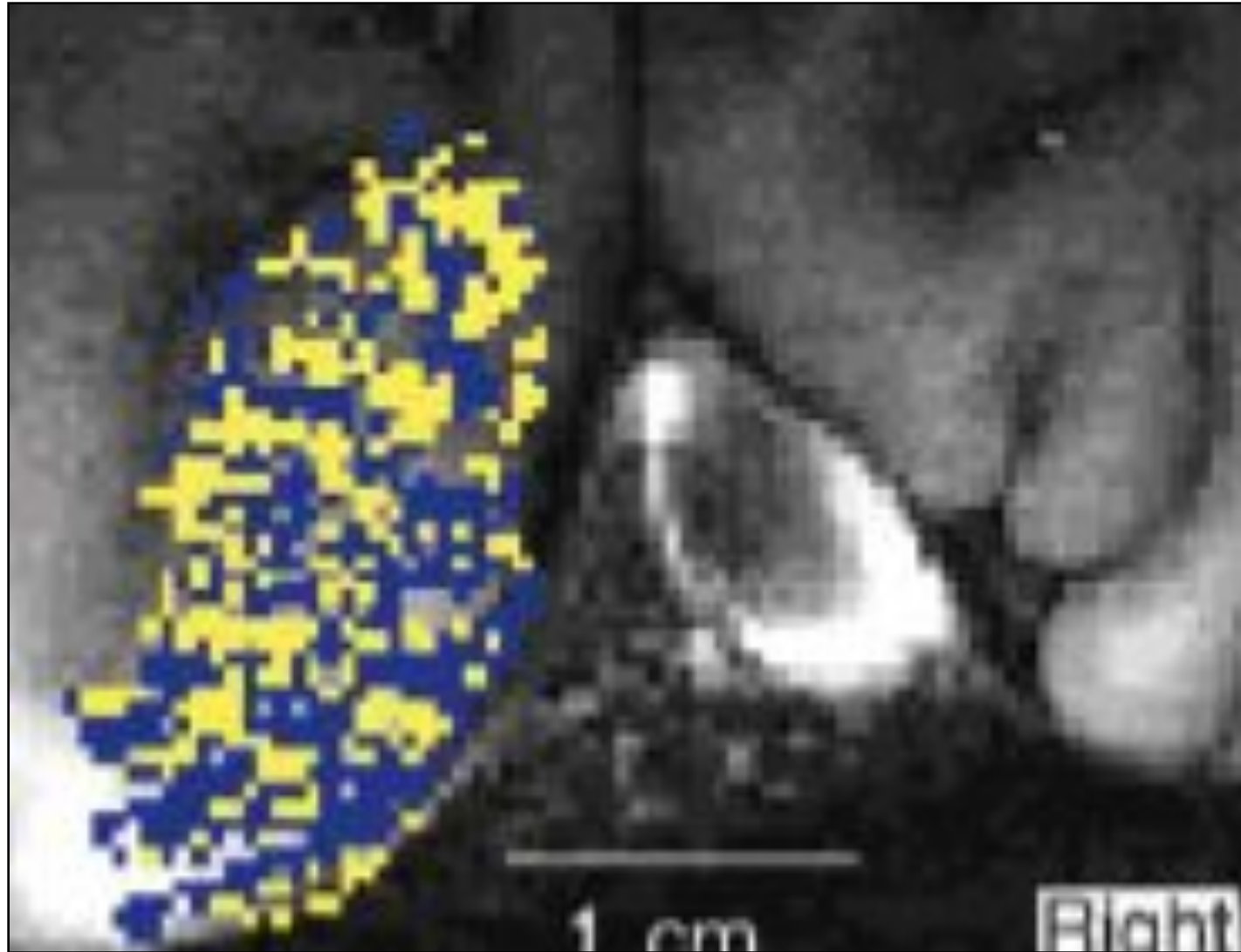


R. D. Frostig et. al, *PNAS* 87:
6082-6086, (1990).



Cheng, et al. (2001)
Neuron, 32:359-374

0.47 x 0.47 in plane resolution



Cheng, et al. (2001) Neuron,32:359-374

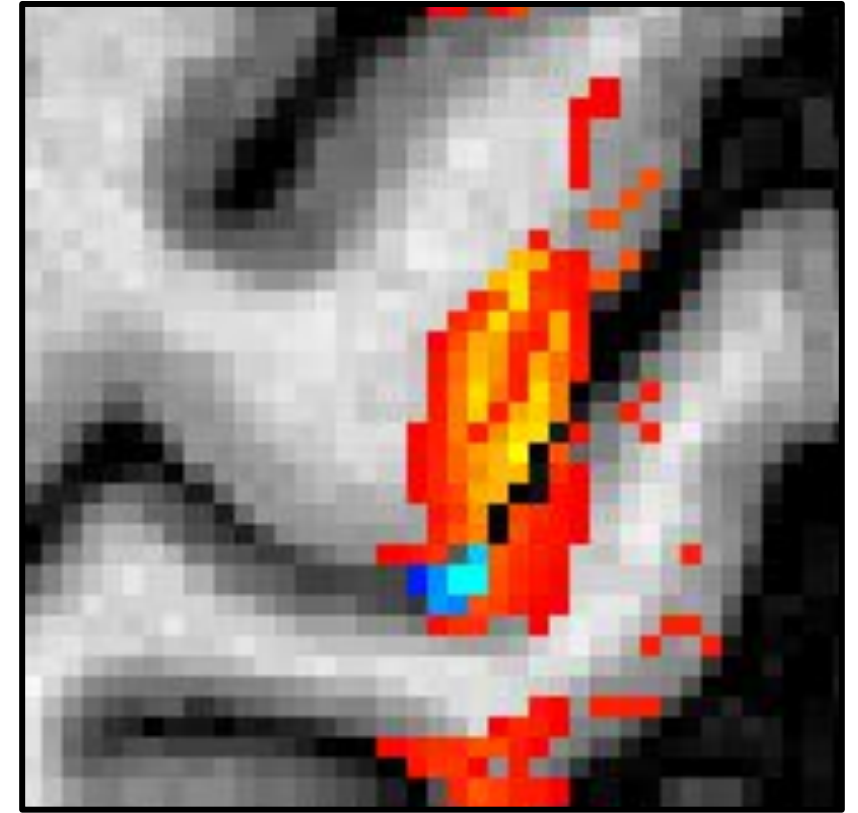
Functional Structure Changes < 0.8 mm



right tapping

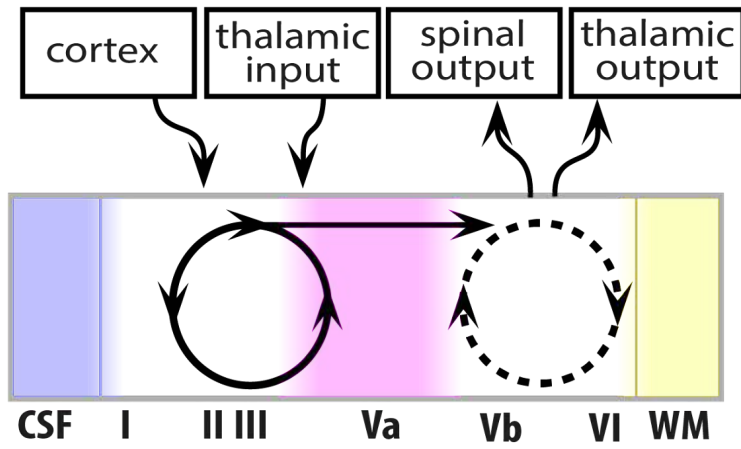


resol. ~~0.75~~ 0.75 mm

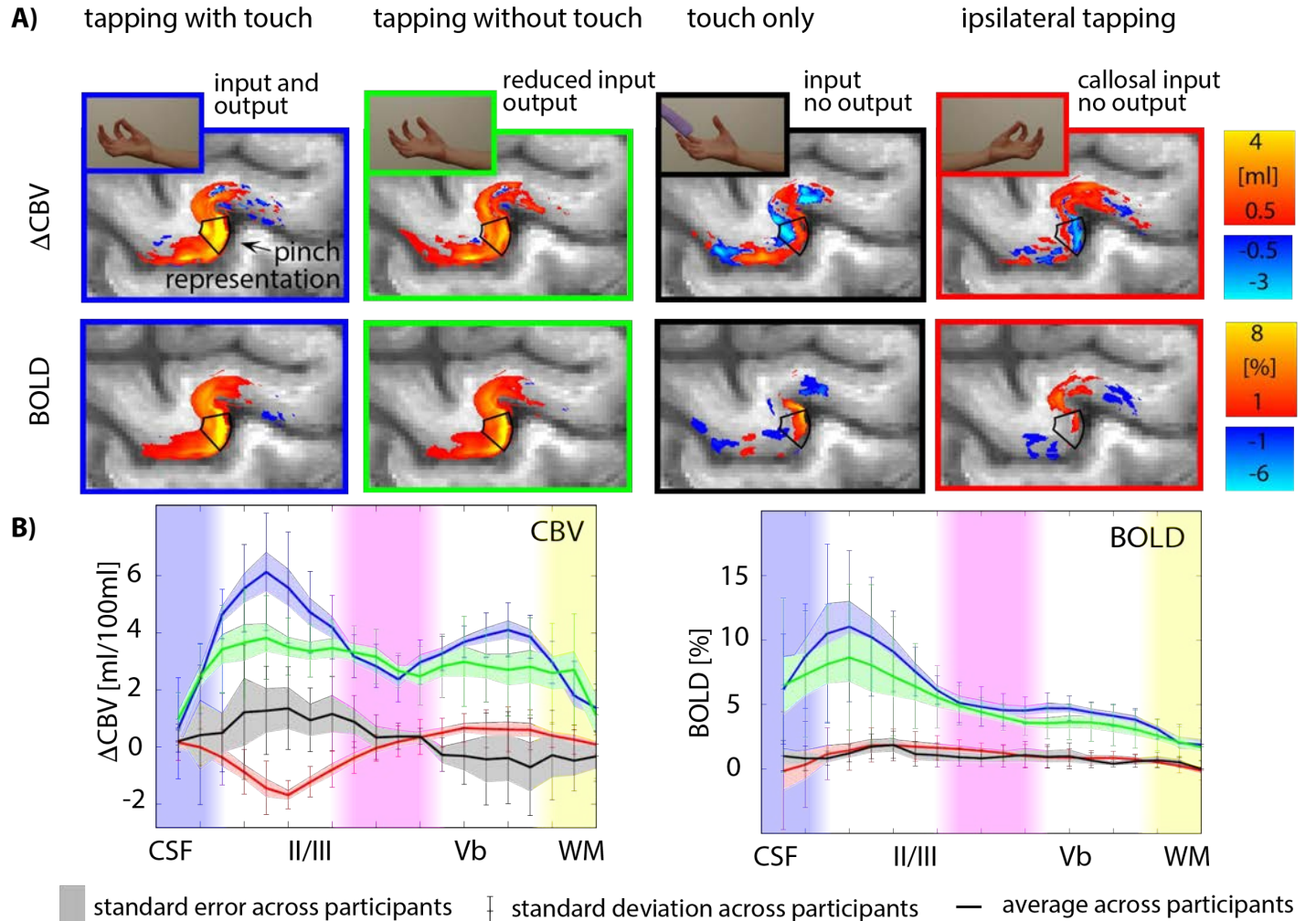


Layer Activity Modulation and Mapping with VASO

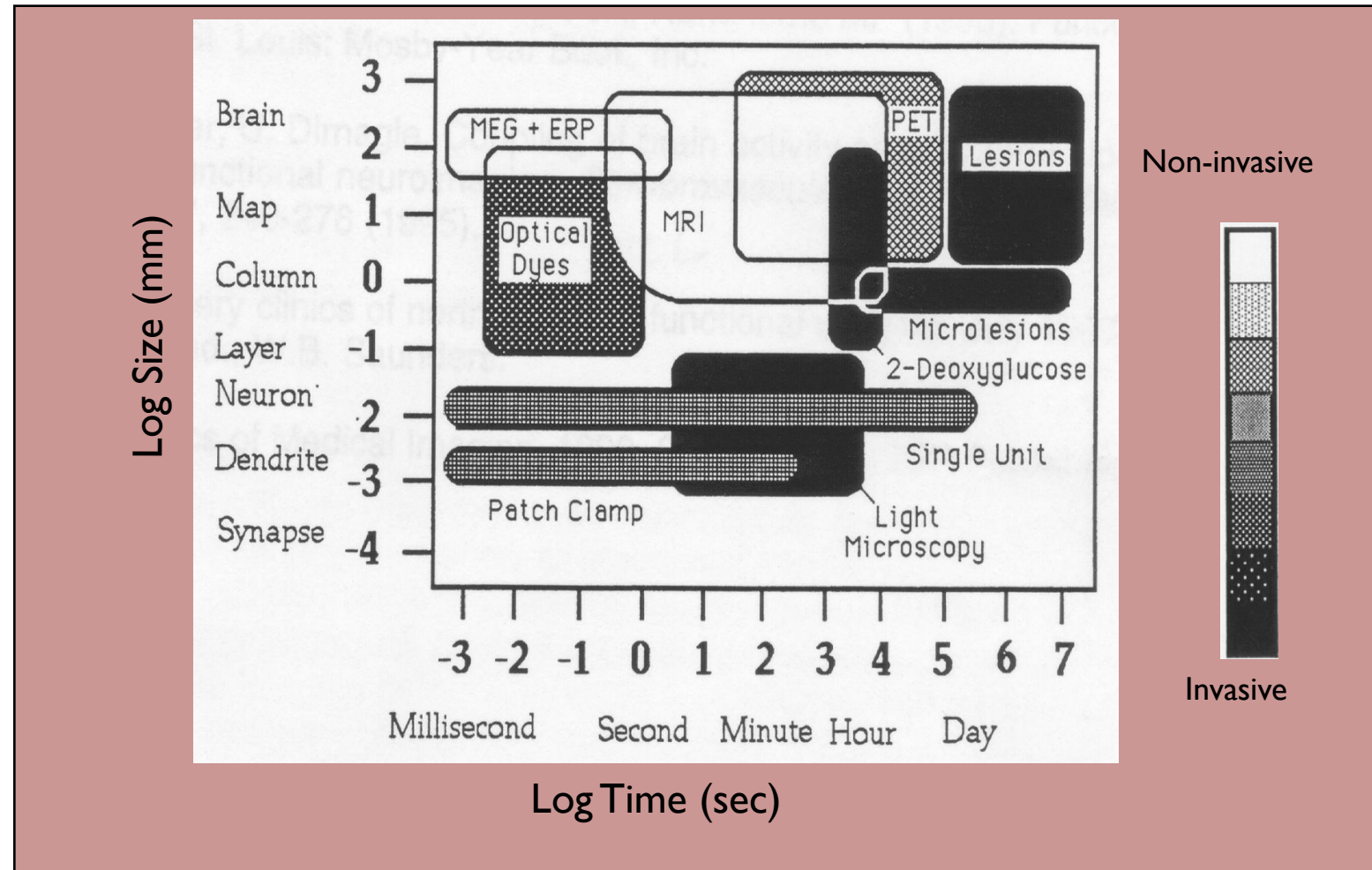
A) expected M1 circuitry based on Mao et al. 2011 and Weiler et al. 2008



3D-EPI, TR=2.5s
FLASH GRAPPA 3
0.8 x 0.8 x 1



Functional Neuroimaging Techniques



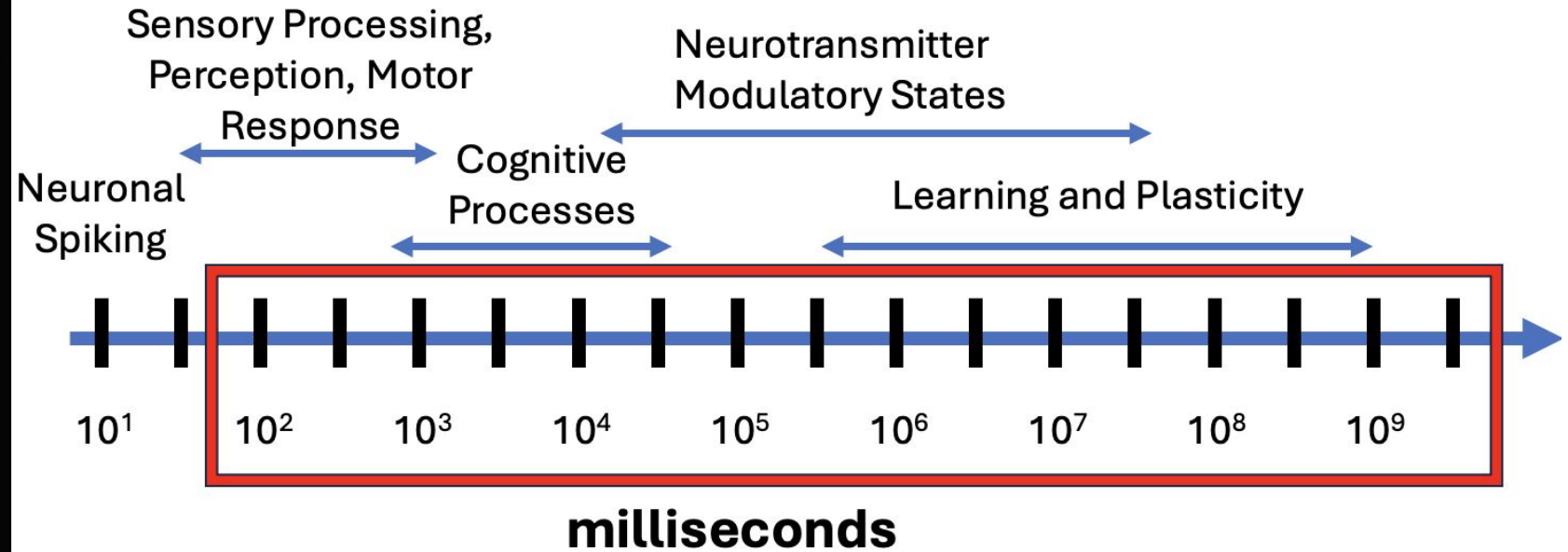
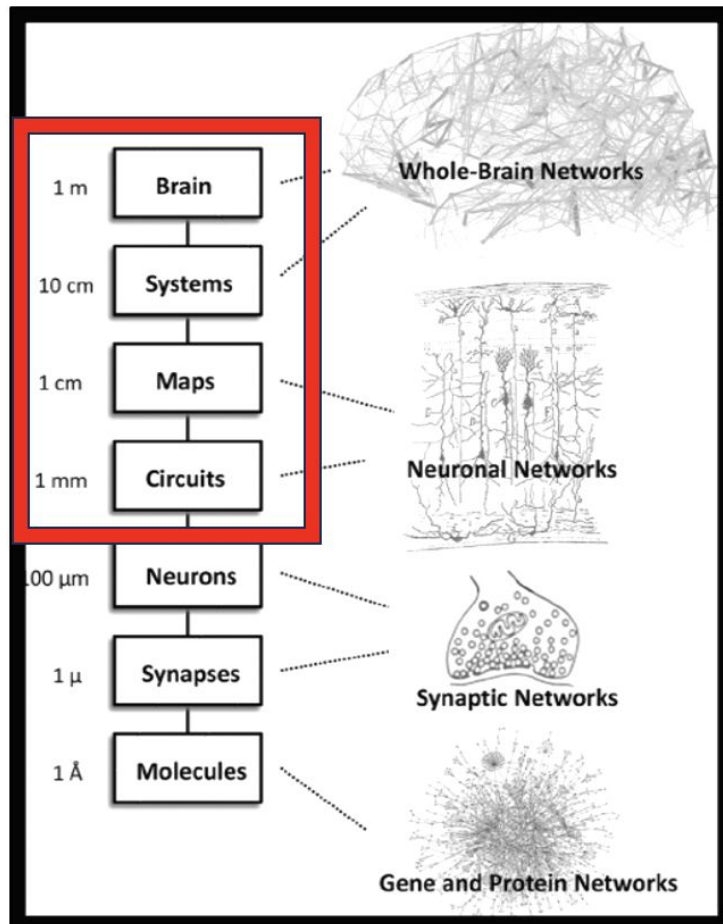
after Churchland and Sejnowski, 1988

Most fMRI research has been towards understanding functional brain organization

The desire is that:

- The signal means something (contains information)
- Is sensitive, precise, and repeatable.
- The spatial and temporal scales are relevant and useful.

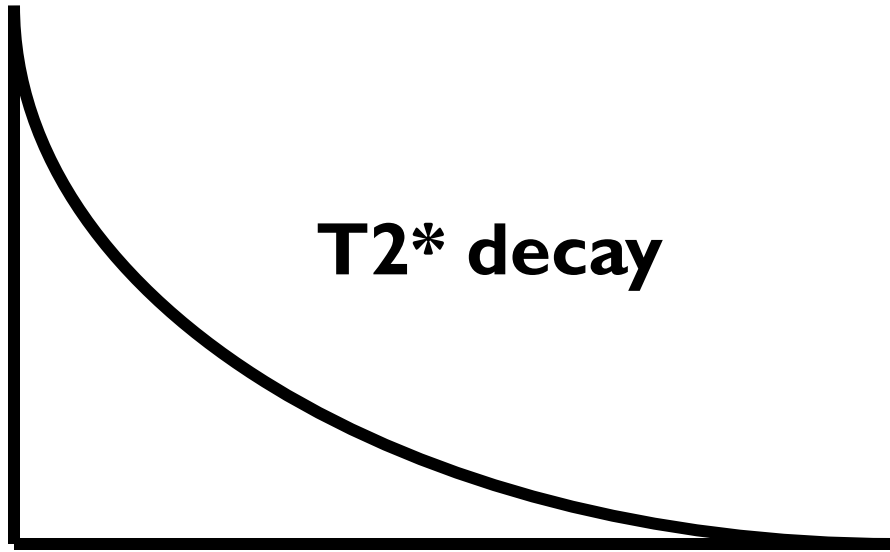
Spatial and Temporal Scales of Brain Function



Five Key Factors For The Emergence of Functional MRI

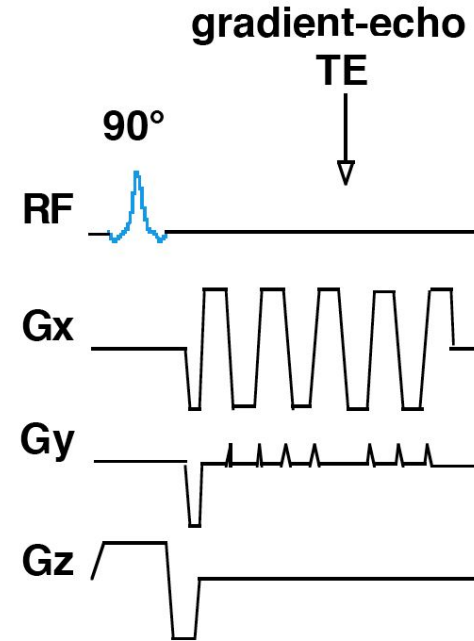
1. **Magnetic properties of red blood cells**
2. **Activation related hemodynamic changes**
3. **Spatial scale of brain activation**
4. **Echo Planar Imaging**
5. **Prevalence of MRI scanners**

Single Shot Echo Planar Imaging (EPI)



EPI Readout Window

≈ 20 to 40 ms

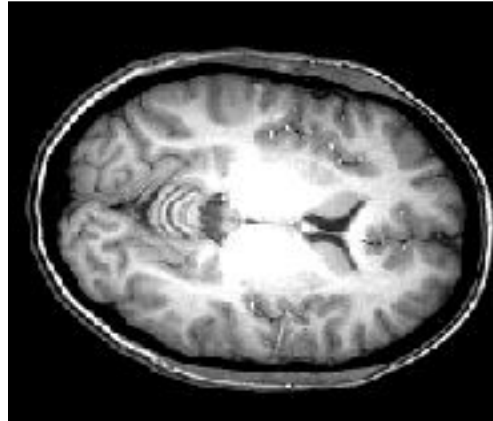
[illegible]

MRI vs. fMRI

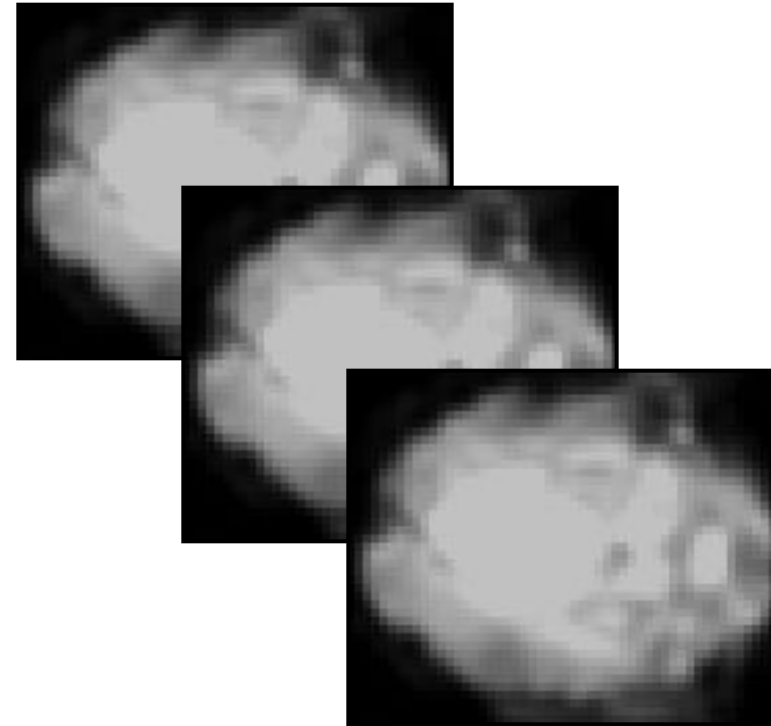
MRI

fMRI

high resolution
(1 mm)

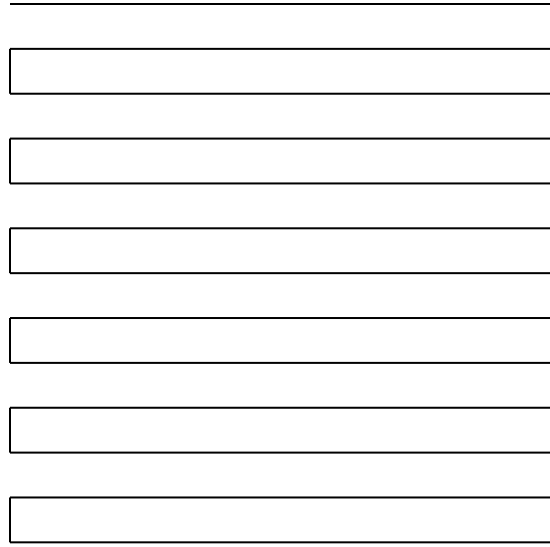


one image

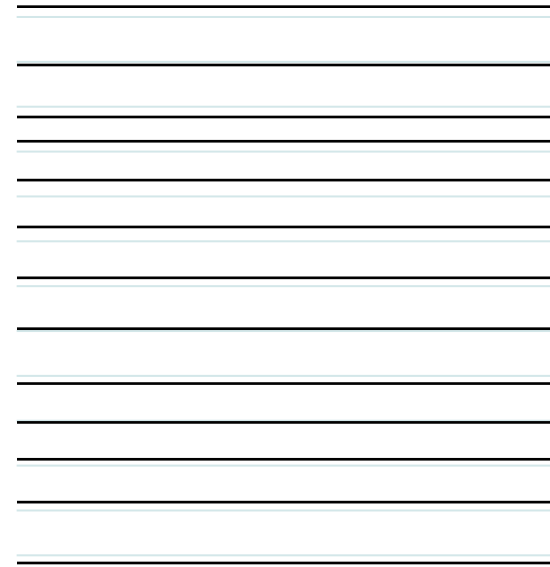


many images
(e.g., every 2 sec for 5
mins)

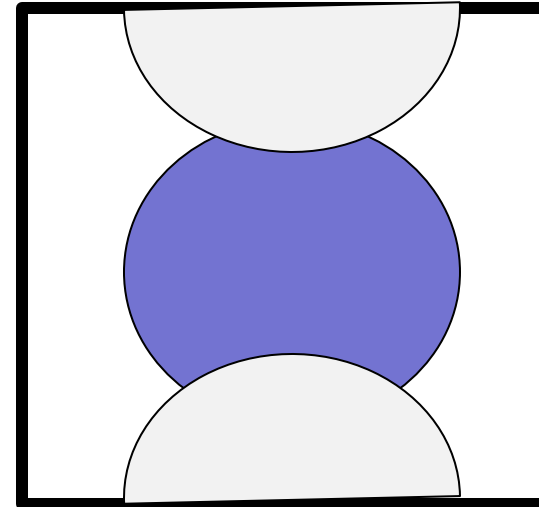
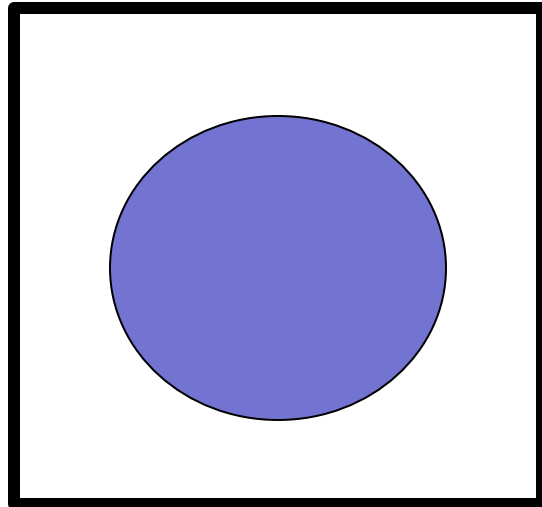
30 ms



10 sec
to
1 min



Phase errors

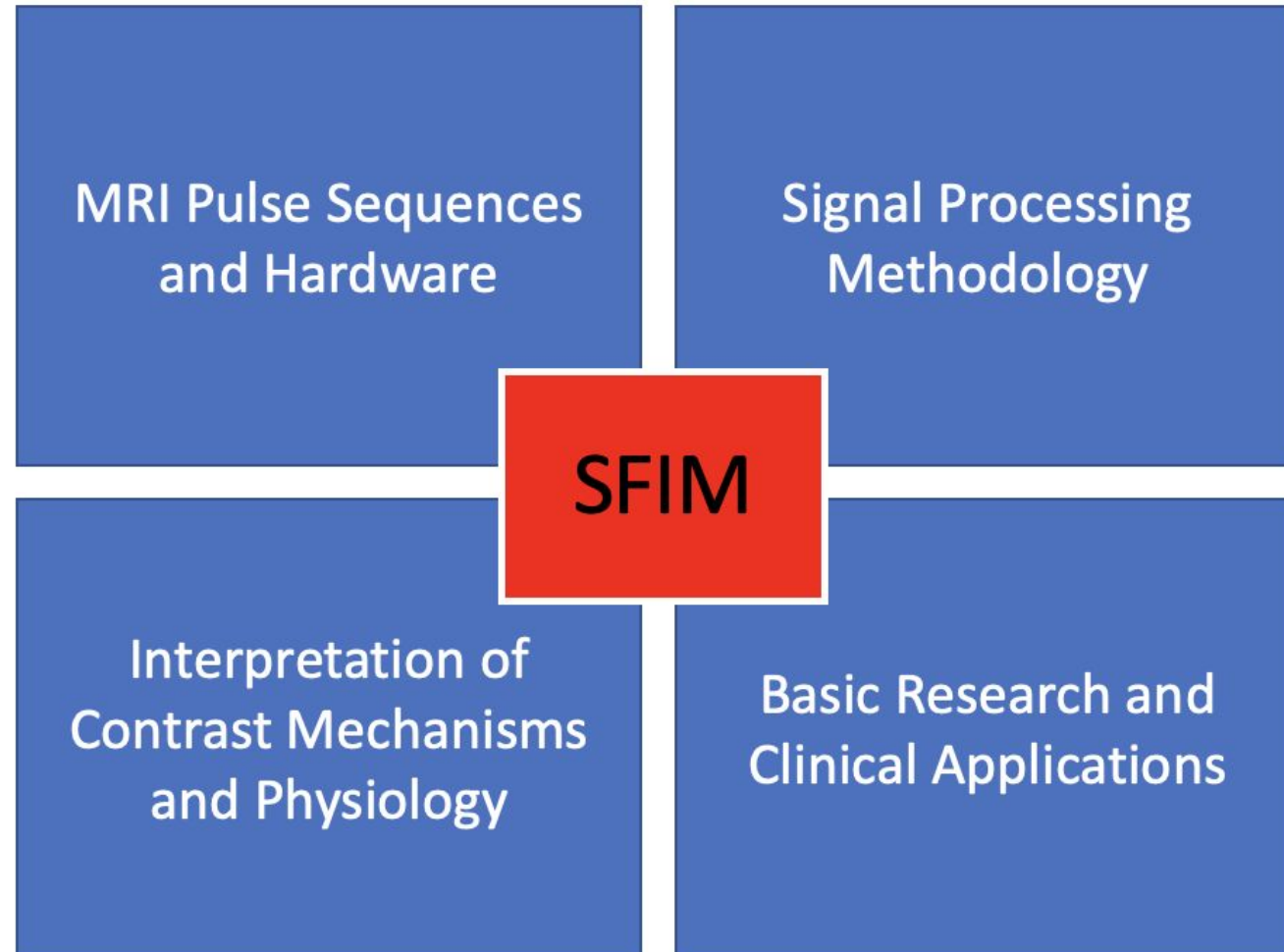


Approximate EPI Timeline

- 1976-84** P. Mansfield conceives of EPI
- 1989** EPI of humans emerges on a handful of scanners
3 x 3 x 3-10 mm³
- 1989** ANMR retrofitted with GE scanners for EPI
- 1991** Home built head gradient coils perform EPI
- 1996** EPI is standard on clinical scanners
- 2000** Gradient performance continues to increase
- 2002** Parallel imaging allows for higher resolution EPI
- 2006** 1.5 x 1.5 x 1.5 mm³ single shot EPI possible
- 2009** At 7T sub – mm single shot EPI for fMRI is possible

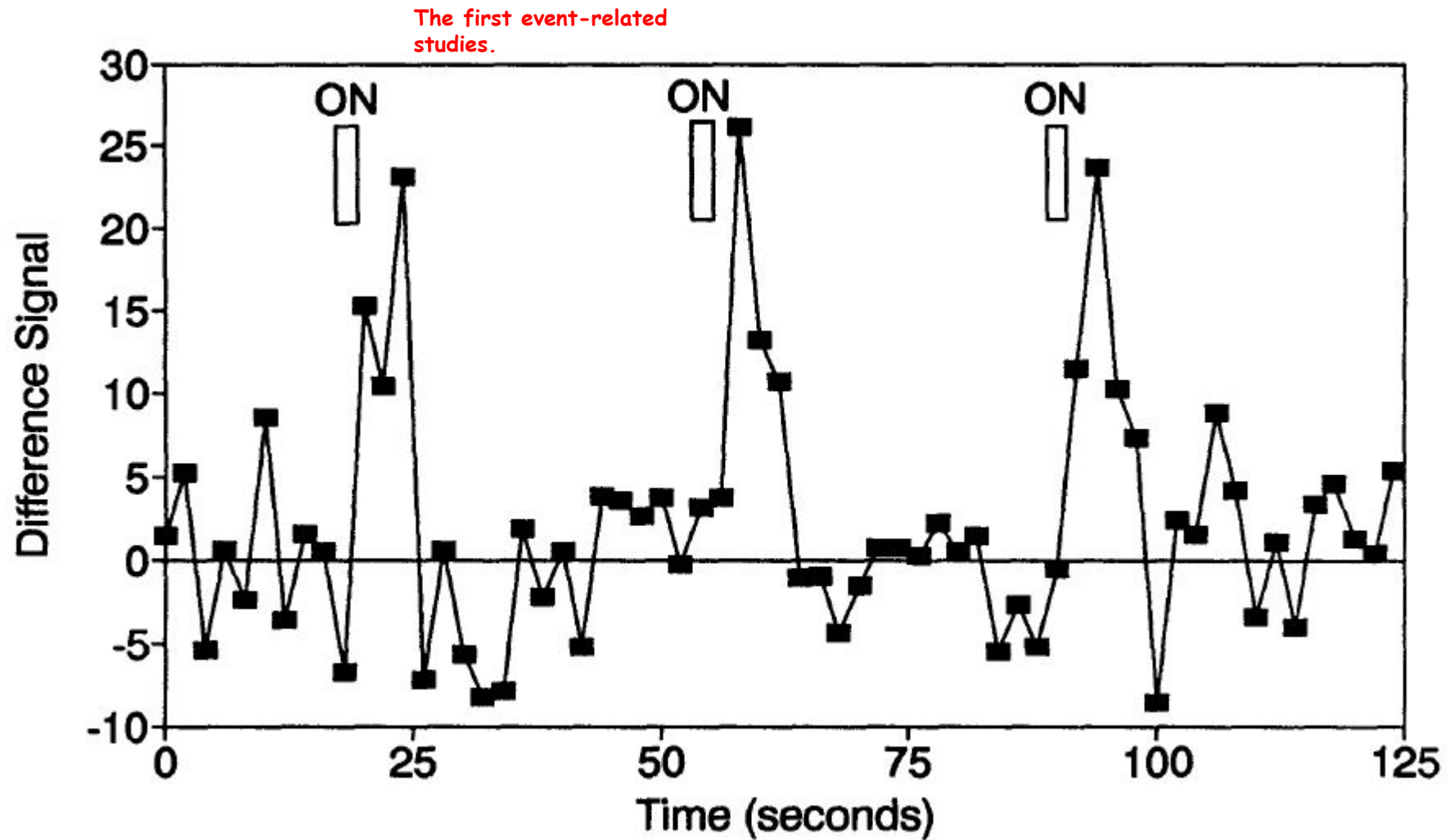
Five Key Factors For The Emergence of Functional MRI

- 1. Magnetic properties of red blood cells**
- 2. Activation related hemodynamic changes**
- 3. Spatial scale of brain activation**
- 4. Echo Planar Imaging**
- 5. Prevalence of MRI scanners**



A bit more history...

- **Event-Related fMRI (1993, 1996)**
- **Retinotopy (1995)**
- **Resting State fMRI (1995...2006)**
- **Ocular Dominance Columns (1997)**
- **High Field and Multi-channel Receive (2000)**
- **fMRI “Decoding” (2001)**
- **Intracortical recordings and fMRI (2001)**
- **DARPA Brain Reading/Decoding Competition (2006)**
- **Approval for Pre-surgical Mapping (2007)**



Blamire, A. M., et al. (1992).
"Dynamic mapping of the human
visual cortex by high-speed
magnetic resonance imaging."
Proc. Natl. Acad. Sci. USA
89: 11069-11073.

Proc. Natl. Acad. Sci. USA
Vol. 93, pp. 14878–14883, December 1996
Neurobiology

Detection of cortical activation during averaged single trials of a cognitive task using functional magnetic resonance imaging

(neuroimaging/single trial/language/prefrontal)

RANDY L. BUCKNER^{†‡§¶}, PETER A. BANDETTINI^{†‡}, KATHLEEN M. O'CRIVEN^{†||}, ROBERT L. SAVOY^{†||},
STEVEN E. PETERSEN^{**††}, MARCUS E. RAICHLE^{§**††}, AND BRUCE R. ROSEN^{†‡}

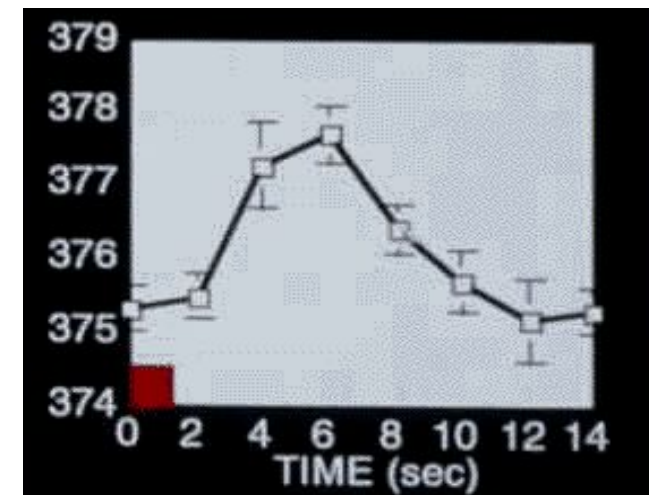
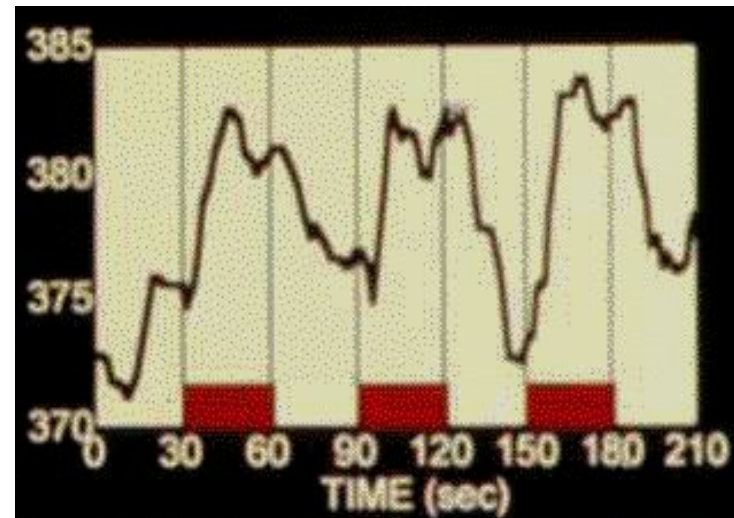
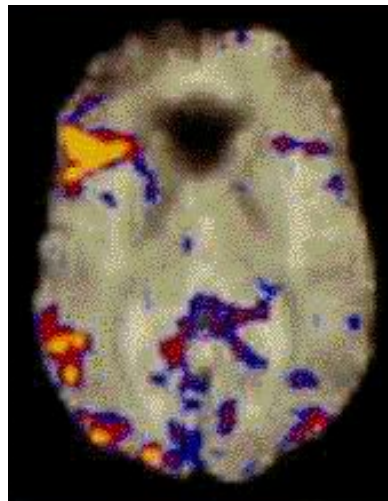
[†]Department of Radiology, Massachusetts General Hospital Nuclear Magnetic Resonance Center, Charlestown, MA 02129; [‡]Harvard University Medical School, Boston, MA 02115; [§]Rowland Institute, Cambridge, MA 02142; and ^{**}Departments of Neurology and Neurosurgery and McDonnell Center for the Study of Higher Brain Function, and Departments of [§]Radiology and ^{††}Anatomy and Neurobiology, Washington University Medical School, St. Louis, MO 63110

Contributed by Marcus E. Raichle, September 4, 1996

BLOCKED:



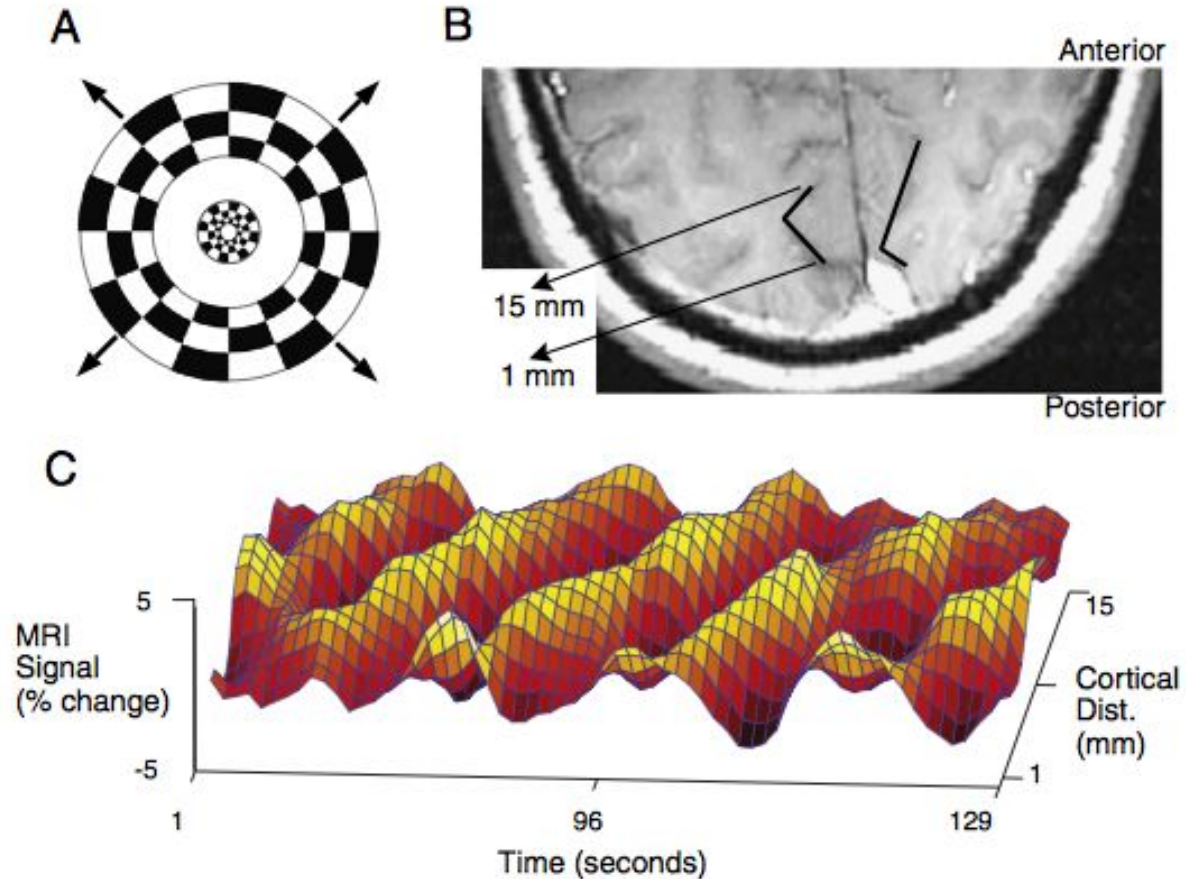
SINGLE TRIAL:



fMRI of human visual cortex

Stephen A. Engel
David E. Rumelhart
Brian A. Wandell
Department of Psychology,
Adrian T. Lee
Gary H. Glover
Department of Radiology,
Eduardo-Jose Chichilnisky
Neuroscience Program,
Michael N. Shadlen
Department of Neurobiology,
Stanford University, Stanford,
California 94305, USA

NATURE · VOL 369 · 16 JUNE 1994



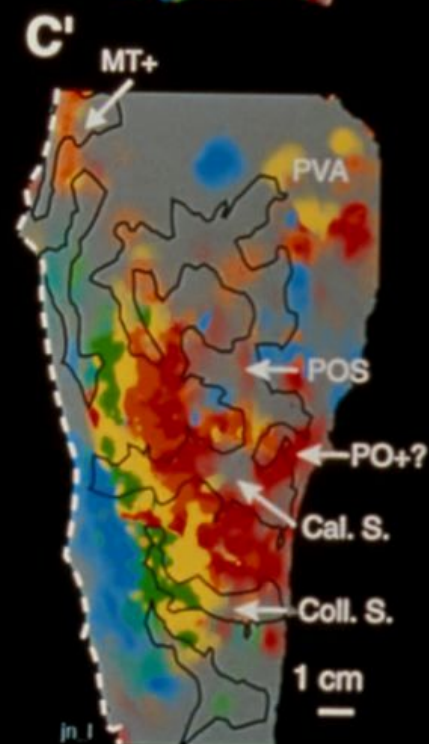
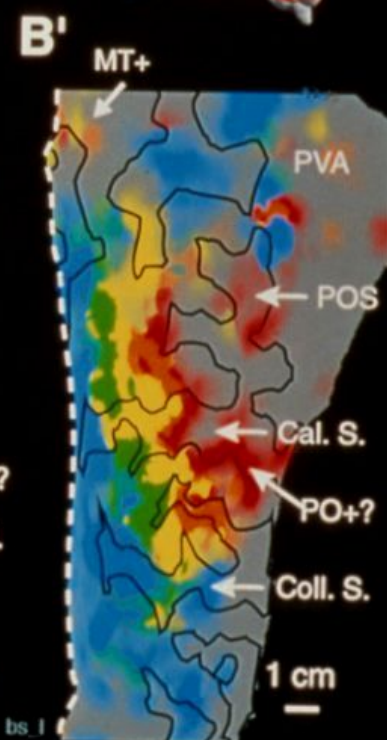
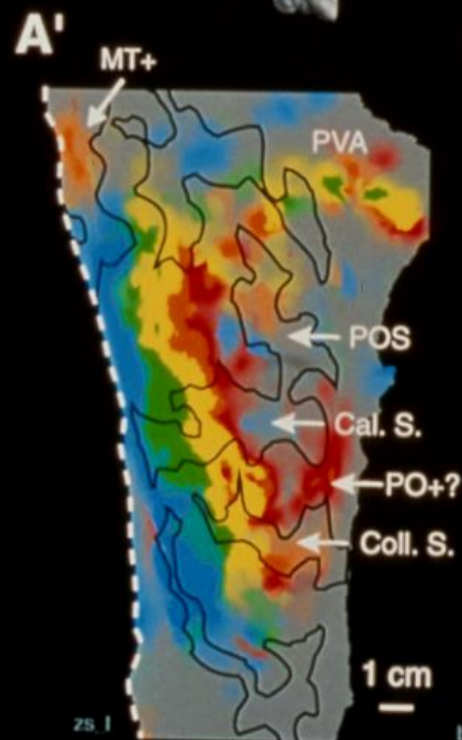
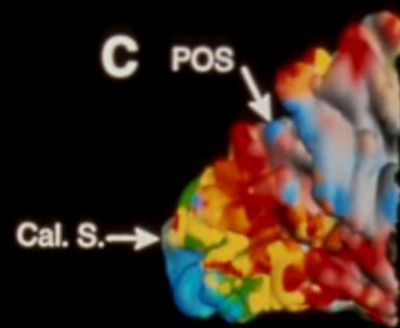
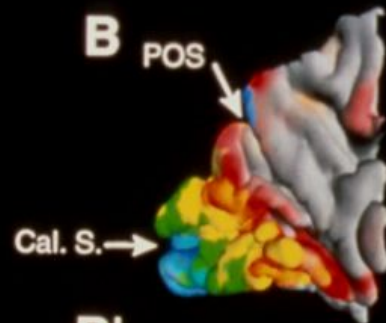
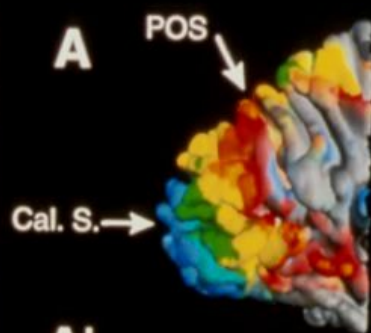
Proc. Natl. Acad. Sci. USA
Vol. 93, pp. 2382–2386, March 1996
Neurobiology

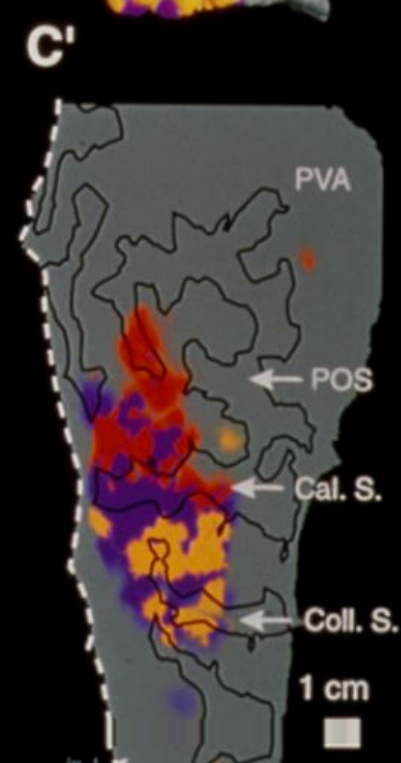
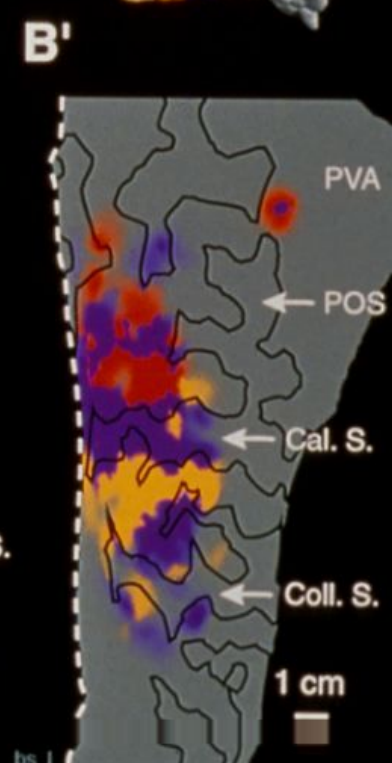
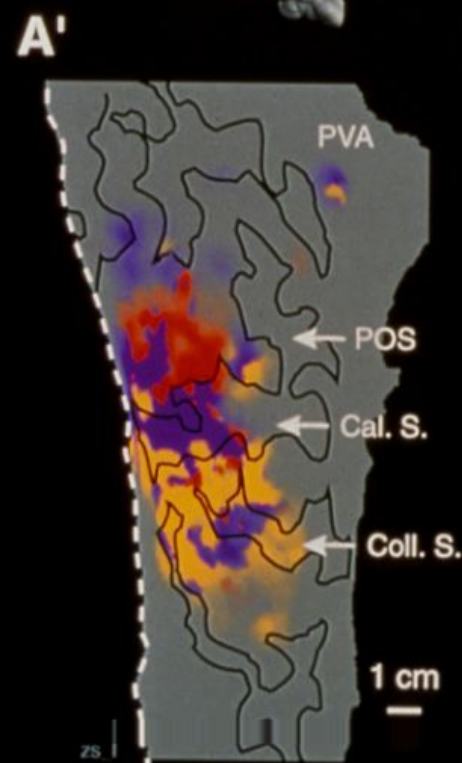
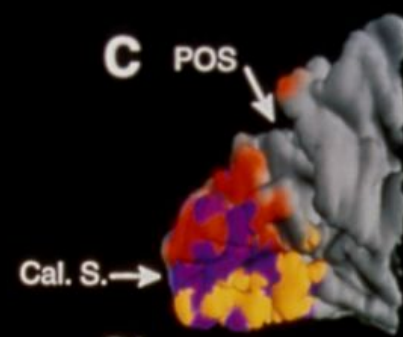
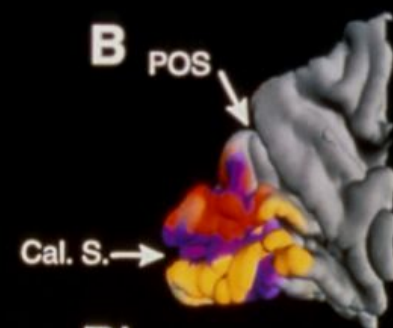
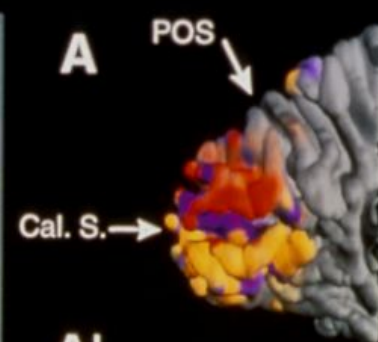
Mapping striate and extrastriate visual areas in human cerebral cortex

EDGAR A. DEYOE*, GEORGE J. CARMAN†, PETER BANDETTINI‡, SETH GLICKMAN*, JON WIESER*, ROBERT COX§, DAVID MILLER¶, AND JAY NEITZ*

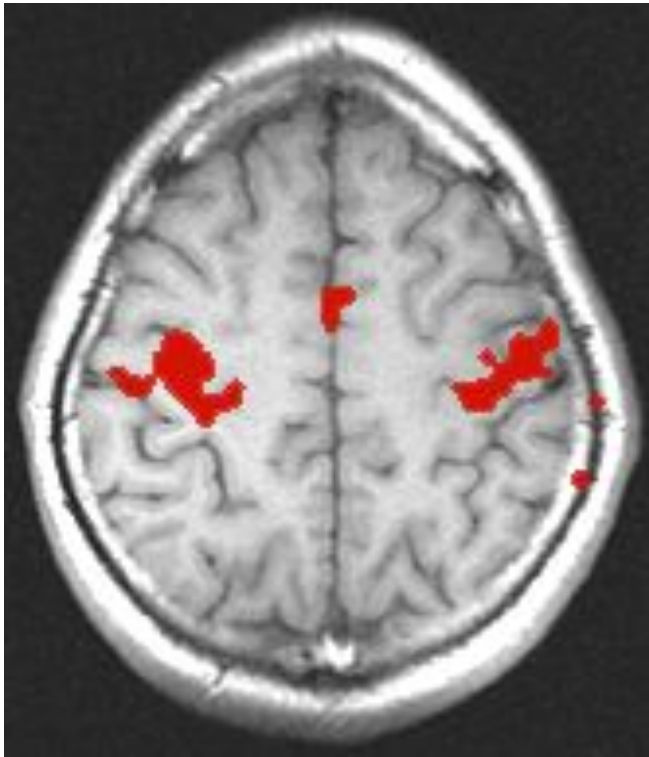
*Department of Cellular Biology and Anatomy, and Biophysics Research Institute, The Medical College of Wisconsin, 8701 Watertown Plank Road, Milwaukee, WI 53226; †The Salk Institute for Biological Studies, La Jolla, CA 92037; ‡Massachusetts General Hospital–NMR Center, Charlestown, MA 02129; §Biophysics Research Institute, The Medical College of Wisconsin, Milwaukee, WI 53226; and ¶Brown University, Providence, RI 02912

Communicated by Francis Crick, The Salk Institute for Biological Sciences, San Diego, CA, November 14, 1995 (received for review August 2, 1995)

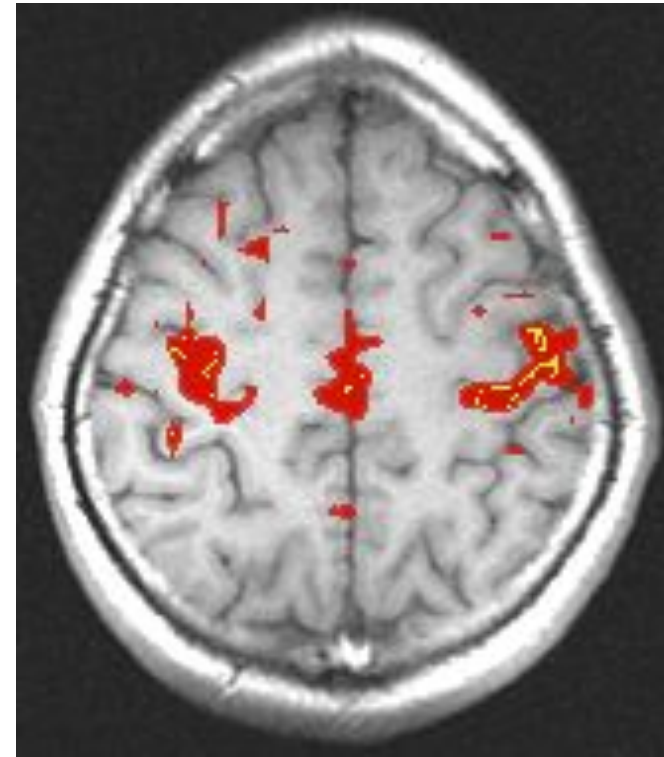




Resting State Correlations



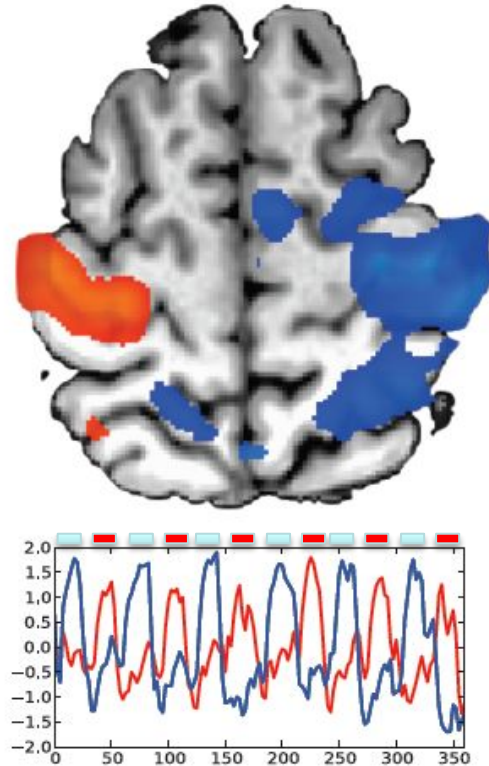
Activation:
correlation with reference function



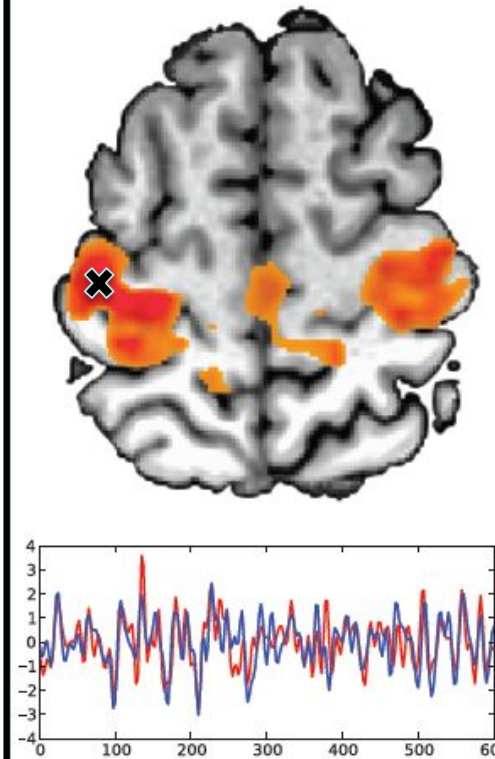
Rest:
seed voxel in motor cortex

Activation-based fMRI and "resting state" fMRI

Task Activation
(Right vs. Left Hand Tapping)

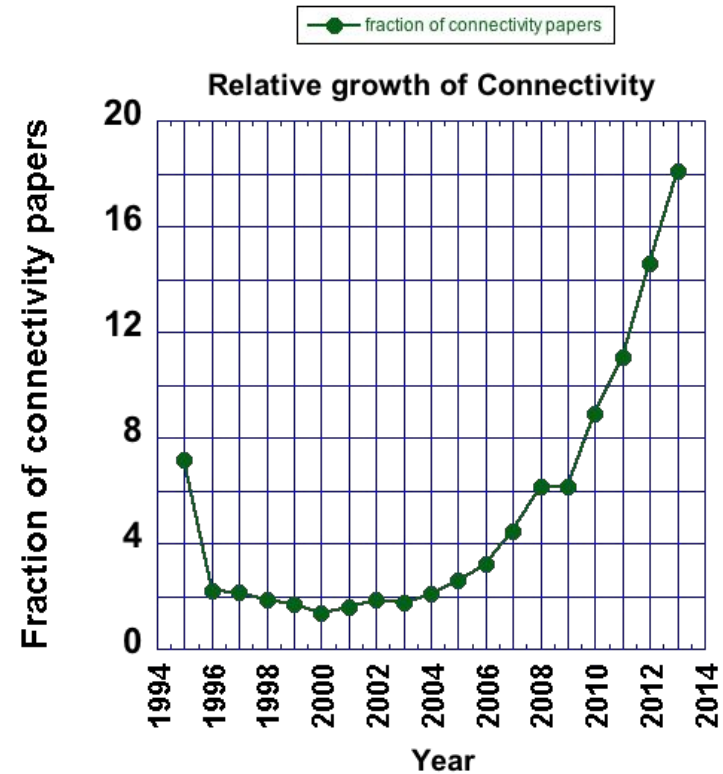
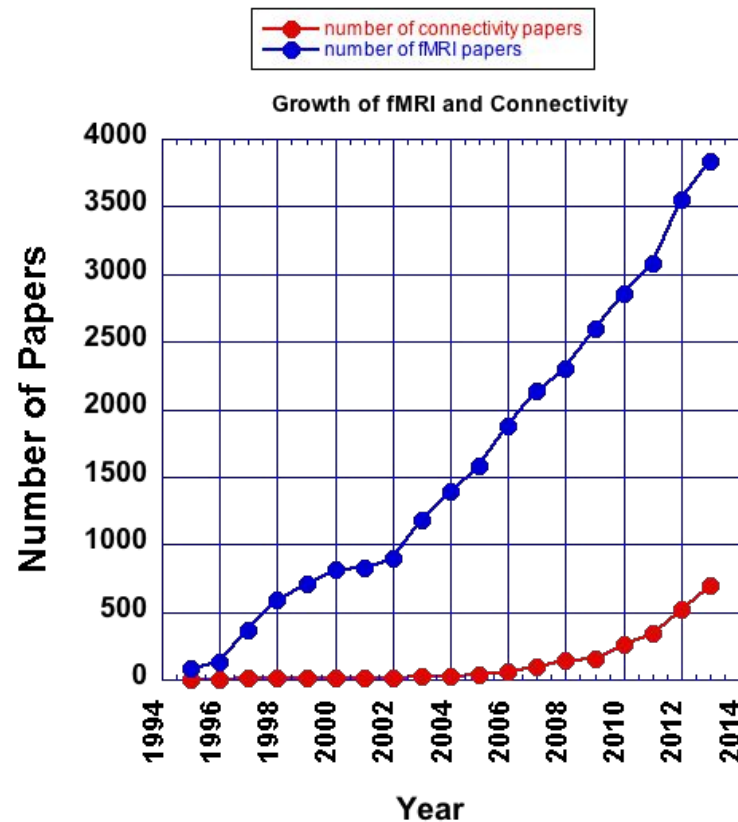


Resting Correlation
(Right Hand Seed)



Resting state fMRI: Why is this area important?

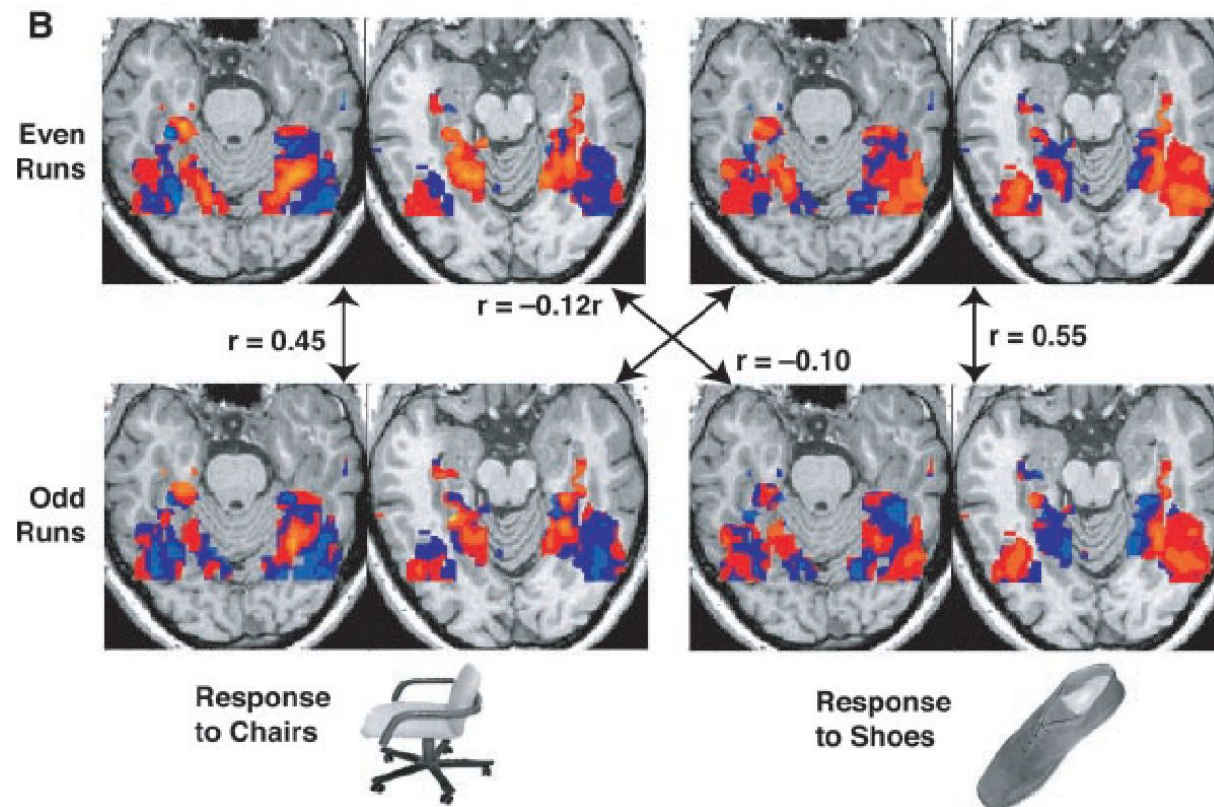
- The number of papers and applications has exploded.
- Neuronal, psychiatric, and developmental disorders may relate to altered connectivity.
- Methods are in their infancy, and rapidly evolving.
- Neuronal correlates of spontaneous fluctuations are not fully understood.



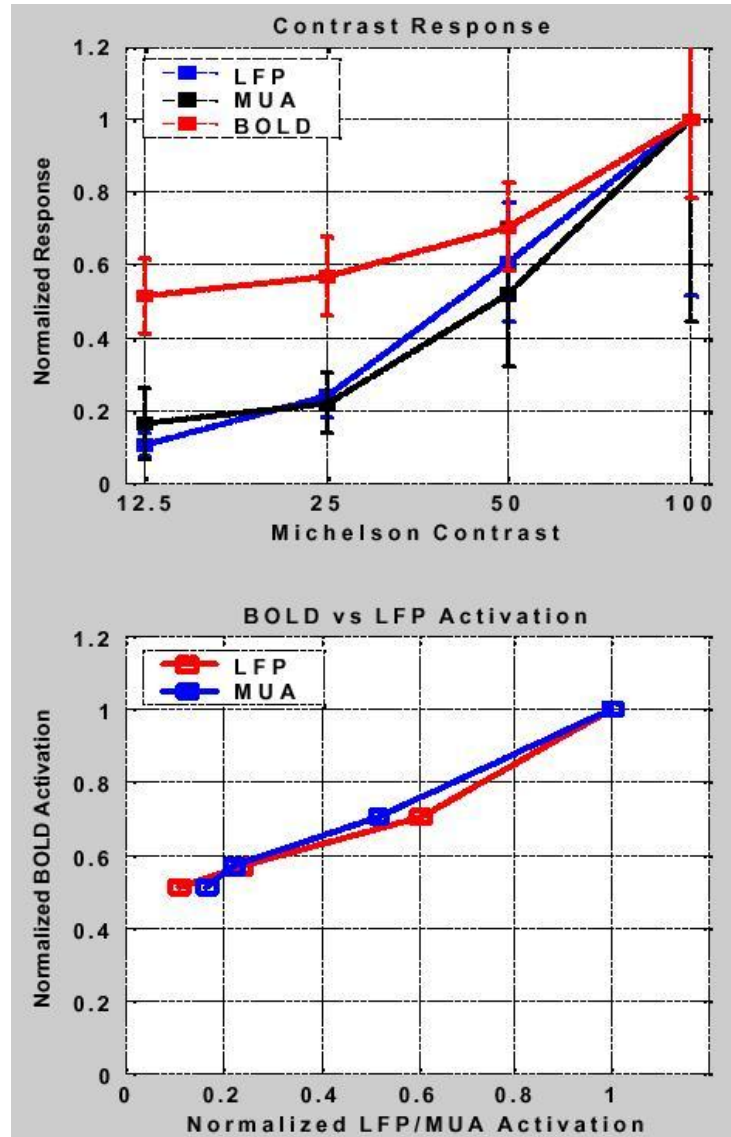
Distributed and Overlapping Representations of Faces and Objects in Ventral Temporal Cortex

James V. Haxby,^{1*} M. Ida Gobbini,^{1,2} Maura L. Furey,^{1,2}
Alumit Ishai,¹ Jennifer L. Schouten,¹ Pietro Pietrini³

SCIENCE VOL 293 28 SEPTEMBER 2001



Logothetis et al. (2001)
“Neurophysiological investigation of the basis of the fMRI signal” Nature, 412, 150-157



Parametric manipulation of brain activation demonstrated that BOLD contrast approximately followed the level of brain activation: visual system (Kwong et al., 1992), auditory system (Binder et al., 1994), and motor system (Rao et al., 1996).

The use of continuous variation of visual stimuli parameters as a function of time was proven a powerful method for fMRI-based retinotopy: (Engel et al., 1994, Deyoe et al., 1994, Sereno et al., 1995).

Event-related fMRI was first demonstrated (Blamire et al., 1992).

Application of event-related fMRI to cognitive activation was shown (Buckner et al., 1996, McCarthy et al., 1997).

Development of mixed event-related and block designs was put forward: (Donaldson et al., 2002).

Paradigms were demonstrated in which the activation timing of multiple brain systems timing was orthogonal, allowing multiple conditions to be cleanly extracted from a single run (Courtney et al., 1997).

High resolution maps were created: For spatial resolution: ocular dominance columns (Menon et al., 1997, Cheng et al., 2001) and cortical layer activation maps were created (Logothetis et al., 2002).

Extraction of information at high spatial frequencies within regions of activation was demonstrated (Haxby et al., 2001).

For temporal resolution: Timings from ms to hundreds of ms were extracted (Ogawa et al., 2000, Menon et al., 1998, Henson et al., 2002, Bellgowan et al., 2003).

The development of “deconvolution” methods allowed for rapid presentation of stimuli (Dale and Buckner, 1997).

Early BOLD contrast models were put forward: (Ogawa et al., 1993, Buxton and Frank, 1997).

More sophisticated models were published that more fully integrated the latest data on hemodynamic and metabolic changes (Buxton et al., 2004).

The development of “clustered volume” acquisition was put forth as a method to avoid scanner noise artifacts: (Edmister et al., 1999).

The findings of functionally related resting state correlations: (Biswal et al., 1995) and regions that consistently show deactivation (Binder et al., 1999, Raichle et al., 2001) were described.

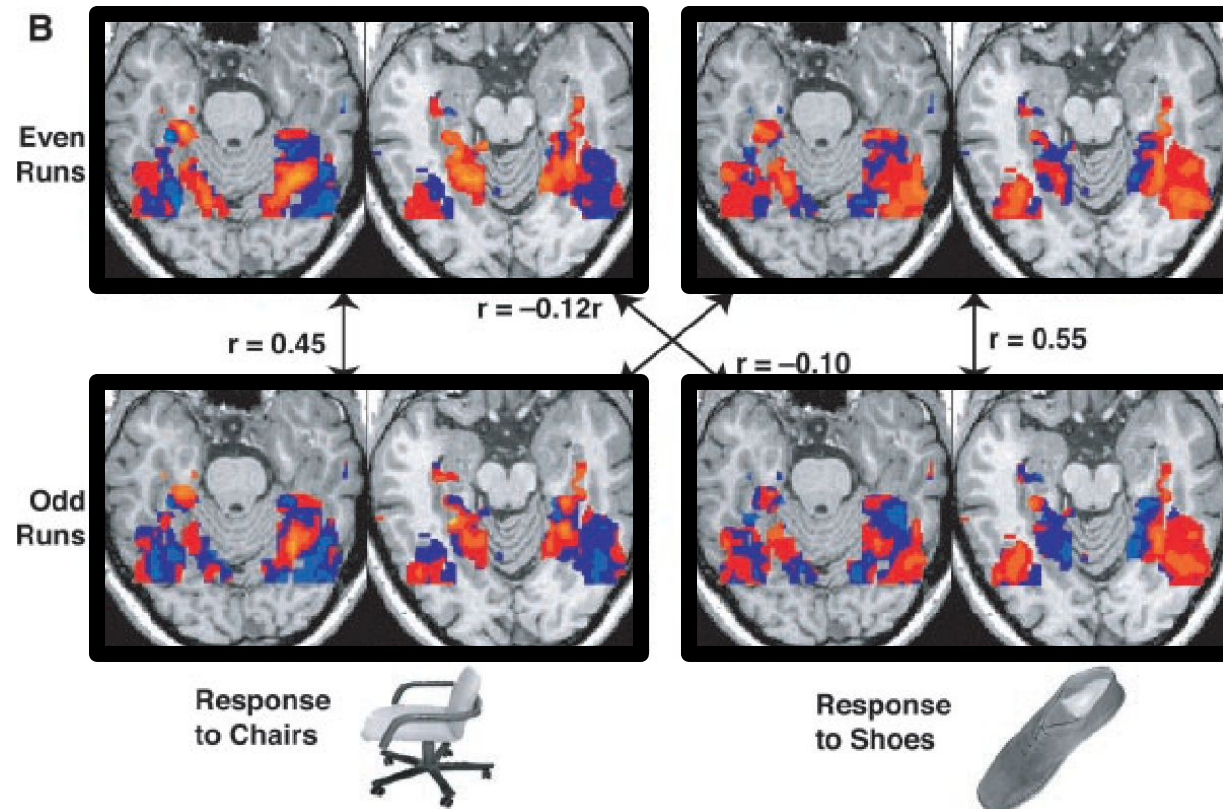
Observation of the pre-undershoot in fMRI (Hennig et al., 1997, Menon et al., 1995, Hu et al., 1997) and correlation with optical imaging was reported (Malonek and Grinvald, 1996).

Simultaneous use of fMRI and direct electrophysiological recording in non-human primate brain during visual stimulation elucidated the relationship between fMRI and BOLD contrast. (Logothetis et al., 2001). Simultaneous electrophysiological recordings in animal models revealed a correlation between negative signal changes and decreased neuronal activity (Shmuel et al., 2002). Simultaneous electrophysiological recordings in animal models provided evidence that inhibitory input could cause an increase in cerebral blood flow (Matheiesen et al., 1998).

Structural equation modeling was developed in the context of fMRI time series analysis: (Buchel and Friston, 1998).

Ventral temporal category representations

Object categories are associated with distributed representations in ventral temporal cortex



Haxby et al. 2001

Overview of fMRI

Functional Contrast:

Blood volume
Blood flow/perfusion
Blood oxygenation

Spatial resolution:

Typical: 3 mm³
Upper: 0.5 mm³

Temporal resolution:

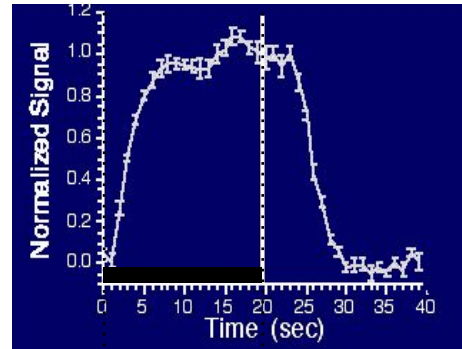
Minimum duration: < 16 ms
Minimum onset diff: 100 ms to 2 sec

Sensitivity:

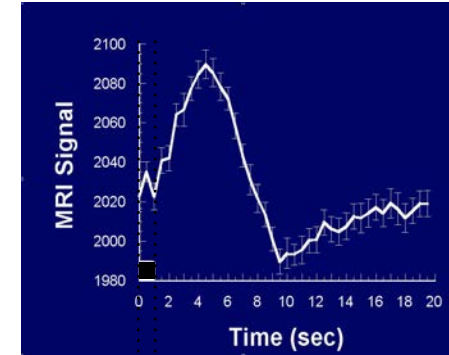
tSNR = 40/1 to 120/1
fCNR = 1/1 to 6/1

Interpretability issues:

Neurovascular coupling, vascular sampling, blood, physiologic noise, motion and other artifacts, etc..

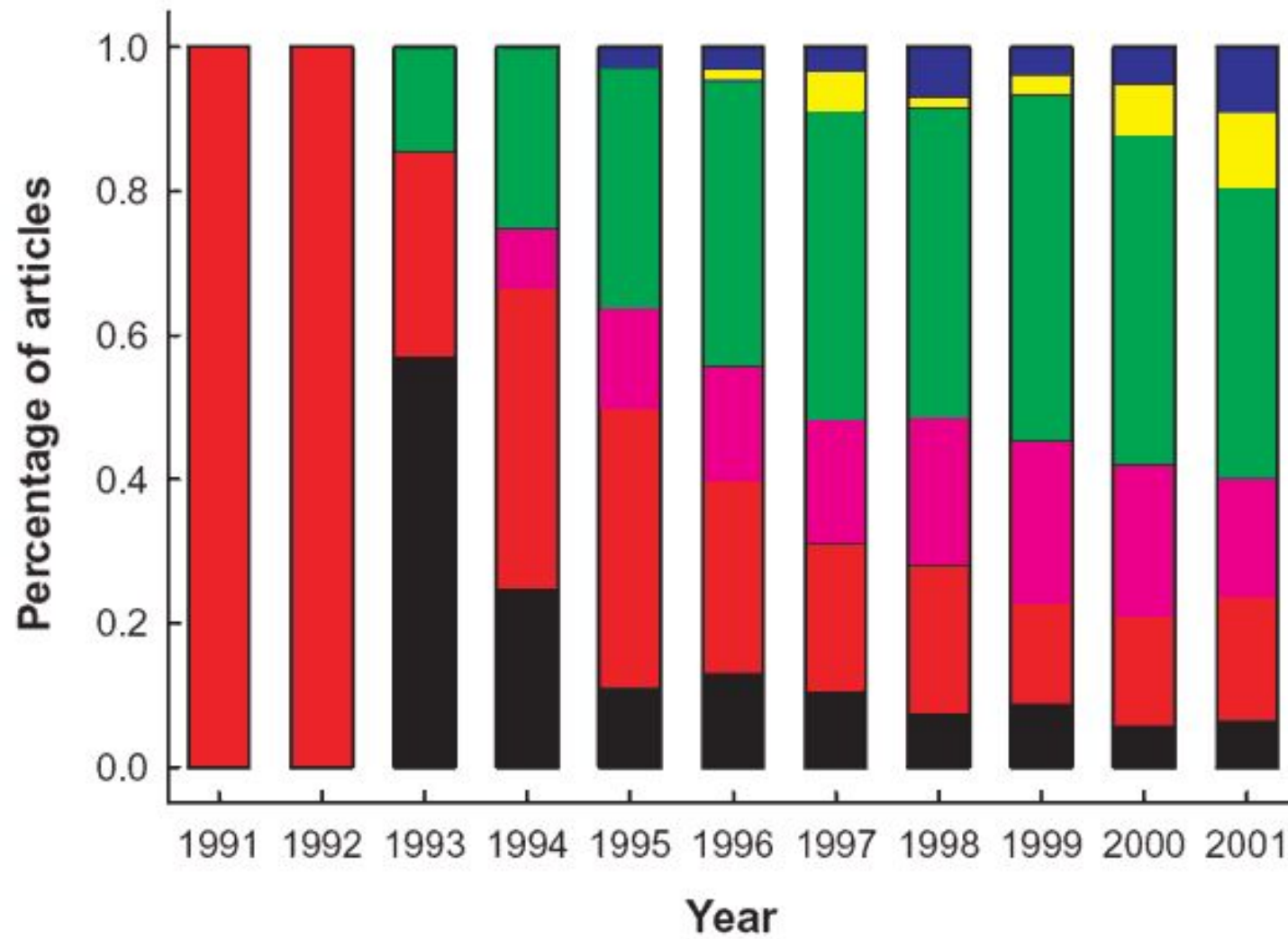


task



task





Motor (black)
Primary Sensory (red)
Integrative Sensory (violet)
Basic Cognition (green)
High-Order Cognition (yellow)
Emotion (blue)

J. Illes, M. P. Kirschen, J. D. E. Gabrieli, Nature Neuroscience, 6 (3) p.205

Functional Contrast

- Volume (gadolinium)
- BOLD
- Perfusion (ASL)
- ΔCMRO_2
- ΔVolume (VASO)
- Neuronal Currents
- Diffusion coefficient
- Temperature

What factors influence the fMRI signal magnitude and timing?

Physiologic

Baseline flow, oxygenation, volume, vessel size, metabolism

Change in flow, oxygenation, volume, vessel size, metabolism

Hematocrit

Blood pressure

Cardiac

Respiration

Drug effects (i.e. Caffeine)

MRI

Pulse sequence (i.e. SE, IR, GE...)

Field strength

TE, TR, Flip angle

Voxel size

Diffusion weighting

Magnetization Transfer Pulse

Neuronal

Location

Timing

LFP / specific frequencies?

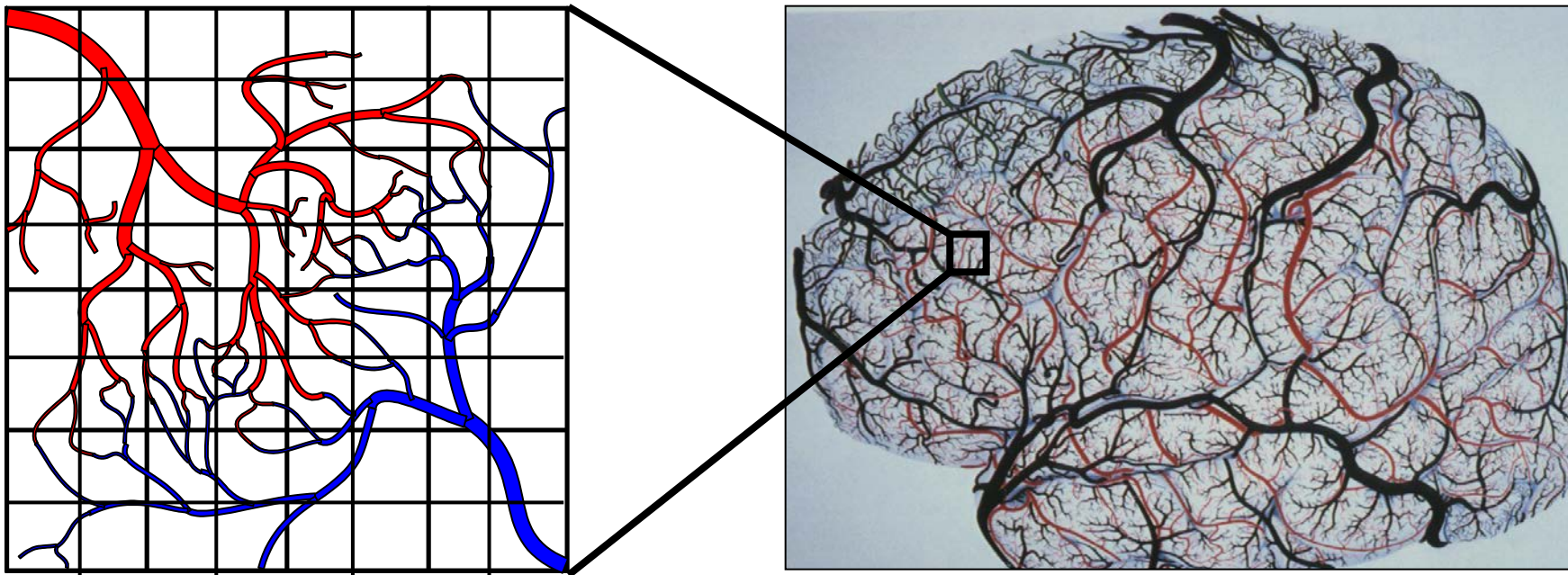
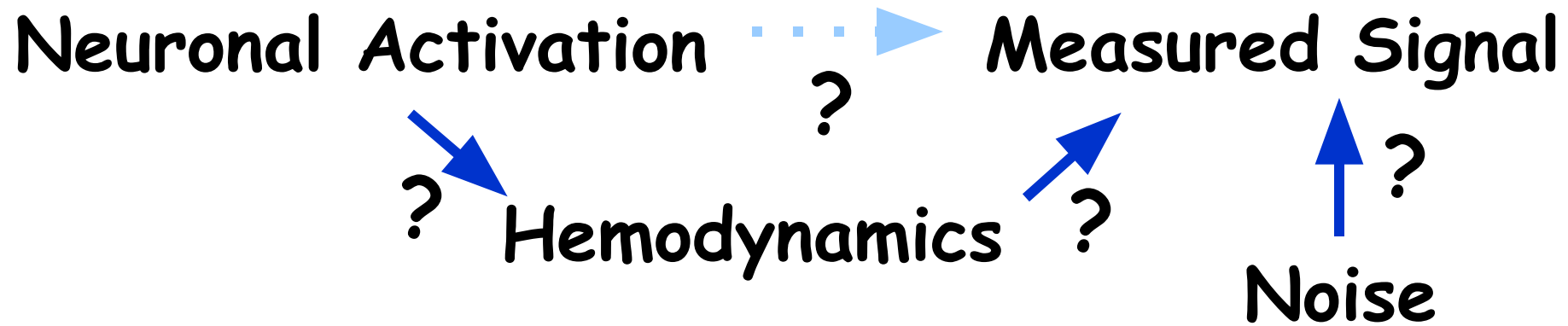
Number / Coherence of Neurons ?

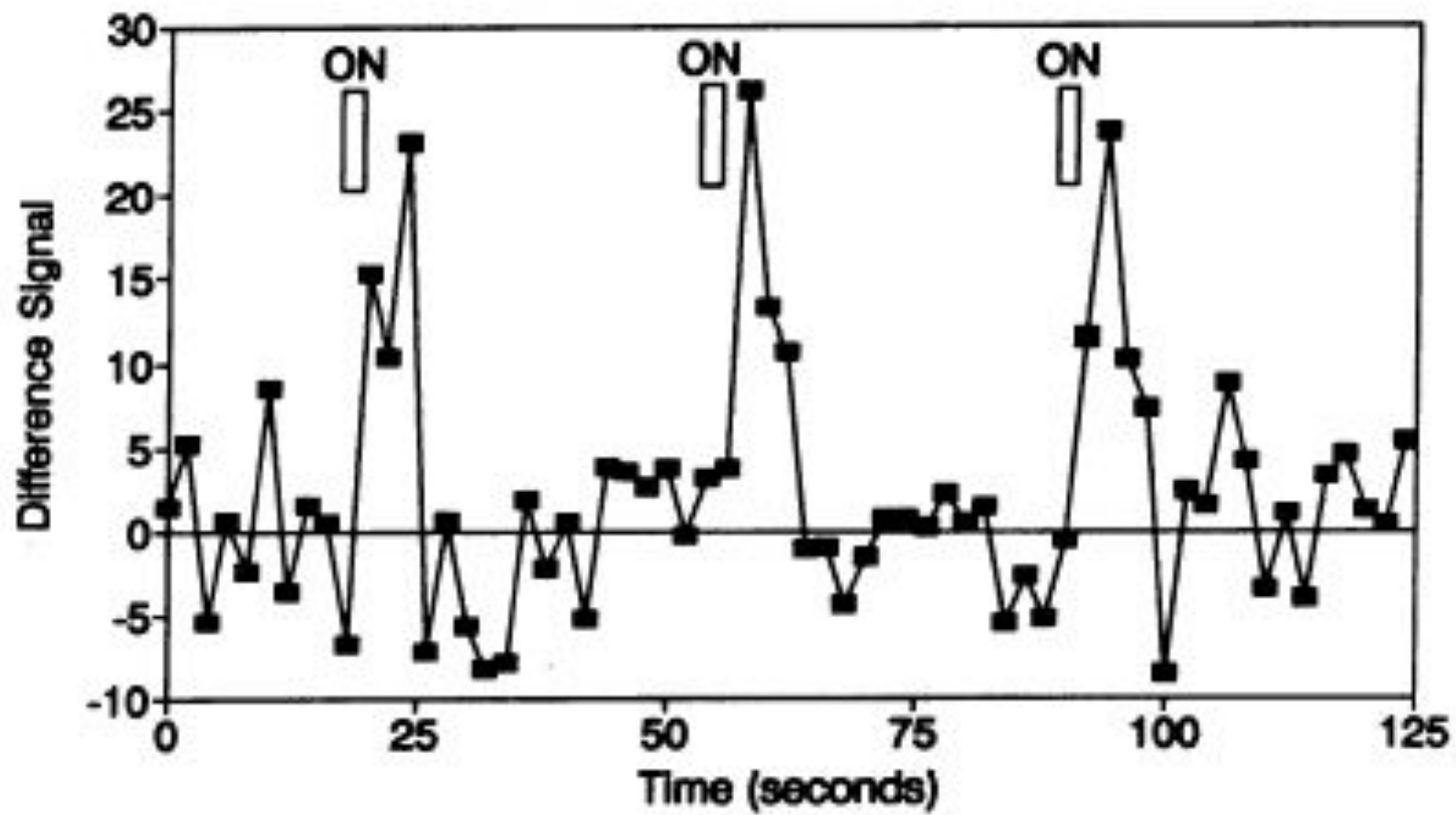
Inhibition/Excitation?

The Challenge: Control for all else and/or minimize number of assumptions while modulating sensitivity to one piece of information.

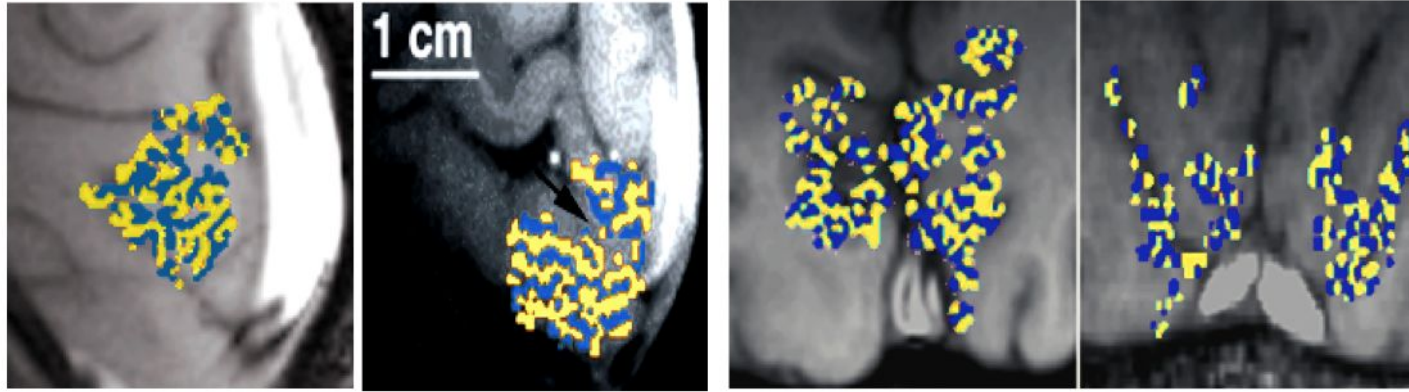
Extracting Information from the fMRI Signal:

- **Spatial Resolution**
- **Temporal Resolution**
- **Sensitivity**



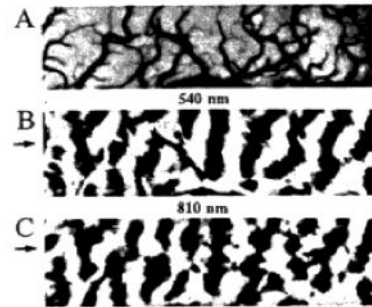


Ocular Dominance Column Mapping

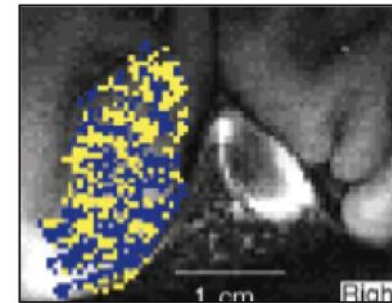


Menon, R. S., S. Ogawa, et al. (1997). J Neurophysiol 77(5): 2780-7.
 0.54 x 0.54 in plane resolution

Optical Imaging



R. D. Frostig et. al, PNAS
 87: 6082-6086, (1990).

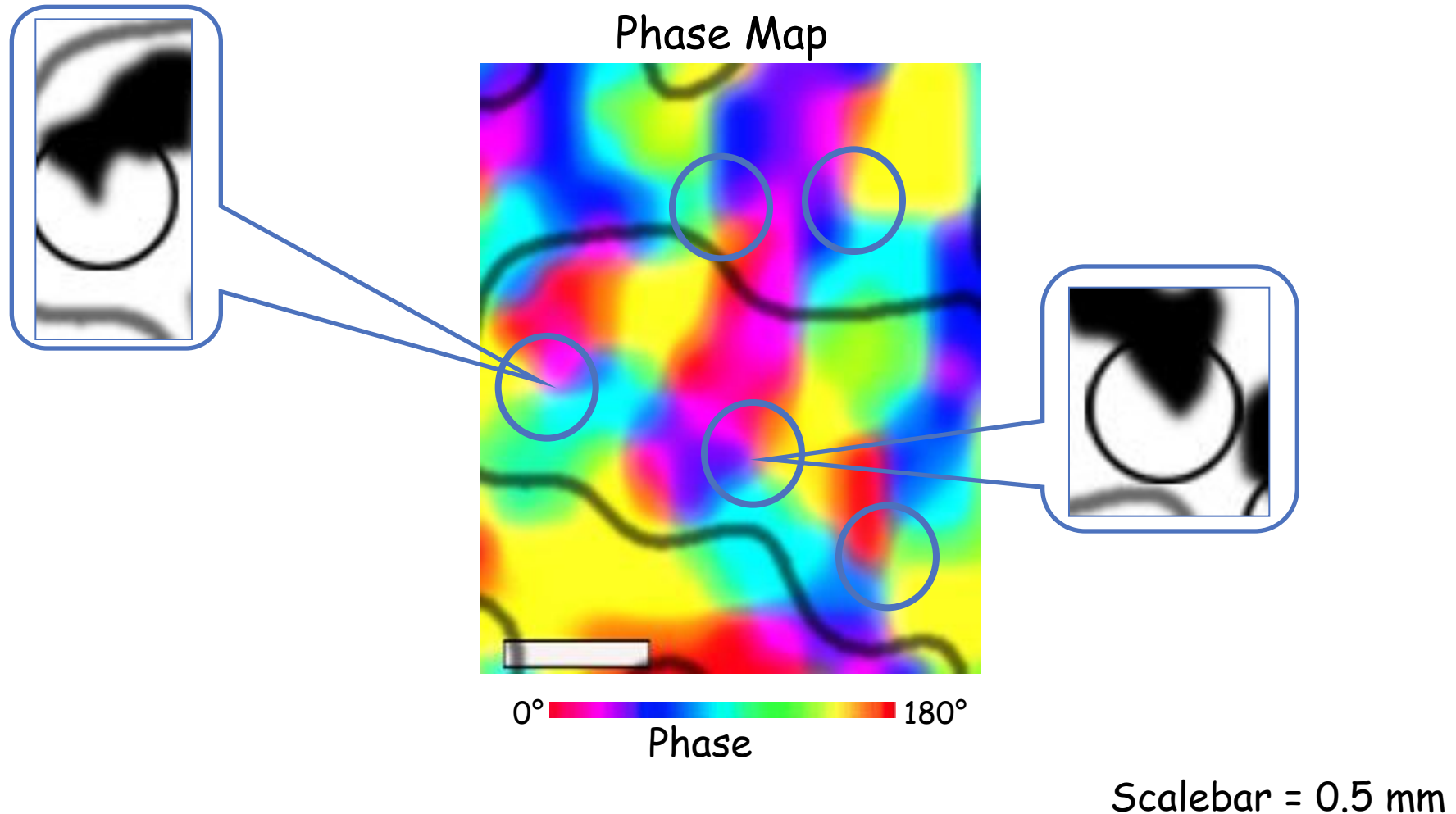


Cheng, et al. (2001)
 Neuron, 32:359-374

0.47 x 0.47 in plane resolution

3.5mm at 1.5T (S. Engel et al - 1994)
 3.9mm (GE), 3.4mm (SE) at 3T (L. Parkes et al - 2005)
 2.3 mm at 7T (A. Schmuel et al - 2007)

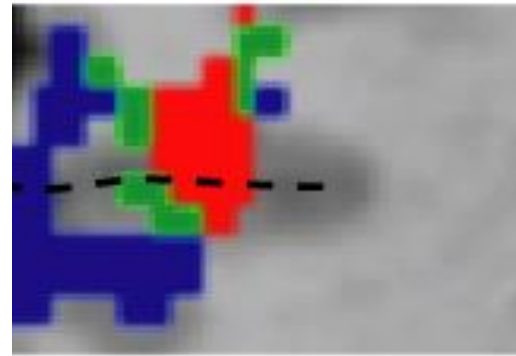
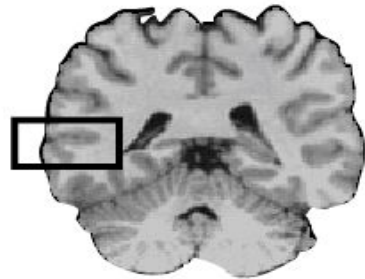
Orientation Columns in Human V1 as Revealed by fMRI at 7T



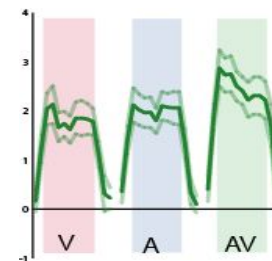
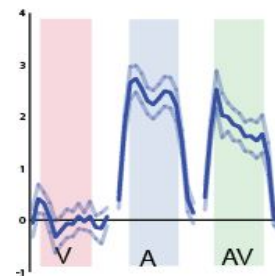
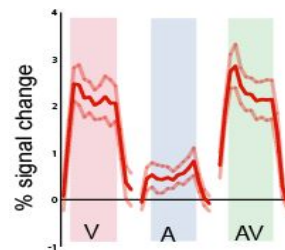
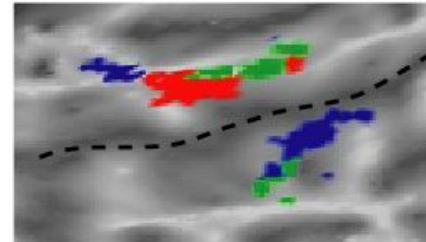
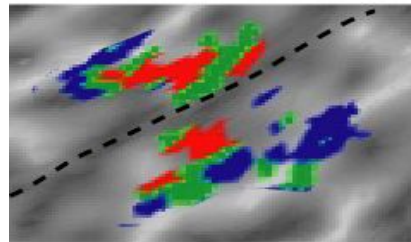
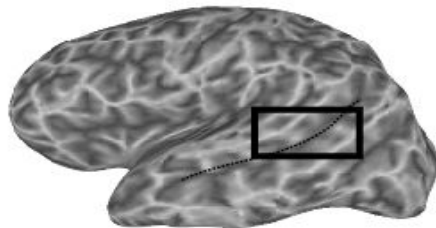
Yacoub et al. PNAS 2008

Multi-sensory integration

M.S. Beauchamp et al.,



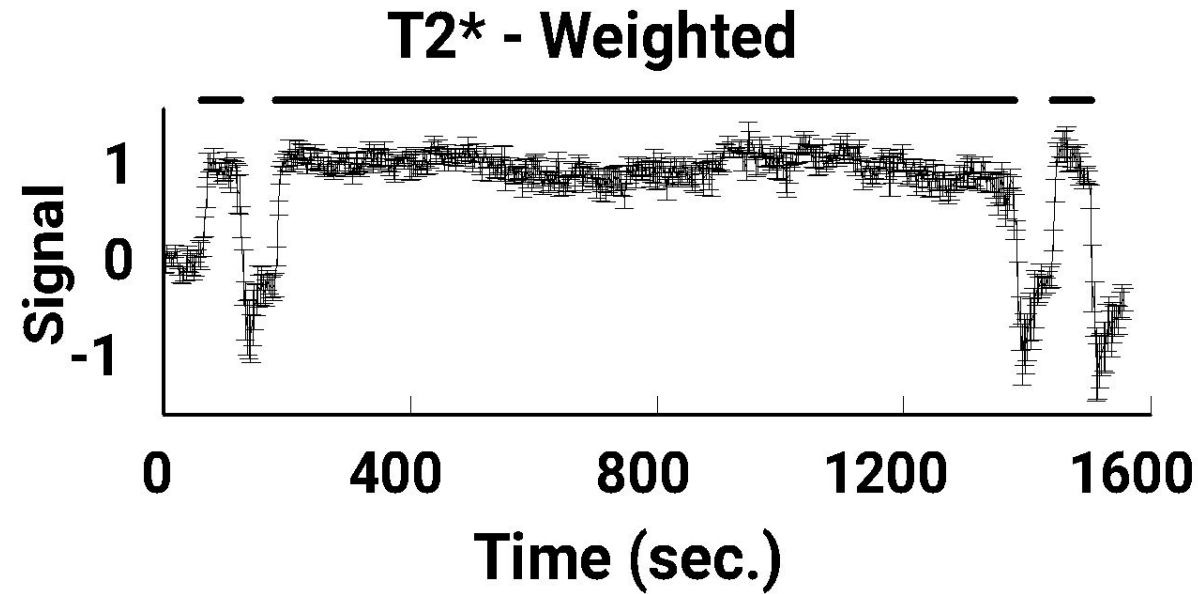
Visual
Auditory
Multisensory



Extracting Information from the fMRI Signal:

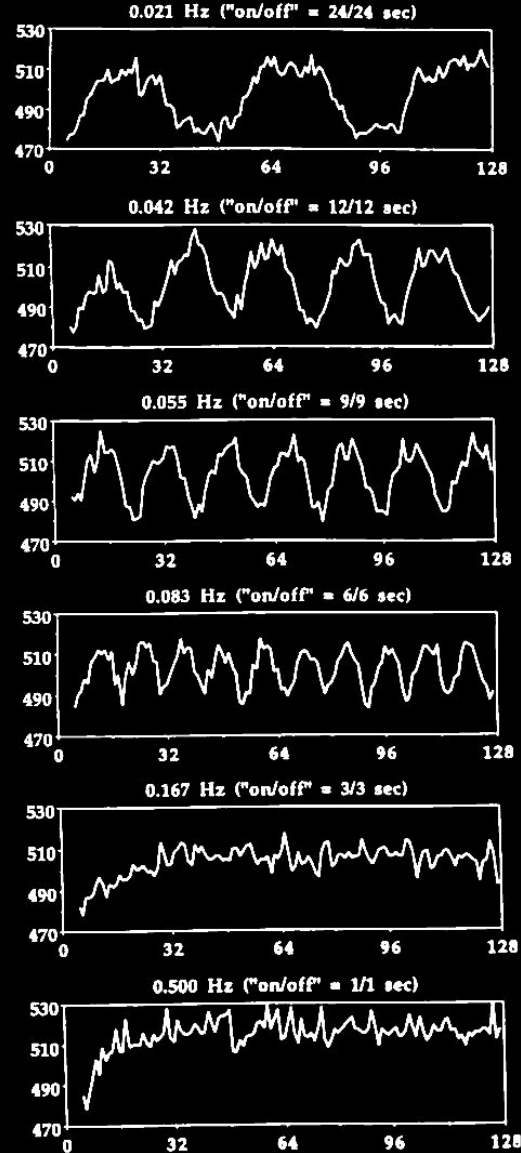
- **Spatial Resolution**
- **Temporal Resolution**
- **Sensitivity**

20 minutes continuous activation



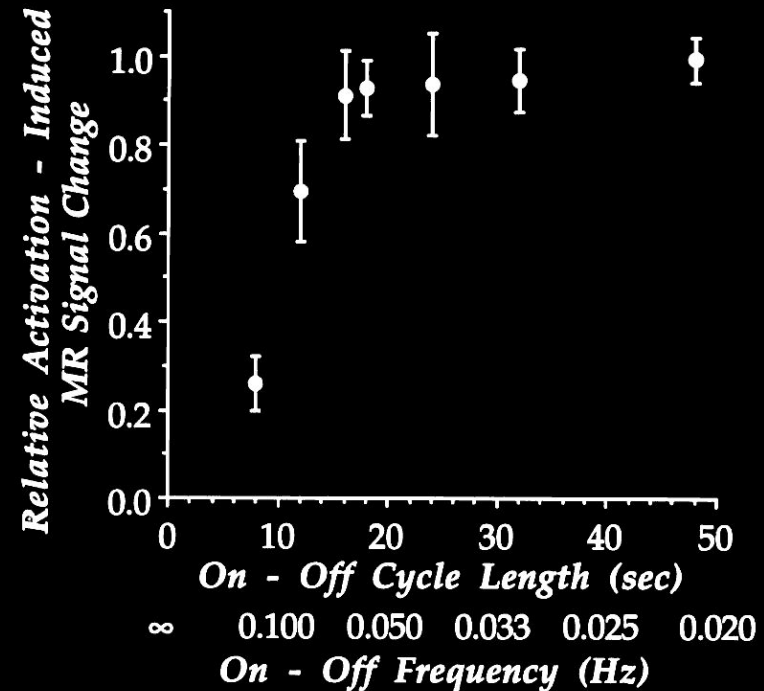
P. A. Bandettini, K. K. Kwong, T. L. Davis, R. B. H. Tootell, E. C. Wong, P. T. Fox, J. W. Belliveau, R. M. Weisskoff, B. R. Rosen, (1997). "Characterization of cerebral blood oxygenation and flow changes during prolonged brain activation." *Human Brain Mapping* 5, 93-109.

MRI Signal

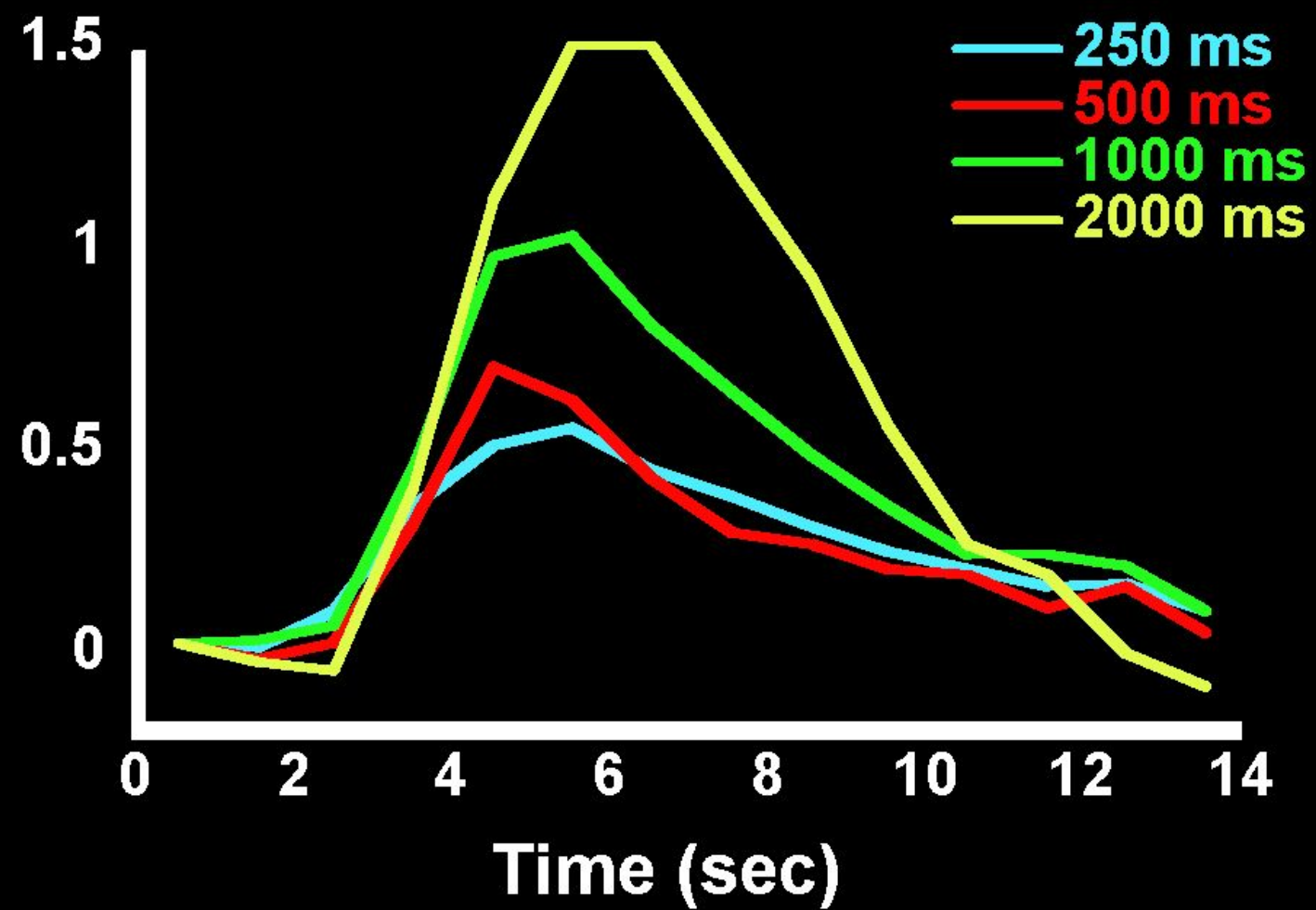


Time (seconds)

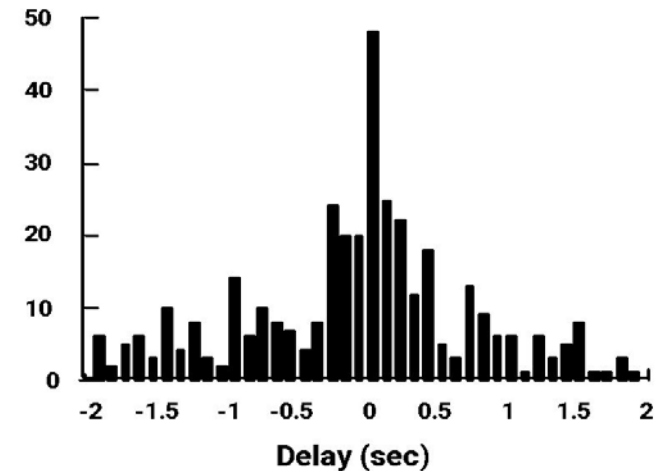
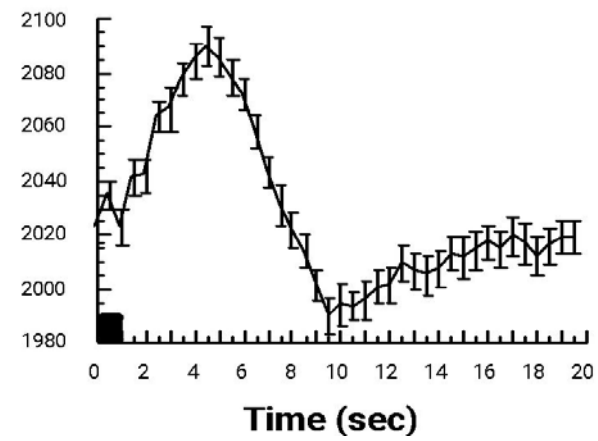
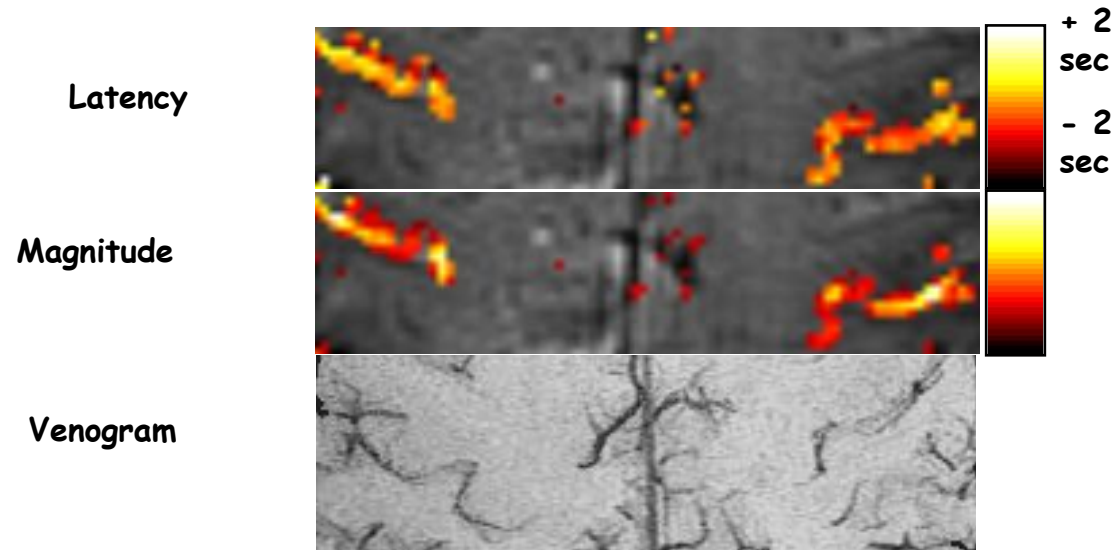
How rapidly can one switch on and off?



P. A. Bandettini,, Functional MRI using the BOLD approach: dynamic characteristics and data analysis methods, in "Diffusion and Perfusion: Magnetic Resonance Imaging" (D. L. Bihan, Ed.), p.351-362, Raven Press, New York, 1995.



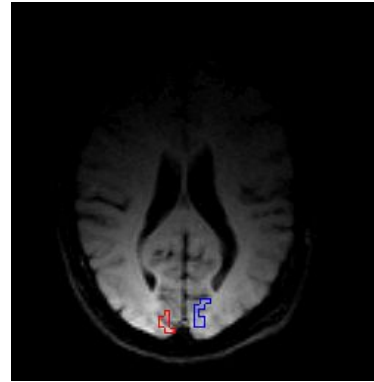
Latency Variation...



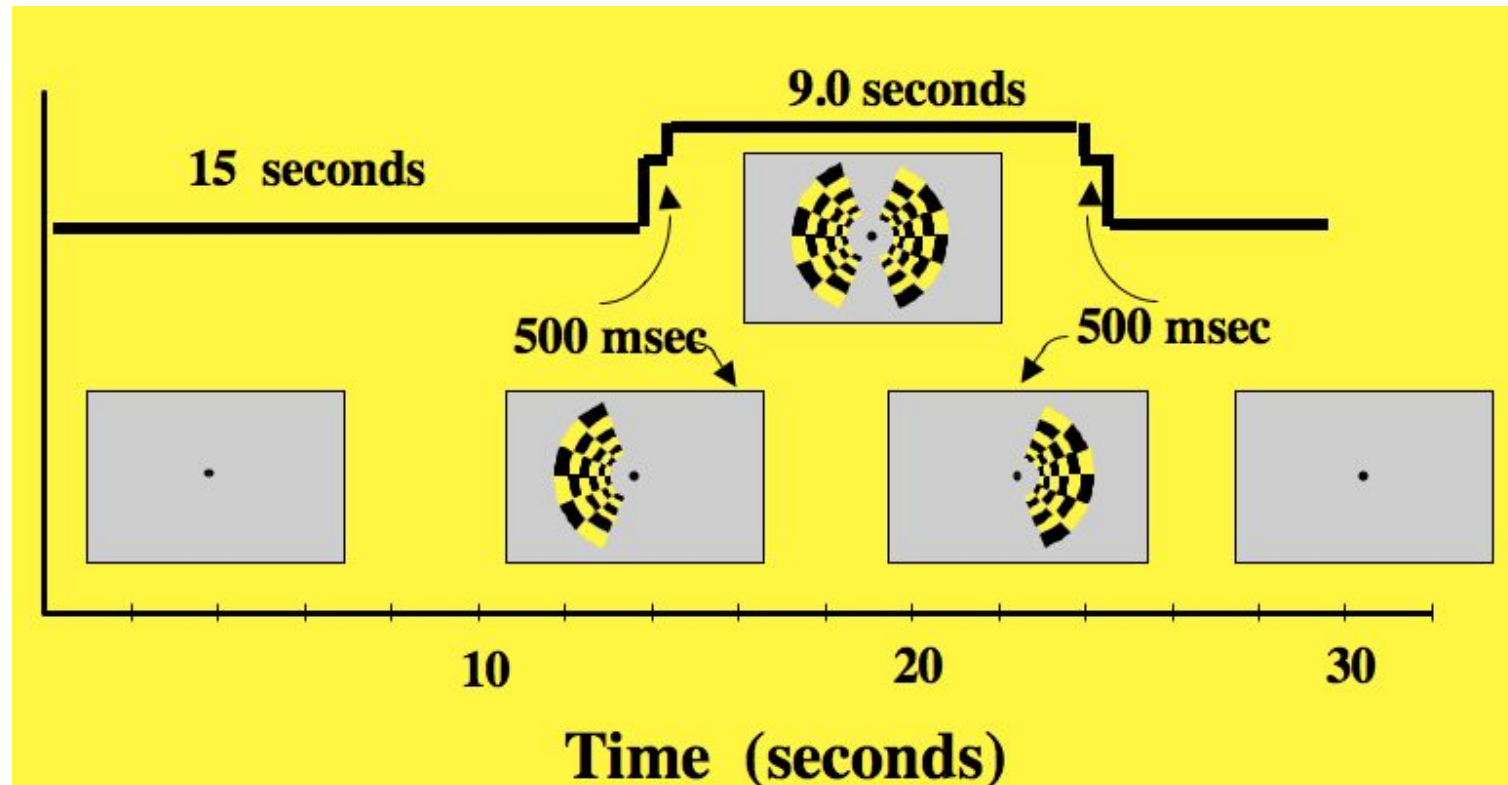
P. A. Bandettini, (1999) "Functional MRI" 205-220.

Hemi-Field Experiment

Right Hemisphere

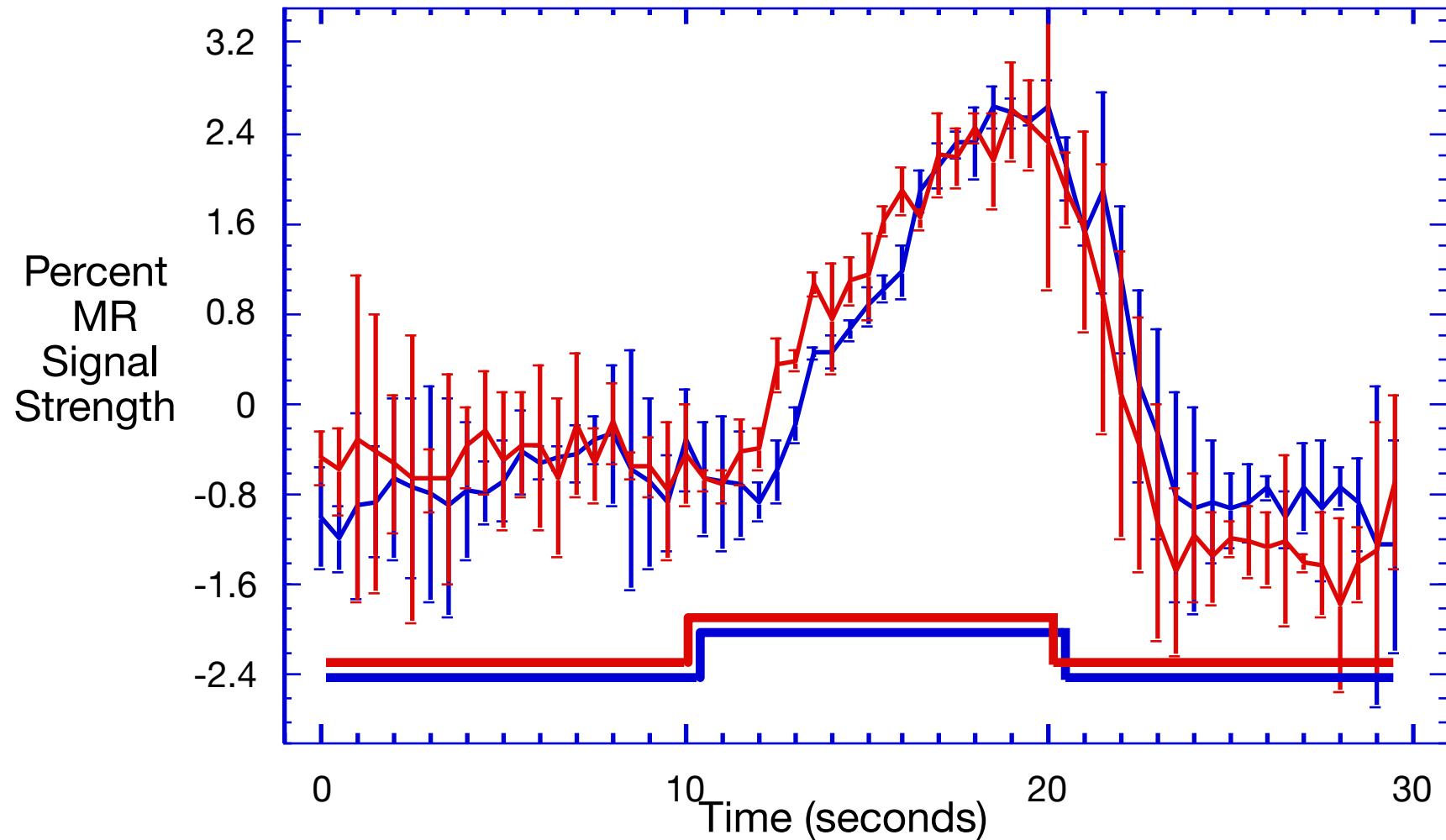


Left Hemisphere



Hemi-field with 500 msec asynchrony

Average of 6 runs



Proc. Natl. Acad. Sci. USA
Vol. 89, pp. 212–216, January 1992
Biophysics

Magnetic resonance imaging of perfusion using spin inversion of arterial water

(cerebral blood flow/adiabatic fast passage/hypercarbia/rat brain/cold injury)

DONALD S. WILLIAMS*, JOHN A. DETRE^{†‡}, JOHN S. LEIGH[†], AND ALAN P. KORETSKY*[§]

*Pittsburgh Nuclear Magnetic Resonance Center for Biomedical Research, and [§]Department of Biological Sciences, Carnegie Mellon University, Pittsburgh, PA 15213; and [†]Metabolic Magnetic Resonance Research Center, Department of Radiology, and [‡]Department of Neurology, University of Pennsylvania School of Medicine, Philadelphia, PA 19104

Communicated by Mildred Cohn, September 19, 1991

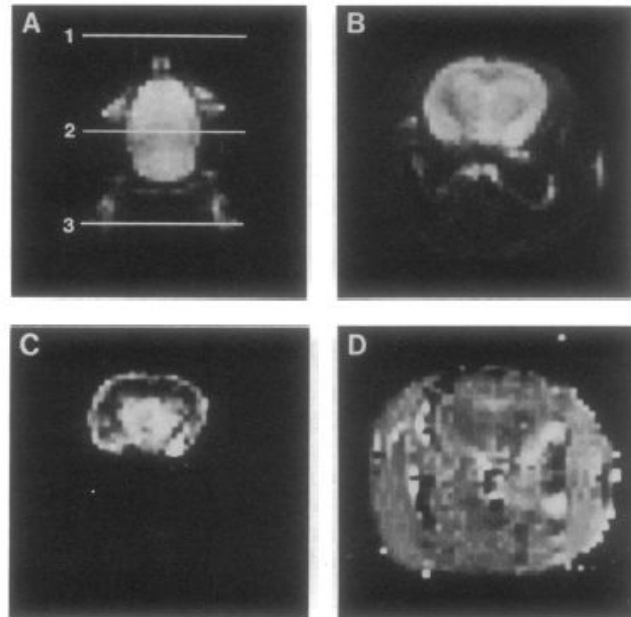


FIG. 2. (A) Coronal image of a rat head. The resonance planes for radiofrequency used for spin inversion by AFP for control and inversion images are indicated by 1 and 3, respectively, and plane 2 is the detection plane. (B) Control transverse image from the detection plane (plane 2 in A). (C) Difference image between control and inversion images. (D) T_{1app} image.

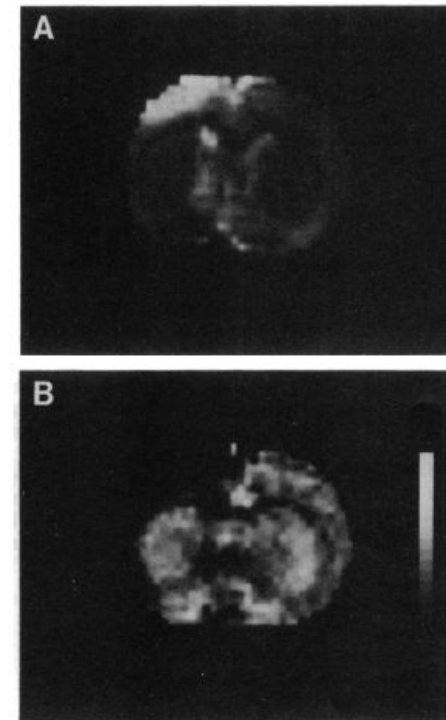
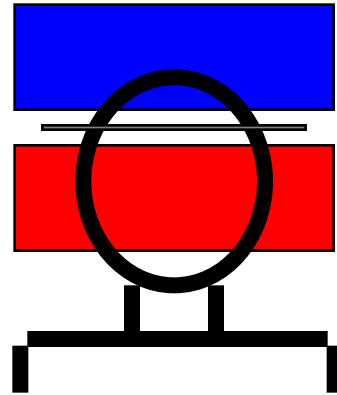


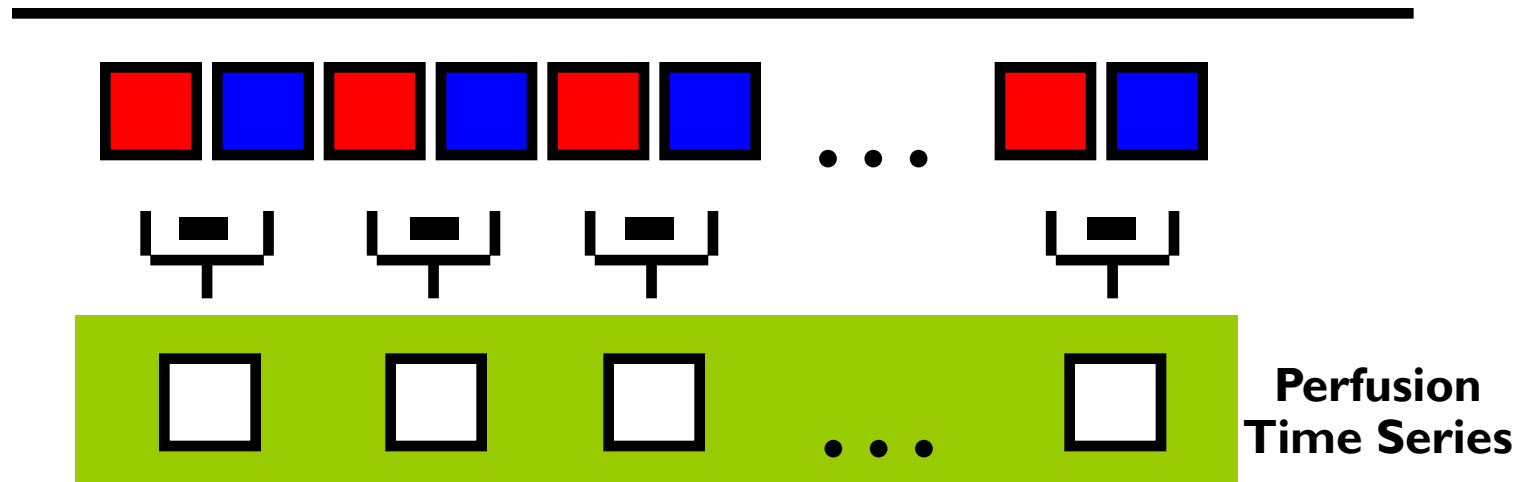
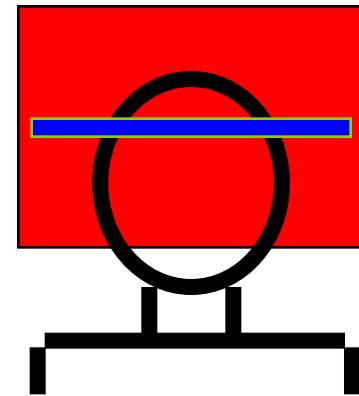
FIG. 5. Comparison of conventional MRI and perfusion imaging of a rat brain subjected to a regional cold injury. (A) Conventional T_2 -weighted image ($TE = 60$ ms, $TR = 2$ s). The injured region shows up as hyperintensity due to a longer T_2 . (B) Perfusion image of the same slice. The grey scale is from 0 to $6 \text{ ml} \cdot \text{g}^{-1} \cdot \text{min}^{-1}$. The injured region is dark due to low flow.

Blood Perfusion Contrast

EPISTAR



FAIR



TI (ms)

FAIR

EPISTAR

200

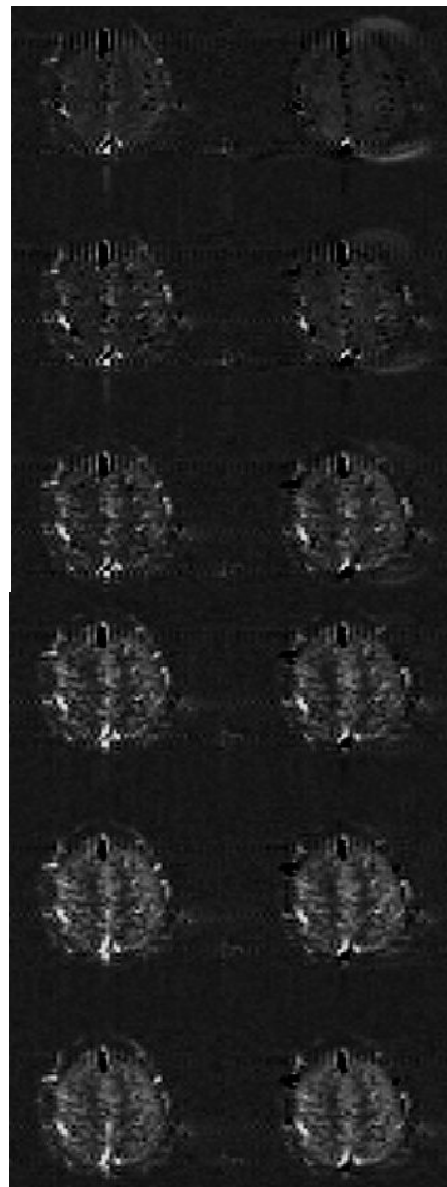
400

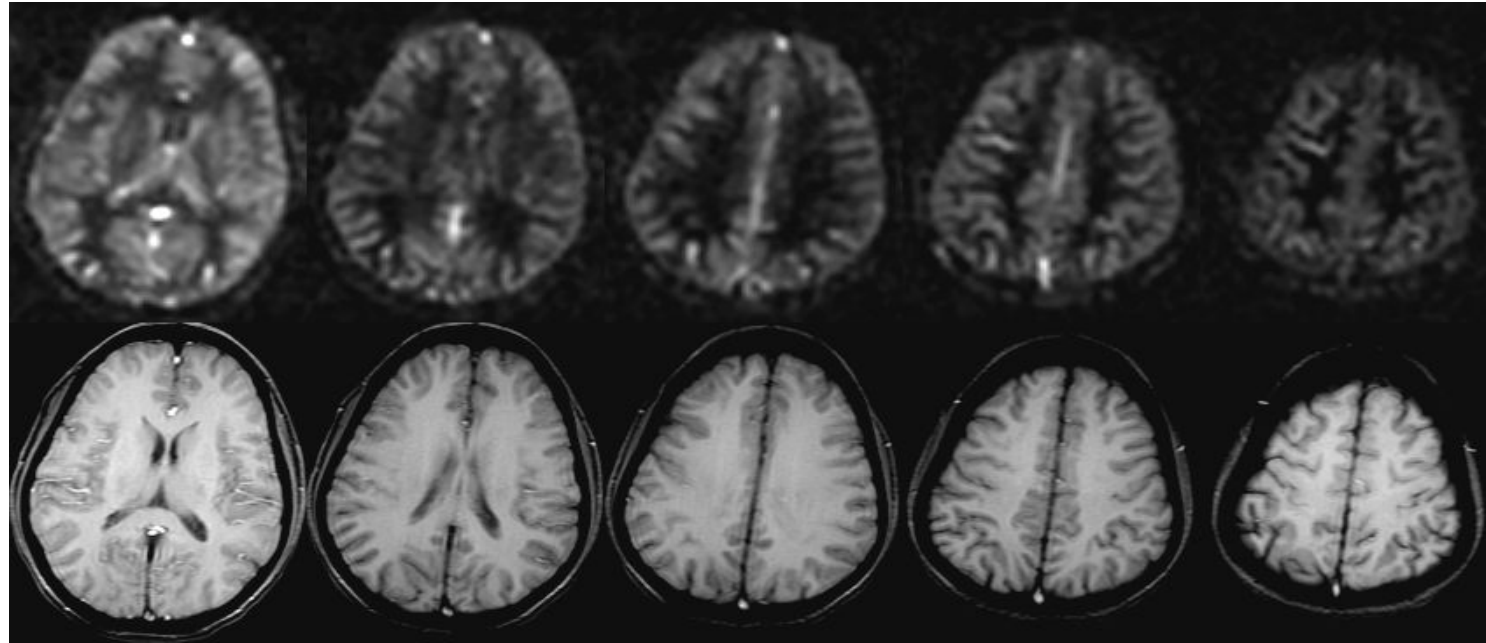
600

800

1000

1200





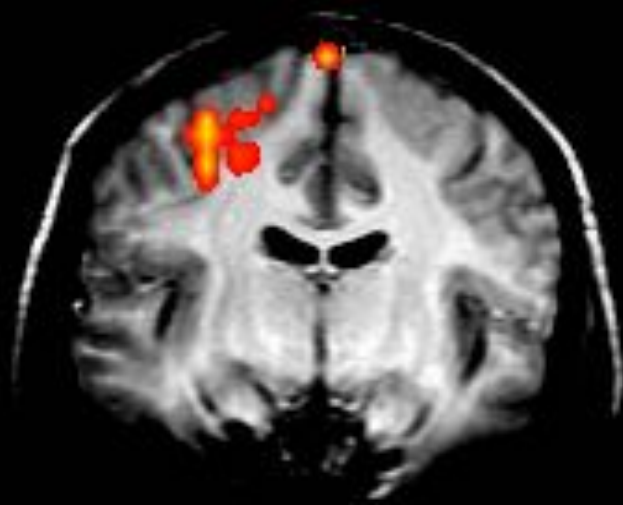
- Williams, D. S., Detre, J. A., Leigh, J. S. & Koretsky, A. S. (1992) "Magnetic resonance imaging of perfusion using spin-inversion of arterial water." **Proc. Natl. Acad. Sci. USA** **89**, 212-216.
- Edelman, R., Siewert, B. & Darby, D. (1994) "Qualitative mapping of cerebral blood flow and functional localization with echo planar MR imaging and signal targeting with alternating radiofrequency (EPISTAR)." **Radiology** **192**, 1-8.
- Kim, S.-G. (1995) "Quantification of relative cerebral blood flow change by flow-sensitive alternating inversion recovery (FAIR) technique: application to functional mapping." **Magn. Reson. Med.** **34**, 293-301.
- Kwong, K. K. et al. (1995) "MR perfusion studies with T1-weighted echo planar imaging." **Magn. Reson. Med.** **34**, 878-887.



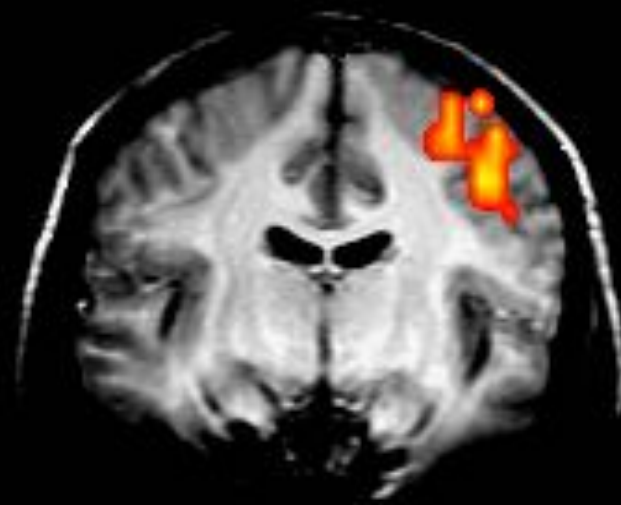
1991

Finger Movement

Left

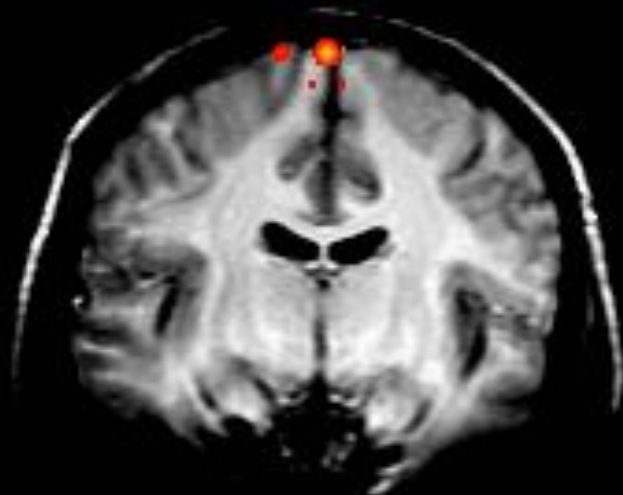


Right

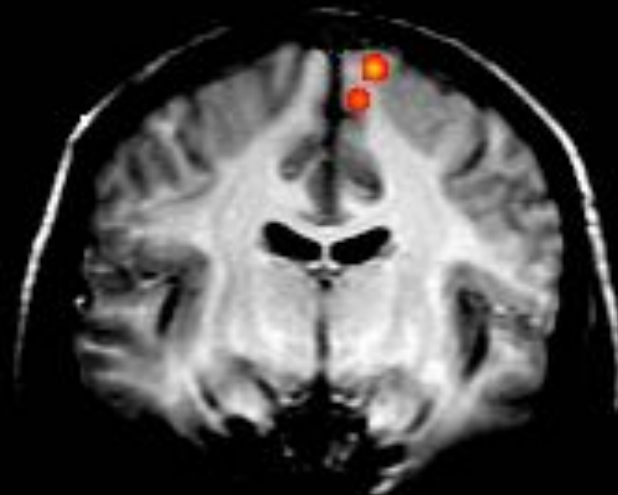


Toe Movement

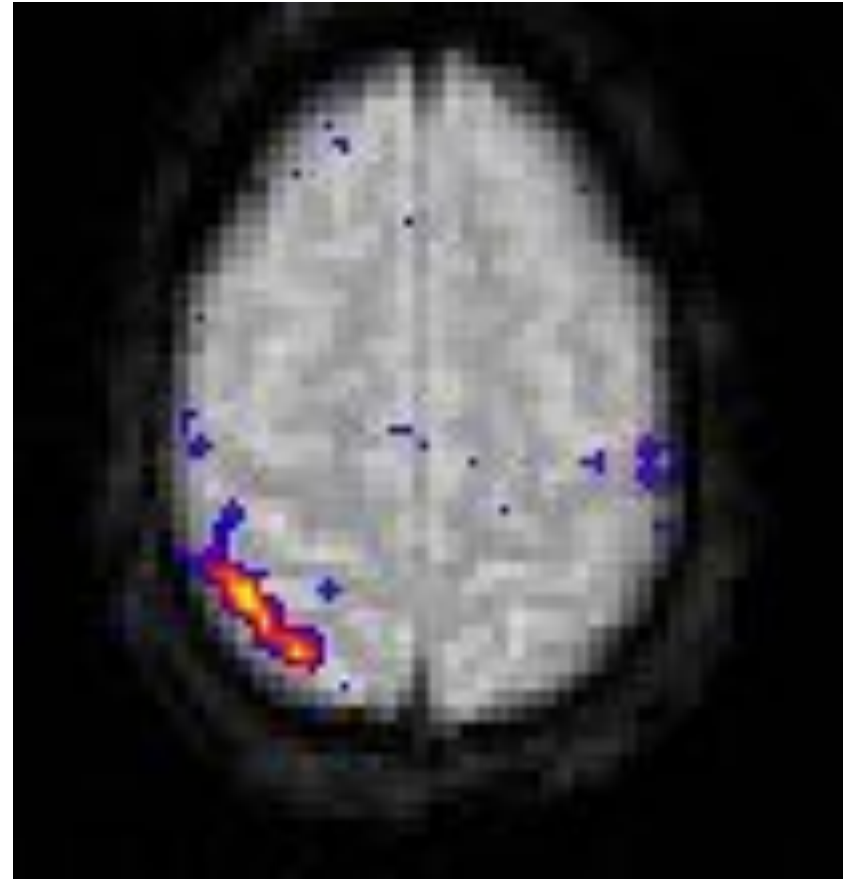
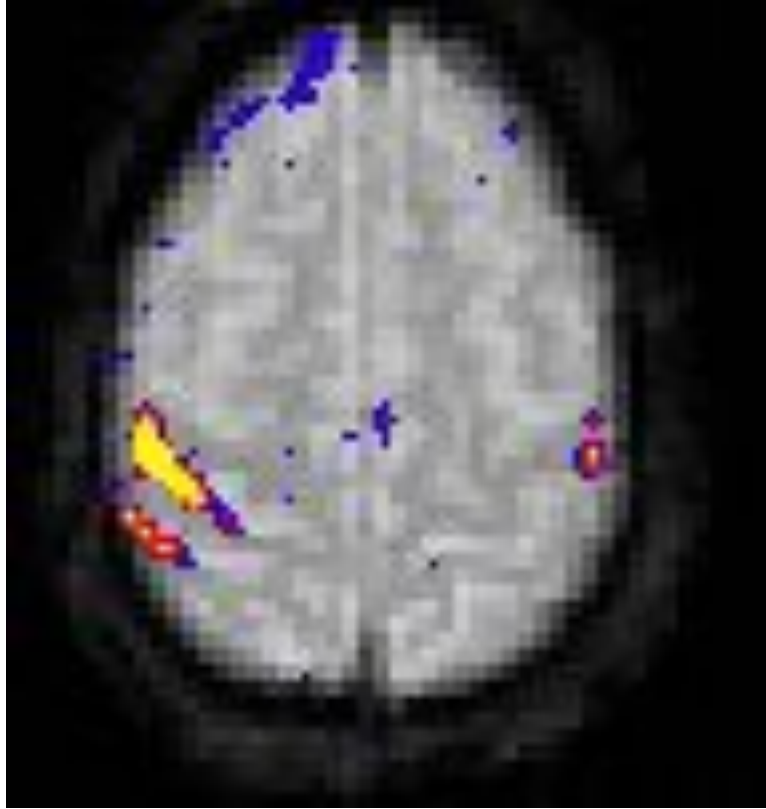
Left



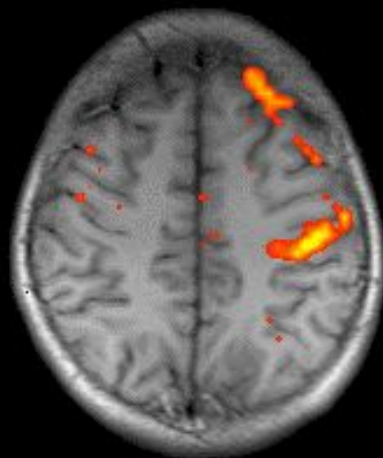
Right



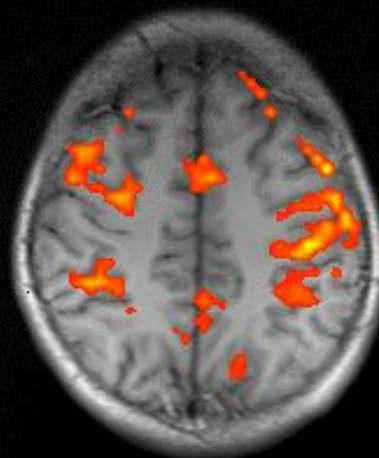
Tapping vs Pure Somatosensory



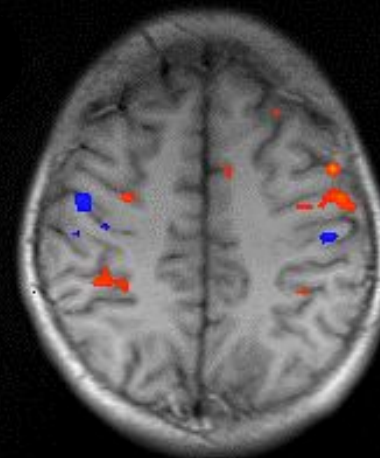
Simple Right



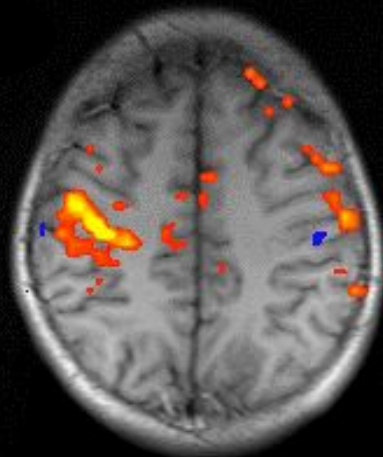
Complex Right



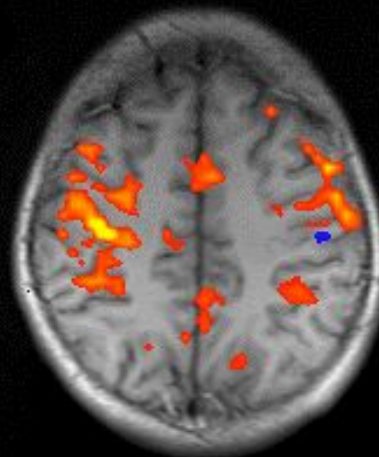
Complex Right



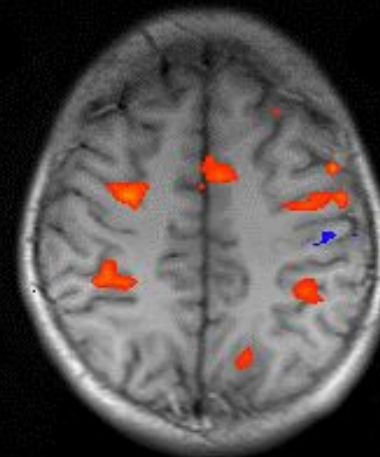
Simple Left



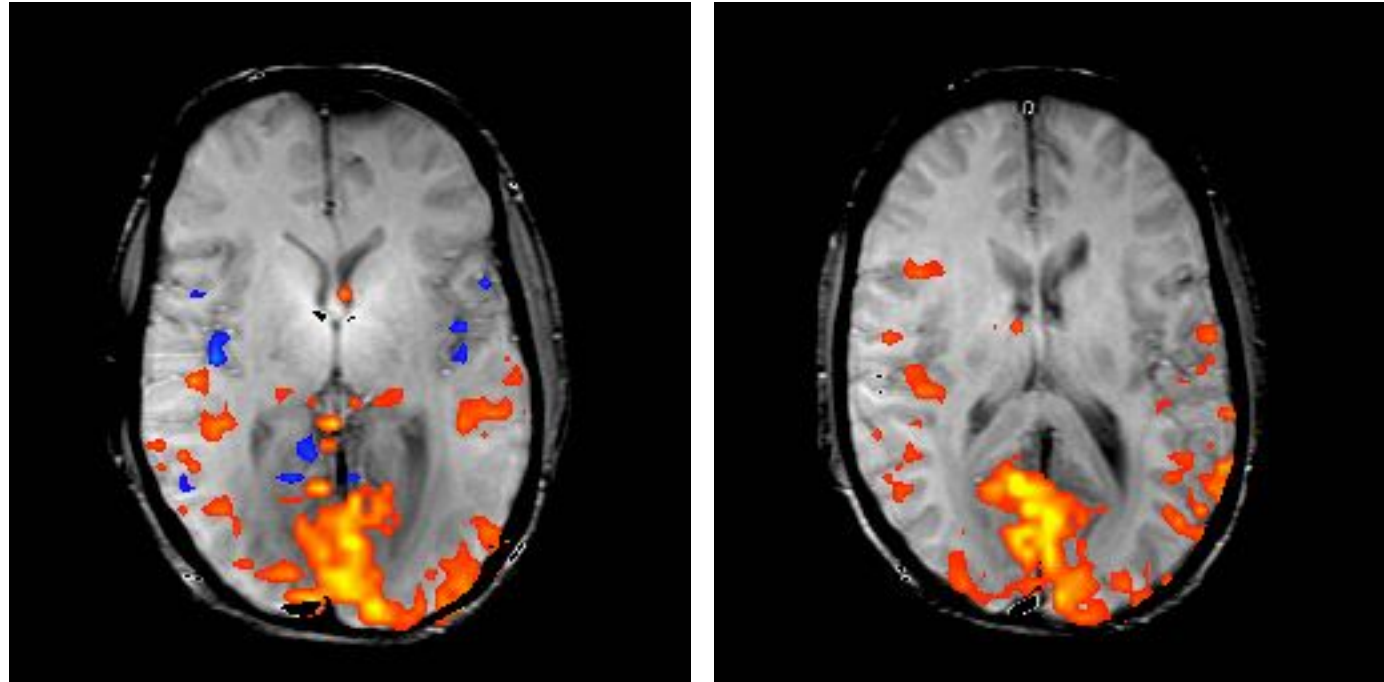
Complex Left



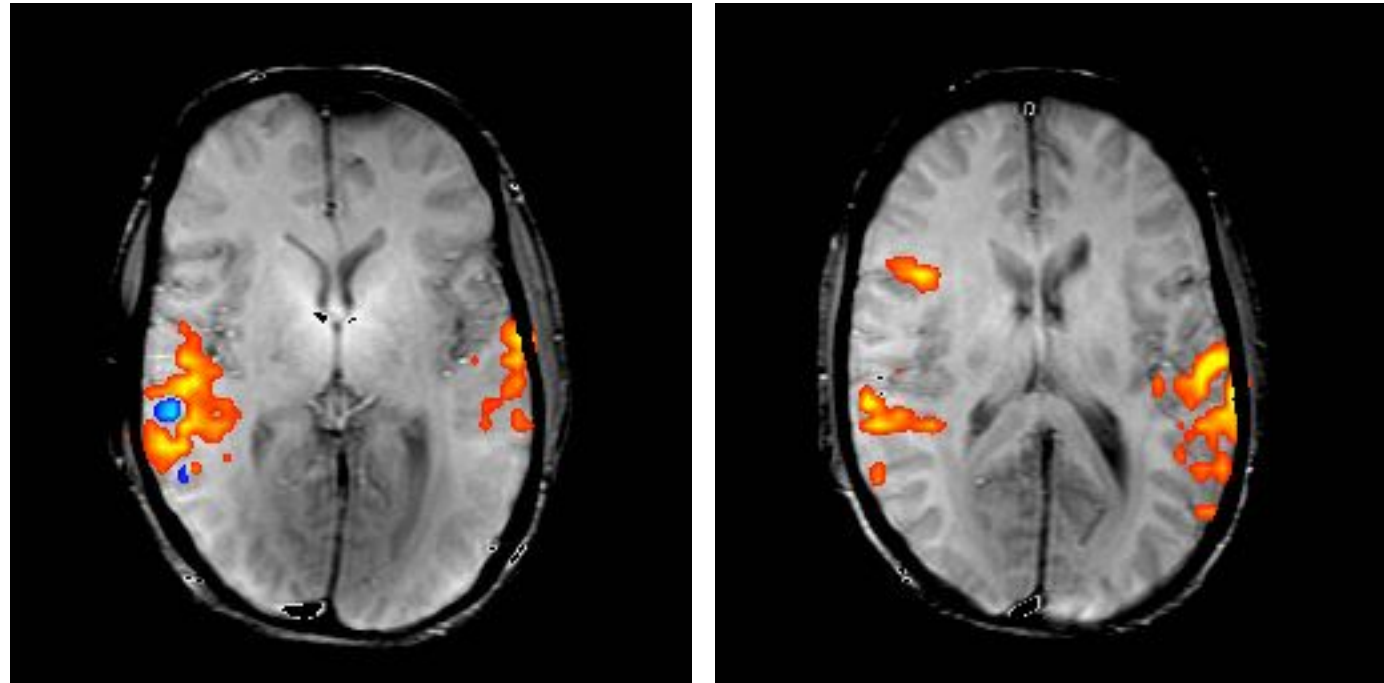
**Imagined
Complex Left**



Reading



Listening to Spoken Words

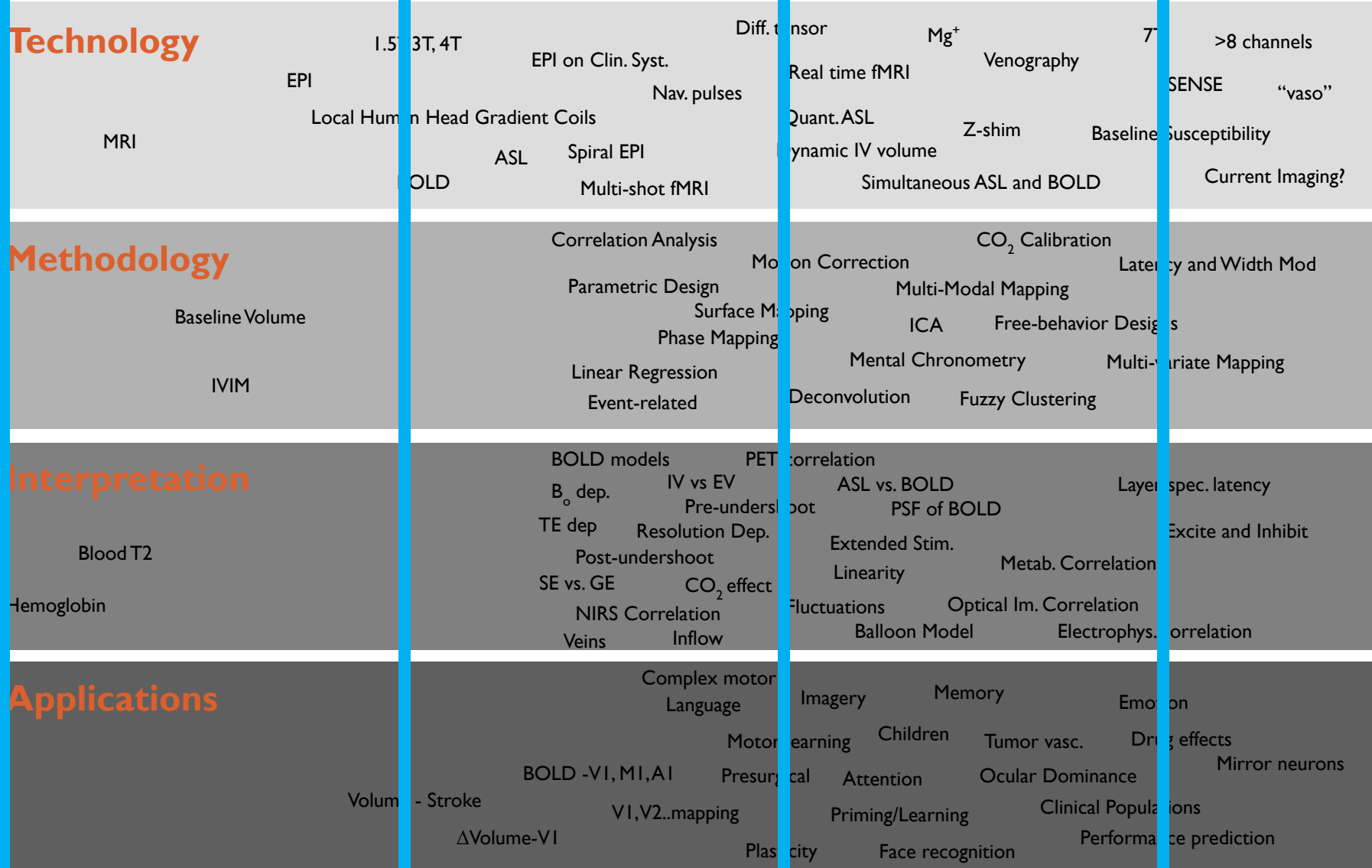
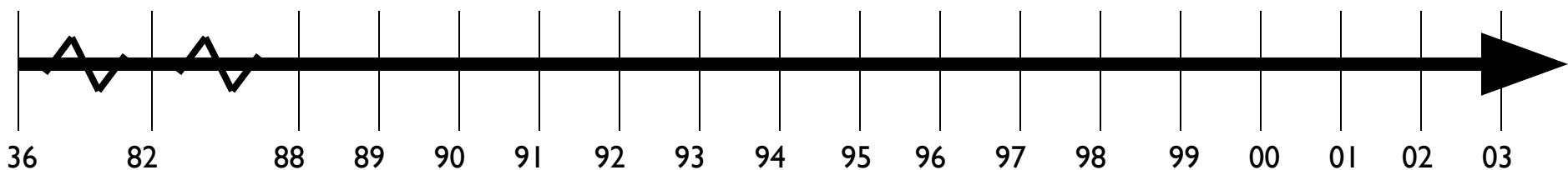


Technology

Methodology

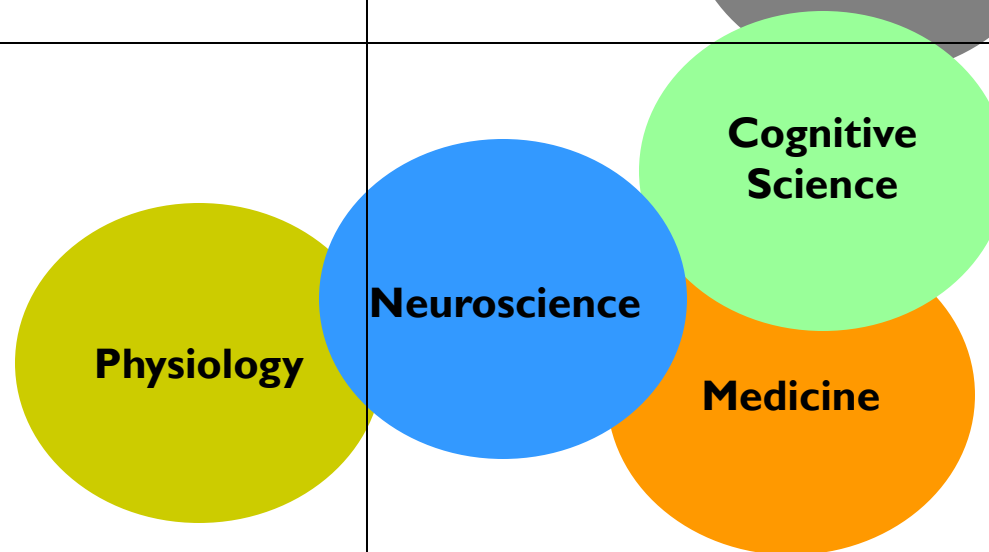
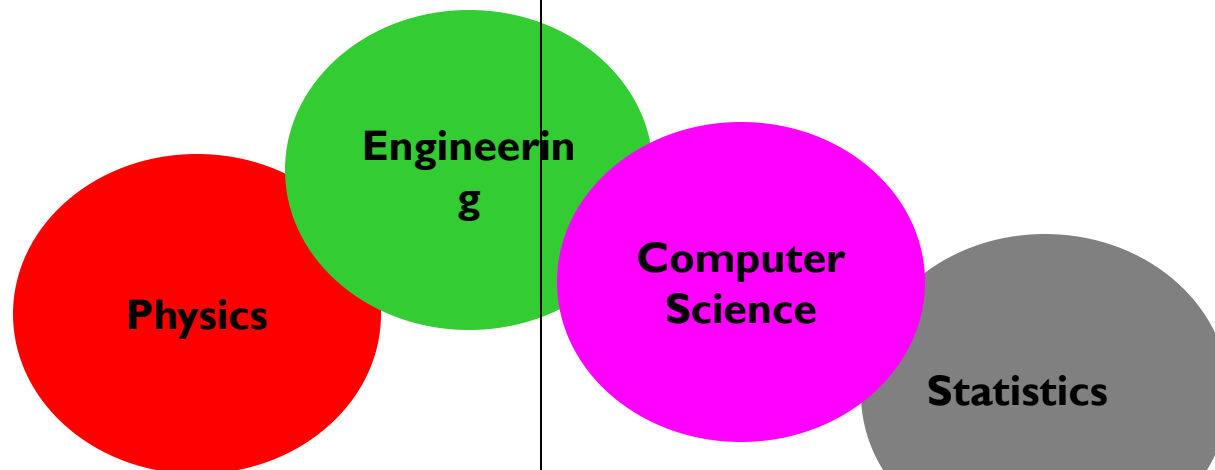
Interpretation

Applications



Technology

Methodology



Interpretation

Applications

Technology

Magnet
RF Coils
Pulse Sequences

Methodology

Paradigm Design
Pre and Post Processing
Subject Interface
Data Display and Comparison

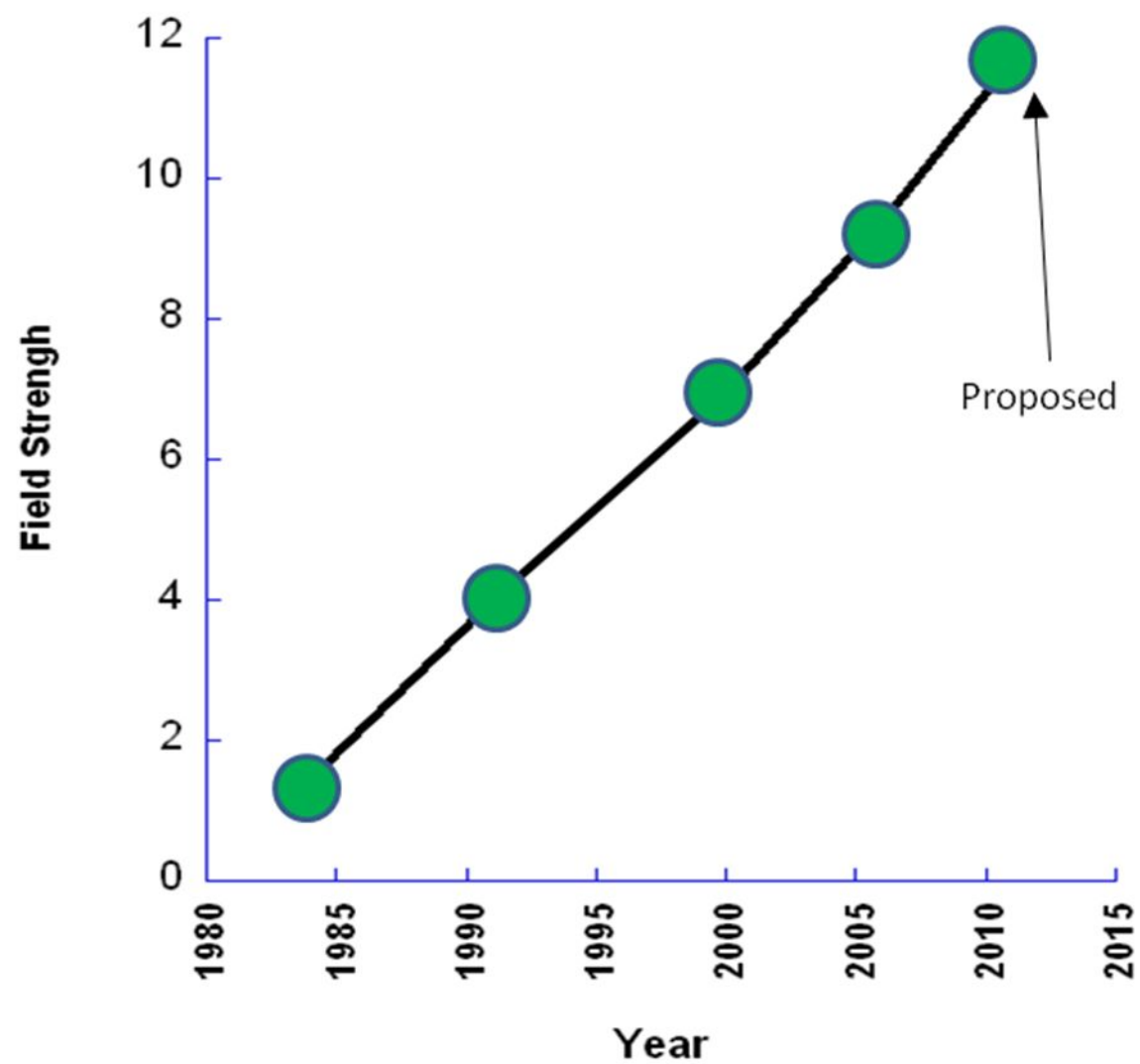
Increases
Decreases
Dynamics
Locations

Interpretation

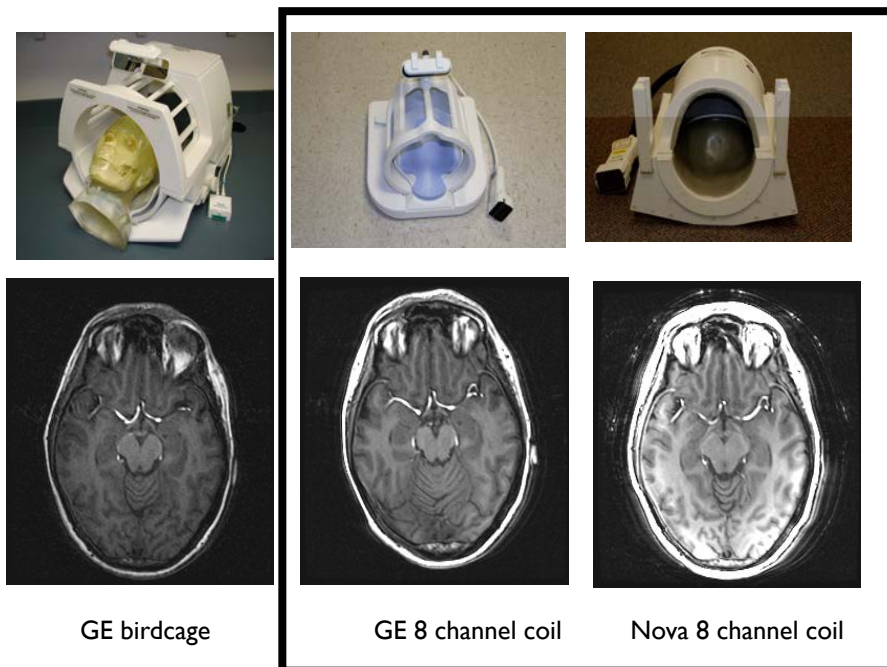
Neuroscience
Physiology
Genetics
Practical Clinical

Applications

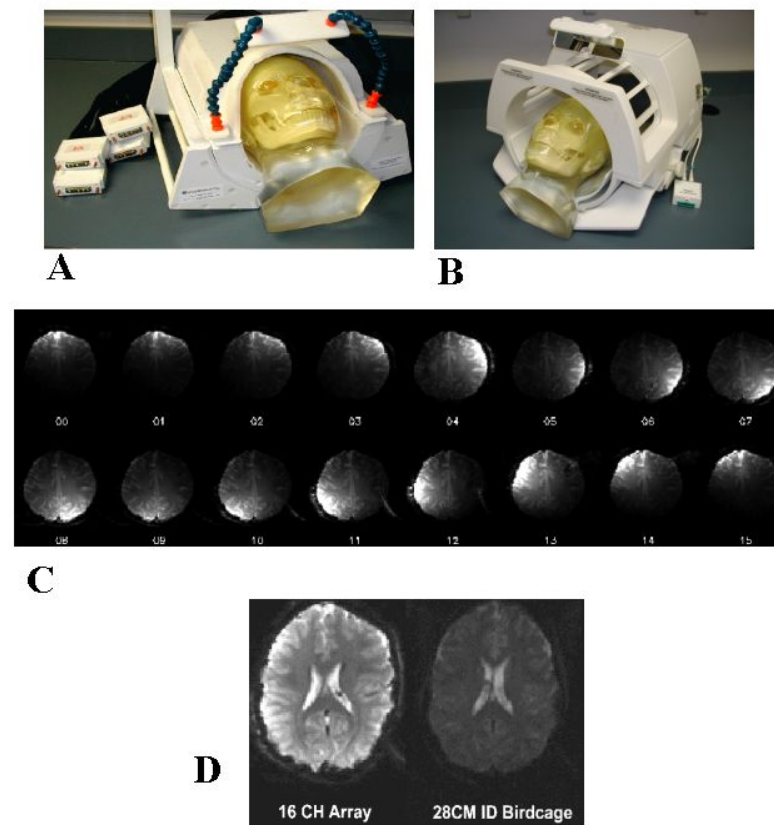
Progression of Human MRI Field Strength

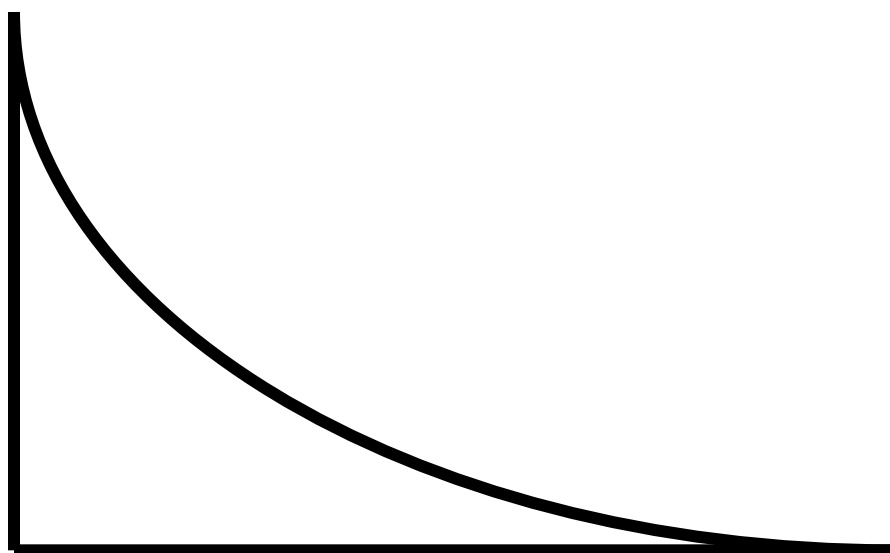


8 channel parallel receiver coil

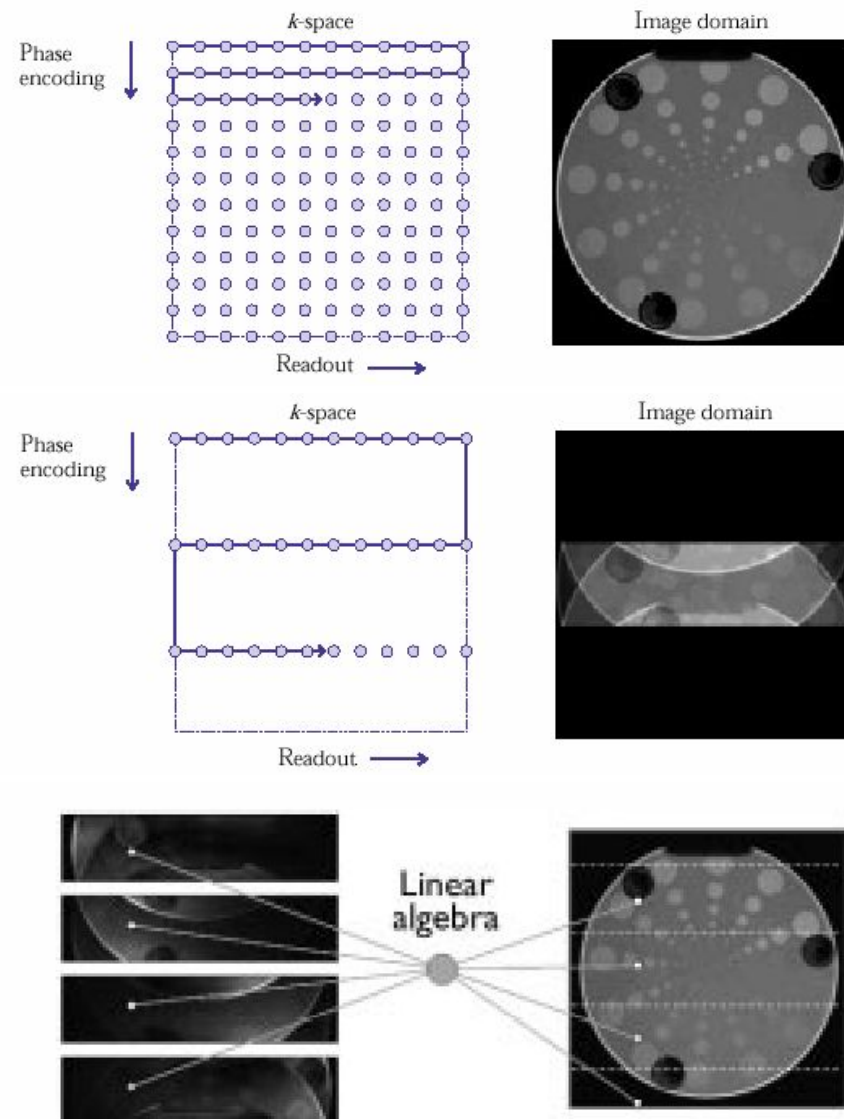


16 channel parallel receiver coil

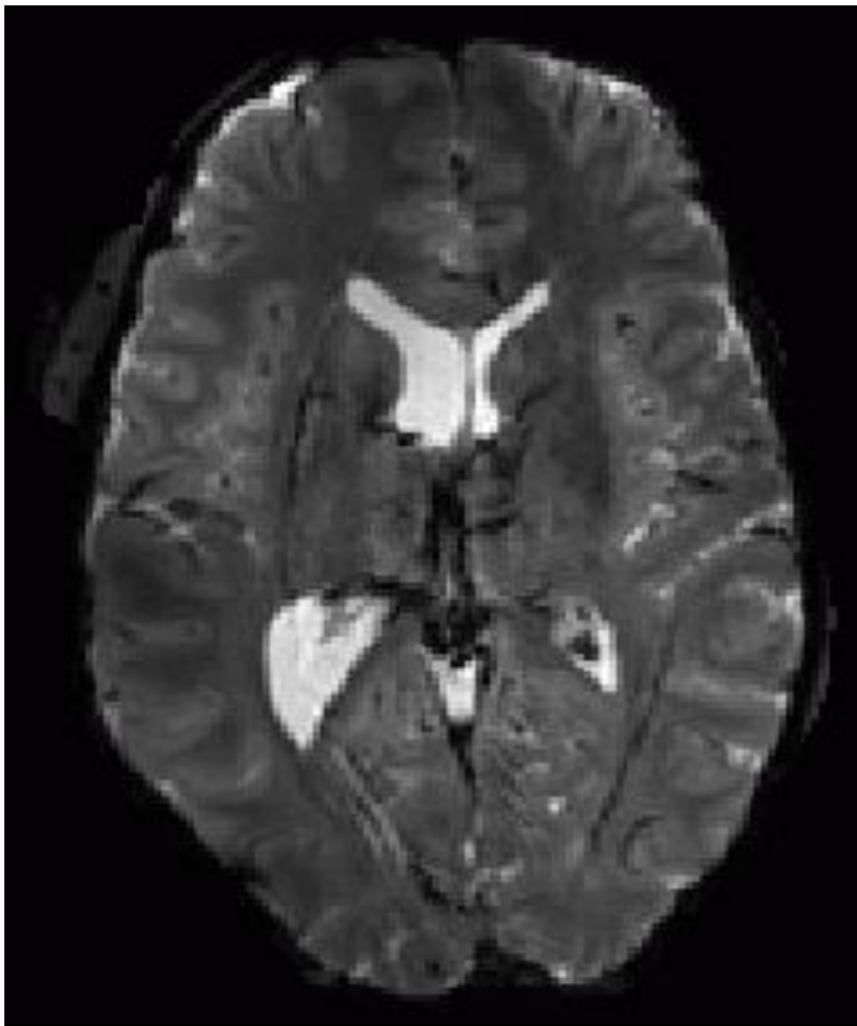




≈ 5 to 30 ms

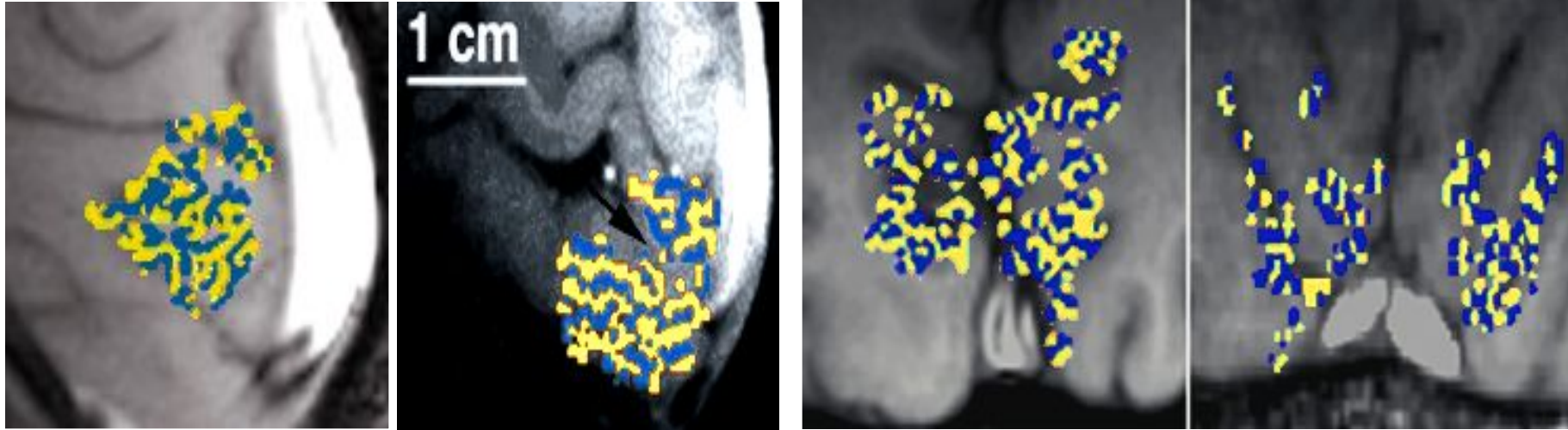


Pruessmann, et al.



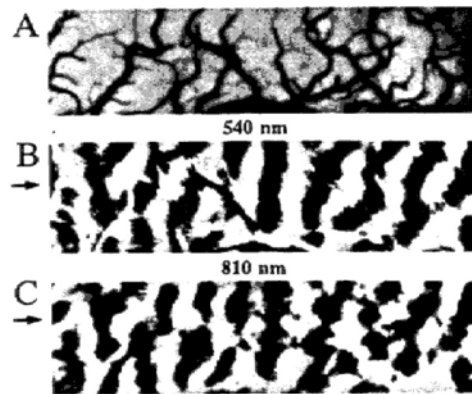
3T single-shot SENSE EPI using 16 channels: 1.25x1.25x2mm

Ocular Dominance Column Mapping

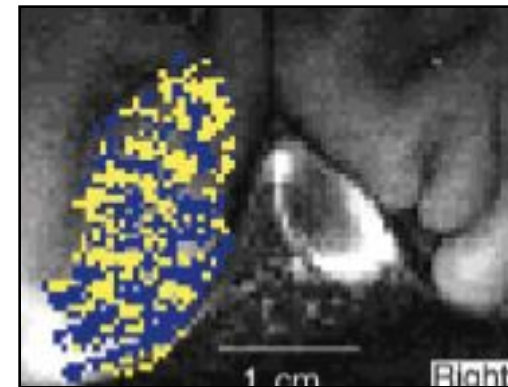


Menon, R. S., S. Ogawa, et al. (1997). *J Neurophysiol* 77(5): 2780-7.
0.54 x 0.54 in plane resolution

Optical Imaging

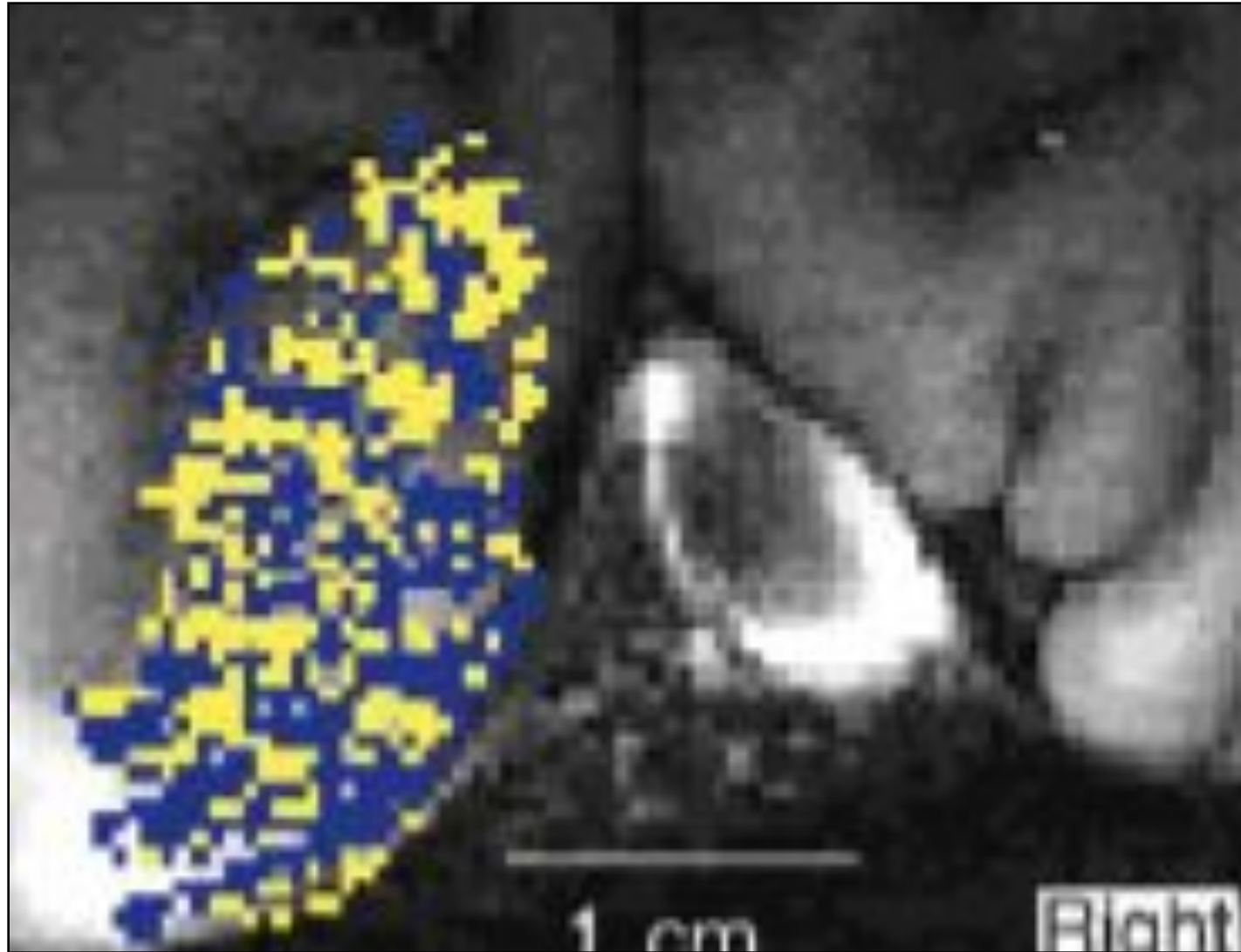


R. D. Frostig et. al, *PNAS* 87:
6082-6086, (1990).

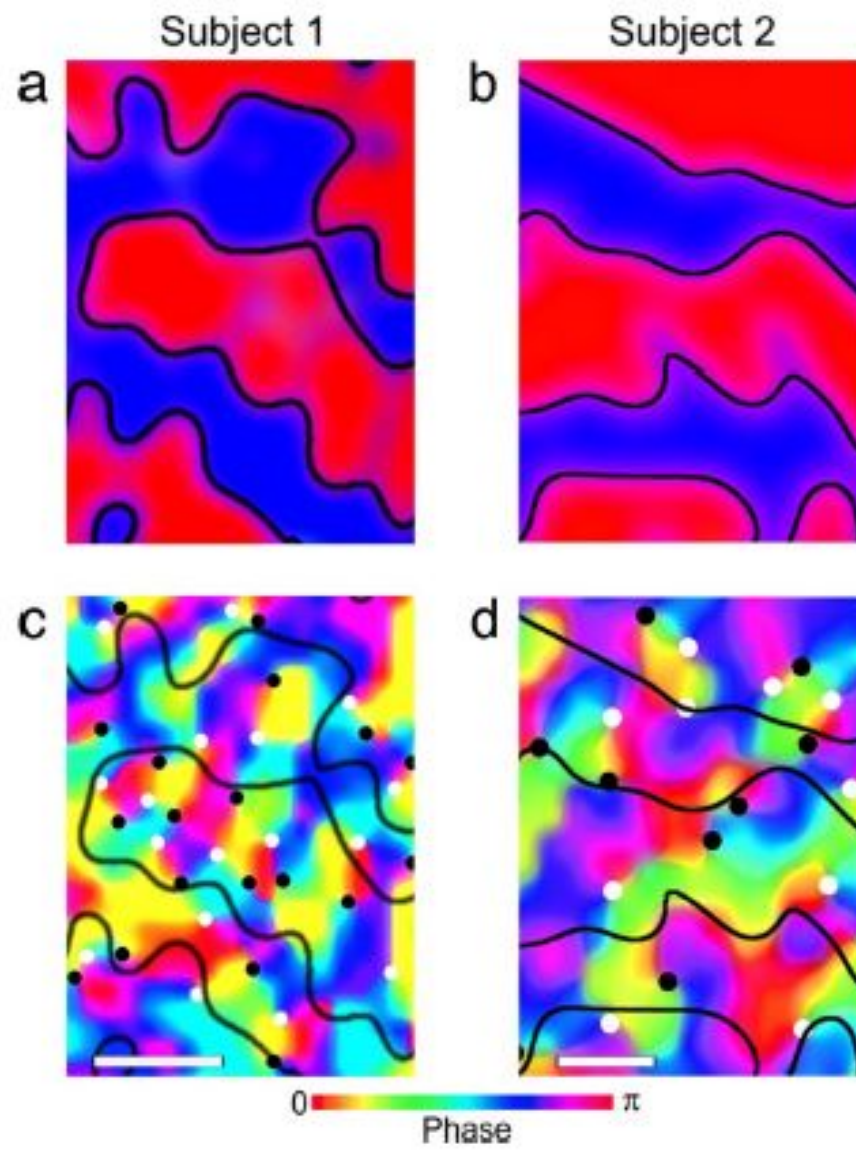


Cheng, et al. (2001)
Neuron, 32:359-374

0.47 x 0.47 in plane resolution

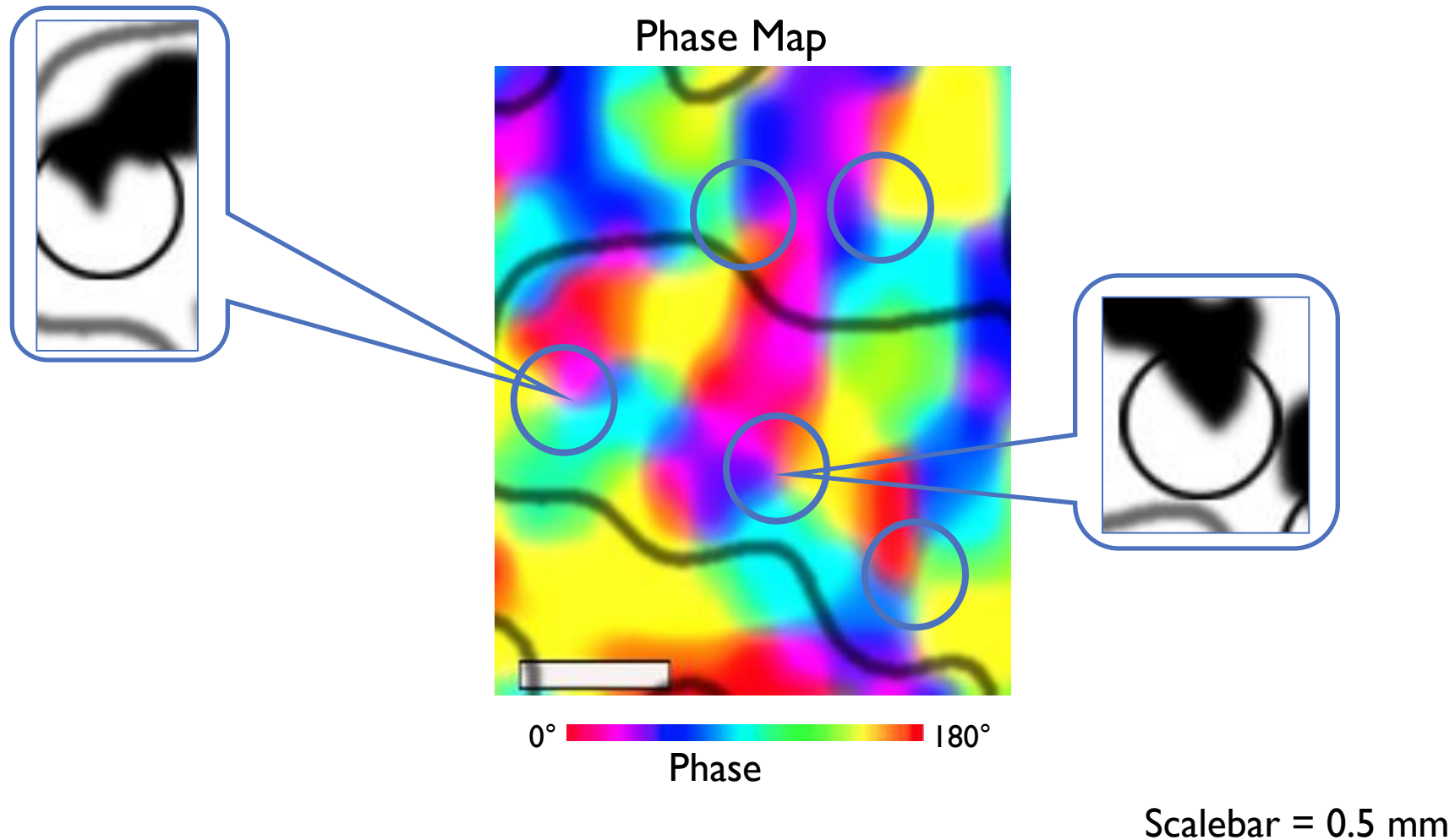


Cheng, et al. (2001) Neuron,32:359-374



Yacoub et al. PNAS 2008

Orientation Columns in Human VI as Revealed by fMRI at 7T



Yacoub et al. PNAS 2008

Technology

Magnet
RF Coils
Pulse Sequences

Methodology

Paradigm Design
Pre and Post Processing
Subject Interface
Data Display and Comparison

Increases
Decreases
Dynamics
Locations

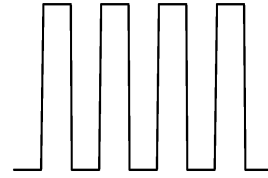
Interpretation

Neuroscience
Physiology
Genetics
Practical Clinical

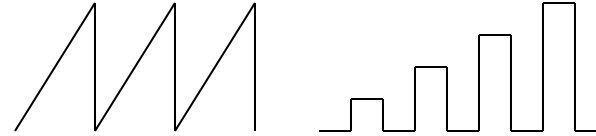
Applications

Neuronal Activation Input Strategies

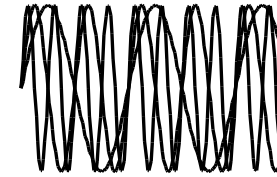
1. Block Design



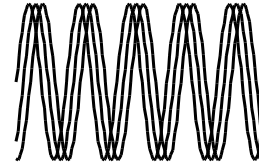
2. Parametric Design



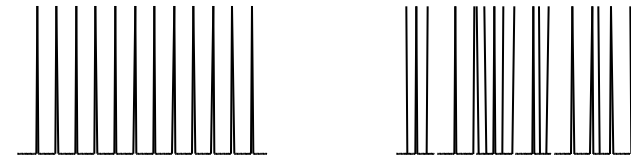
3. Frequency Encoding



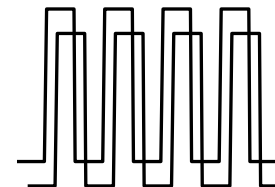
4. Phase Encoding



5. Event Related



6. Orthogonal Design

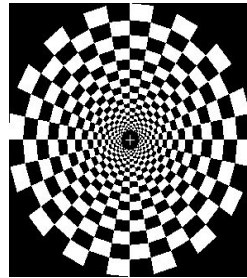


7. Free Behavior Design

Selective Averaging of Rapidly Presented Individual Trials Using fMRI

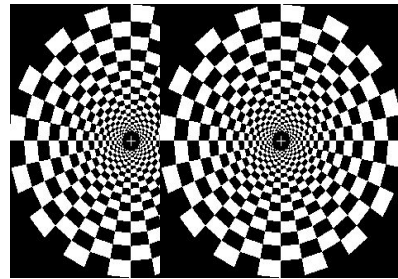
Anders M. Dale* and Randy L. Buckner

*Massachusetts General Hospital Nuclear Magnetic Resonance Center and the Department of Radiology,
Harvard Medical School, Boston, Massachusetts 02129*



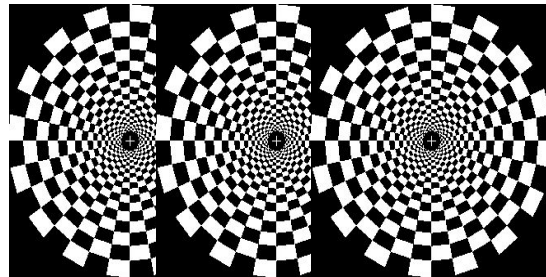
0 sec

20 sec



0 sec 2 sec

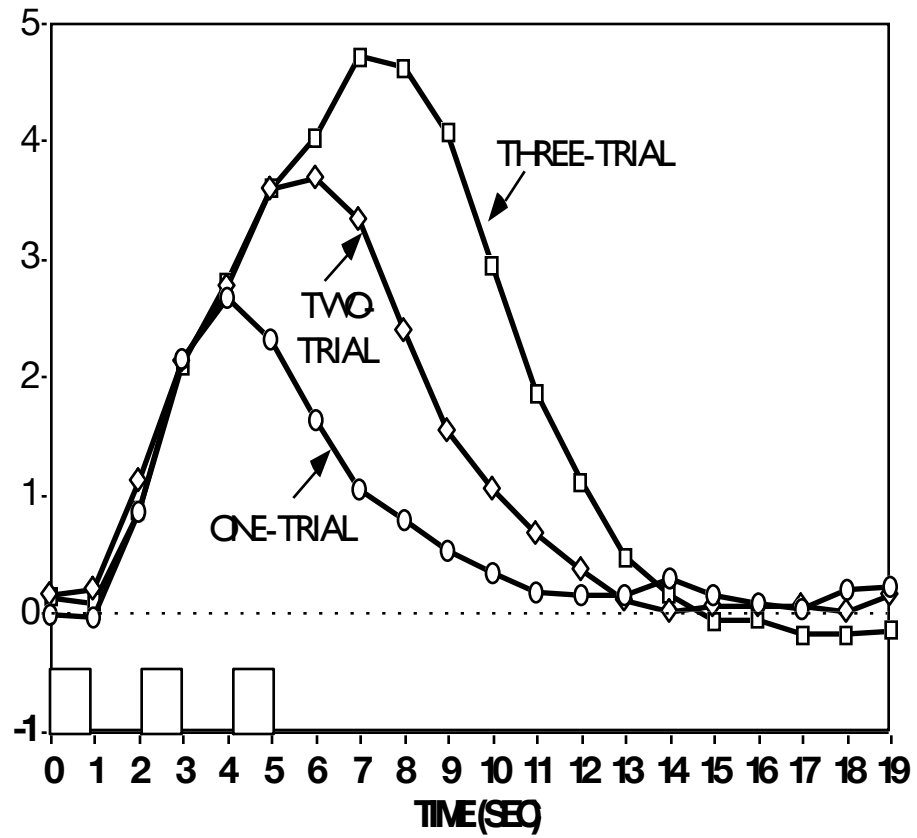
20 sec



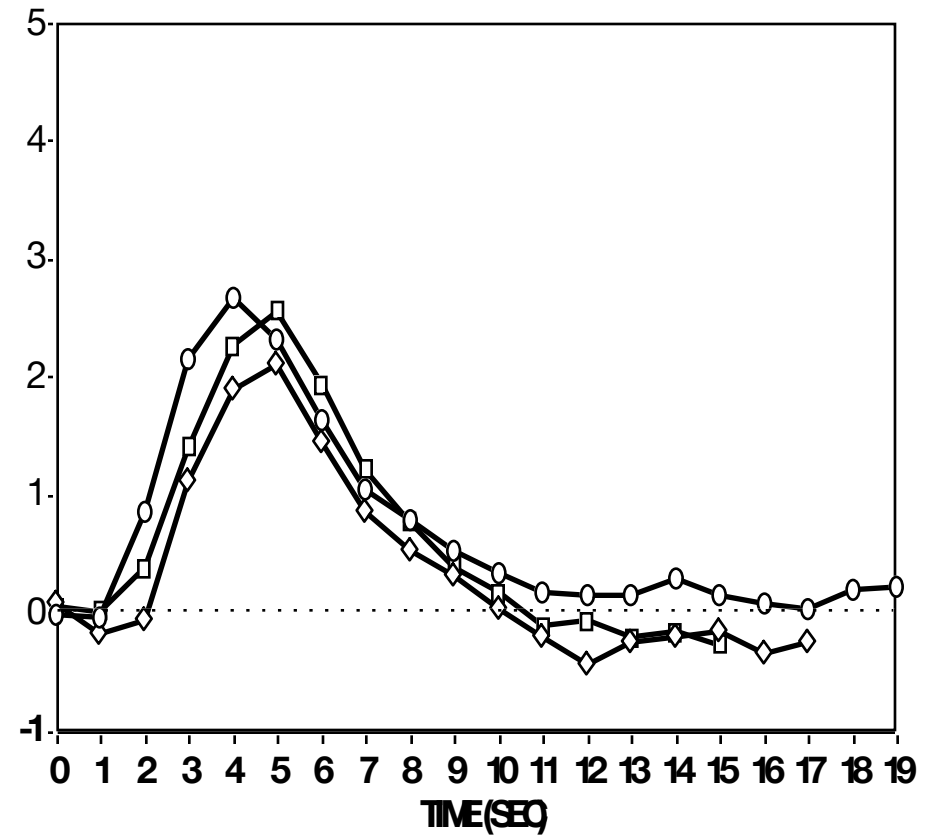
0 sec 2 sec 4 sec

20 sec

RAW DATA



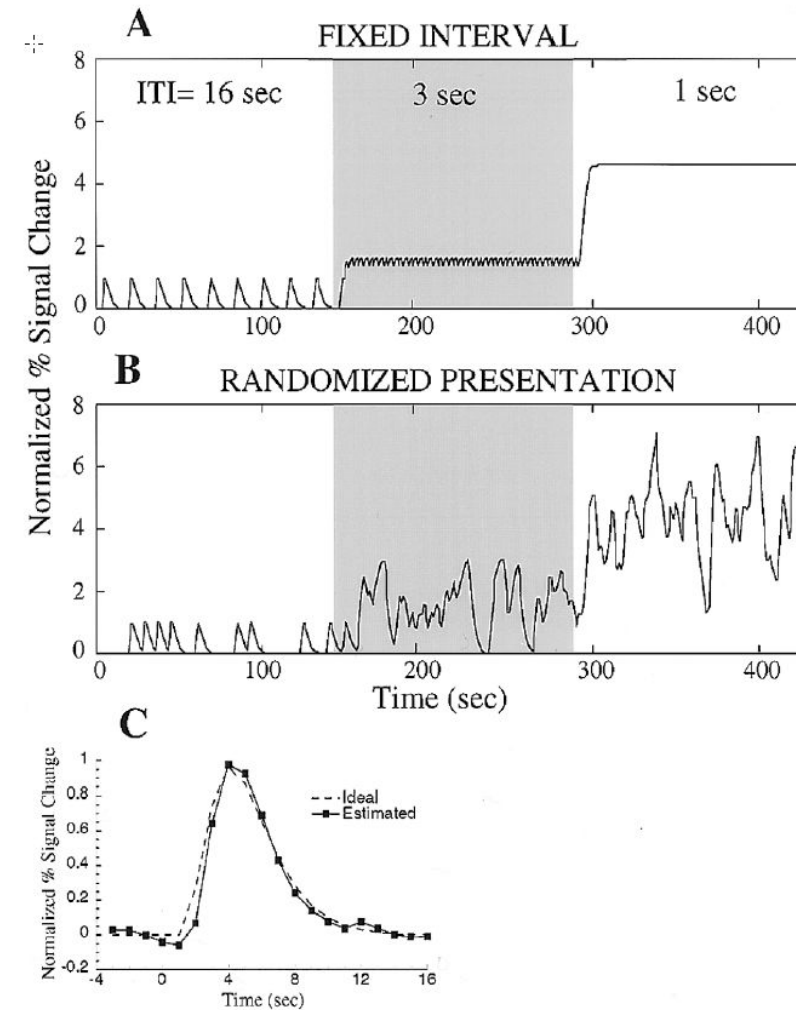
ESTIMATED RESPONSES



Randomized event-related experimental designs allow for extremely rapid presentation rates using functional MRI

Marc A. Burock,^{1,2} Randy L. Buckner,³
Marty G. Woldorff,⁴ Bruce R. Rosen¹
and Anders M. Dale^{1,CA}

¹Massachusetts General Hospital, Nuclear Magnetic Resonance Center, Bldg 149, 13th Street, Charlestown, MA 02129; ²Harvard-MIT Division of Health Sciences and Technology, Cambridge, MA 02129; ³Washington University, Department of Psychology, St. Louis, MO 63130; ⁴University of Texas Health Science Center, Research Imaging Center, San Antonio, TX 78284, USA



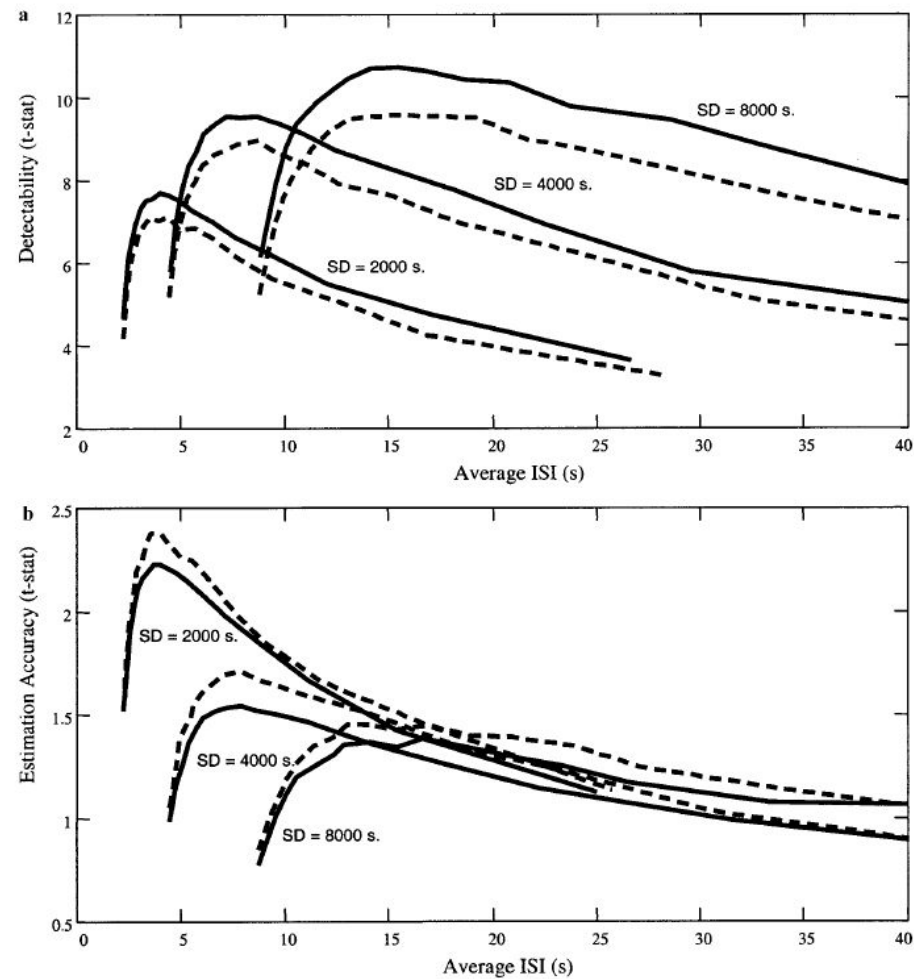
RAPID COMMUNICATION

Detection versus Estimation in Event-Related fMRI: Choosing the Optimal Stimulus Timing

Rasmus M. Birn, Robert W. Cox,* and Peter A. Bandettini

*3T Functional Neuroimaging Core, National Institute of Mental Health, and *Scientific and Statistical Computing Core,
National Institute of Mental Health, Bethesda, Maryland*

Received December 28, 2000



Fluctuations

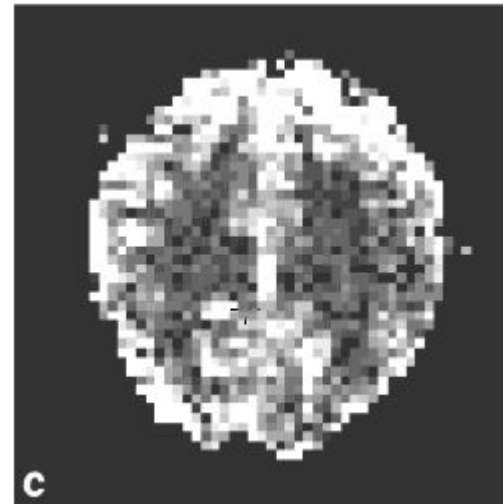
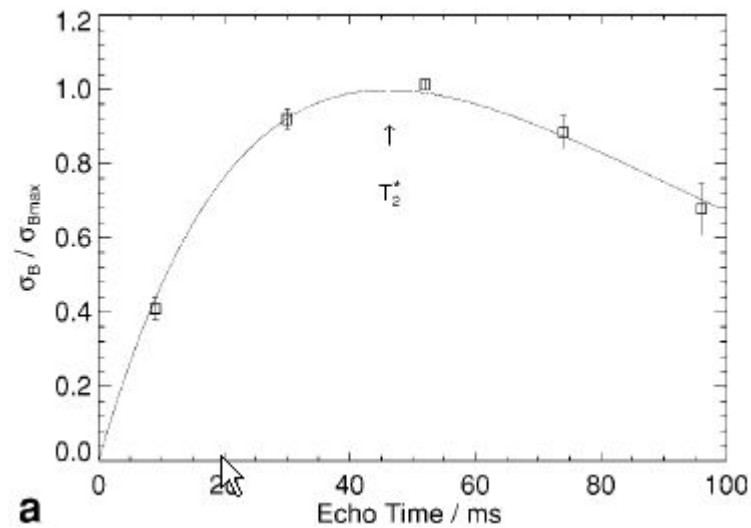
Patterns

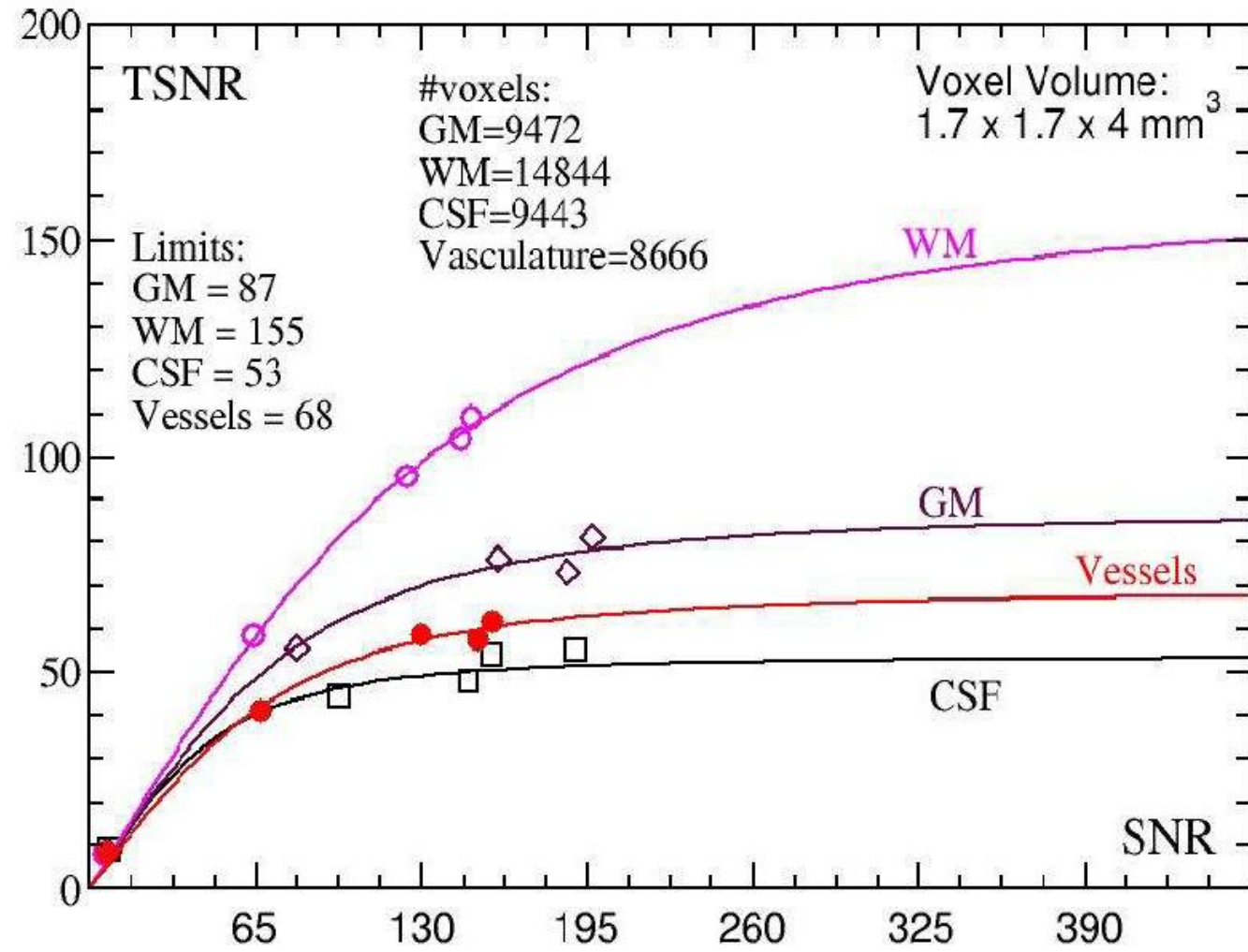
Fluctuations

Patterns

Physiological Noise in Oxygenation-Sensitive Magnetic Resonance Imaging

Gunnar Krüger* and Gary H. Glover

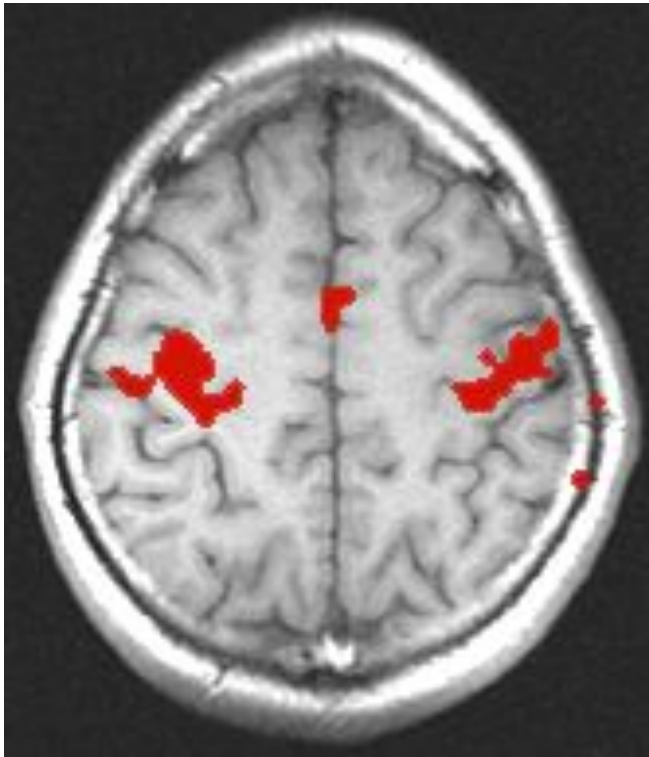




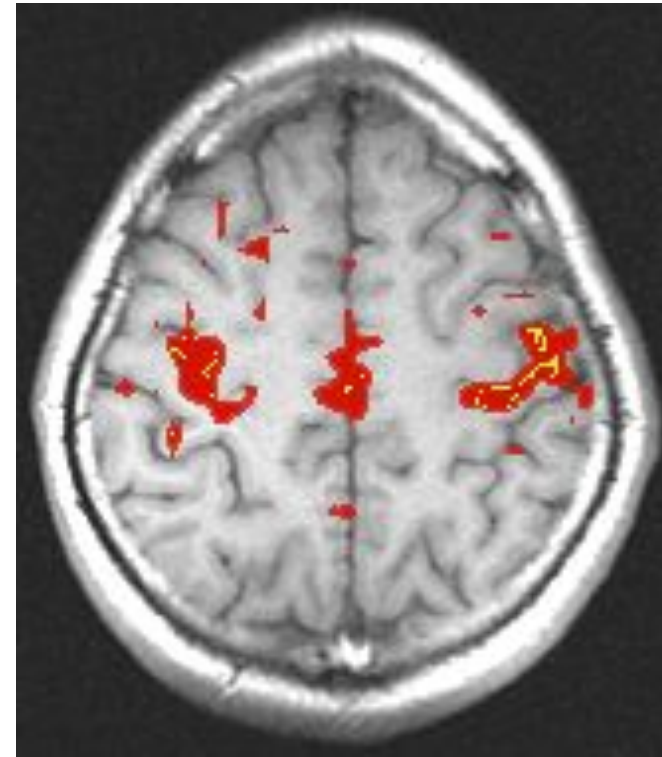
Sources of time series fluctuations:

- Blood, brain and CSF pulsation
- Vasomotion
- Breathing cycle (B_0 shifts with lung expansion)
- Bulk motion
- Scanner instabilities
- Changes in blood CO_2 (changes in breathing)
- Spontaneous neuronal activity

Resting State Correlations



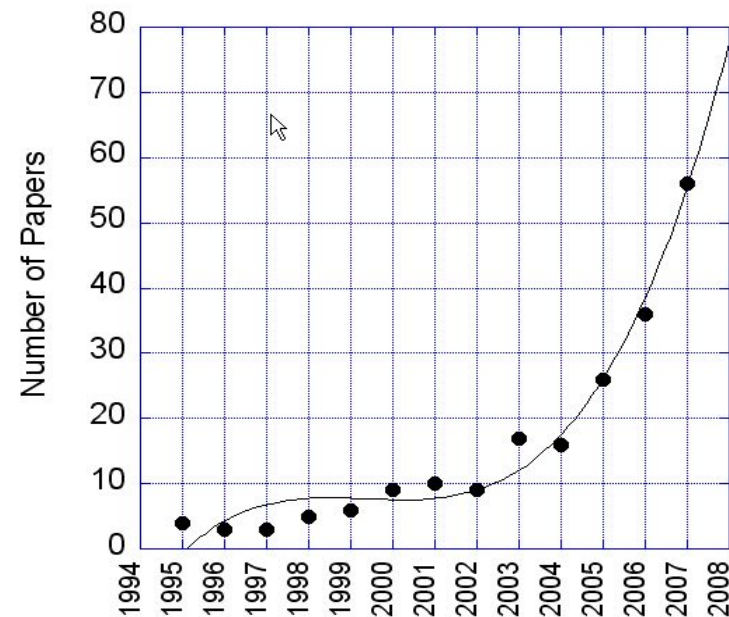
Activation:
correlation with reference function



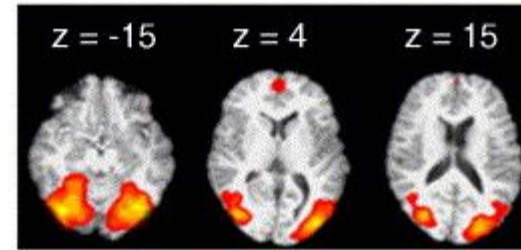
Rest:
seed voxel in motor cortex

Resting state networks identified with ICA

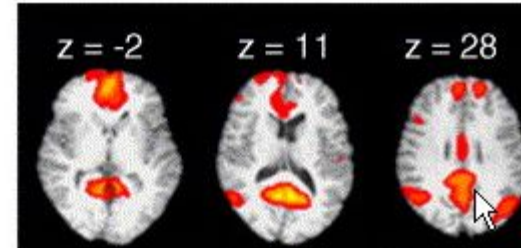
M. DeLuca, C.F. Beckmann, N. De Stefano, P.M. Matthews, S.M. Smith, **fMRI resting state networks define distinct modes of long-distance interactions in the human brain.** *NeuroImage*, 29, 1359-1367



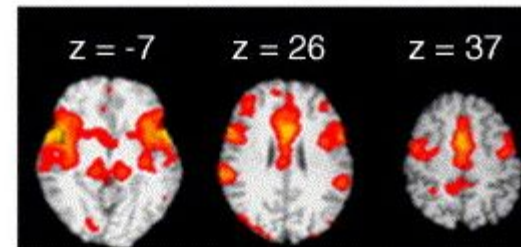
RSN1



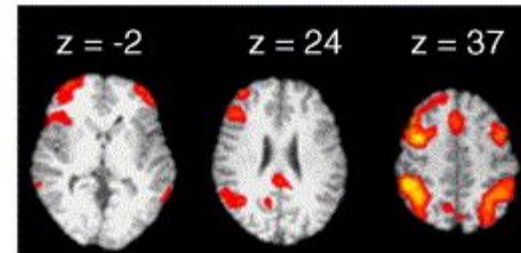
RSN2



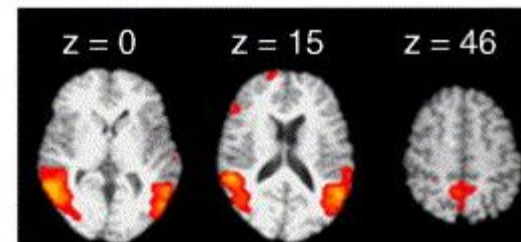
RSN3



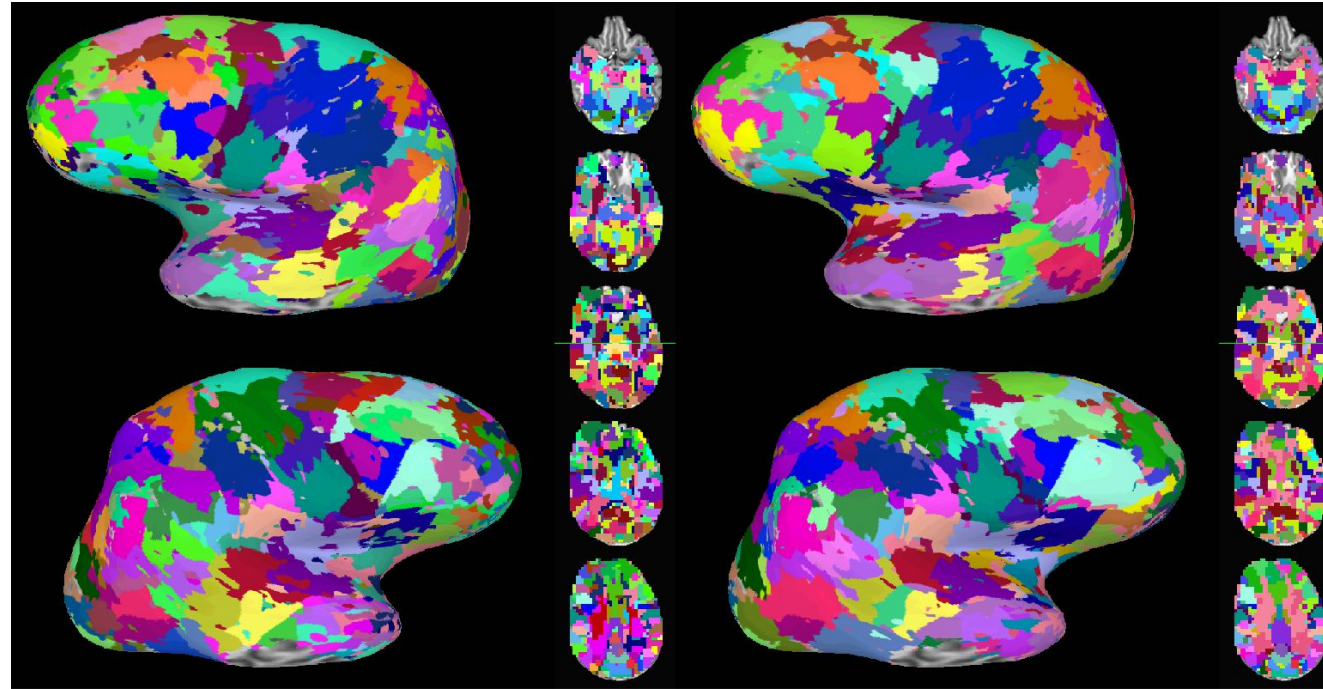
RSN4



RSN5



Resting State: Subdividing the Entire Brain

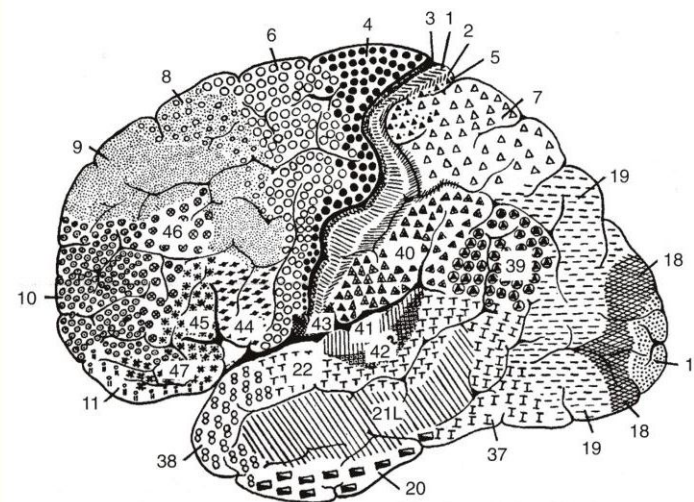


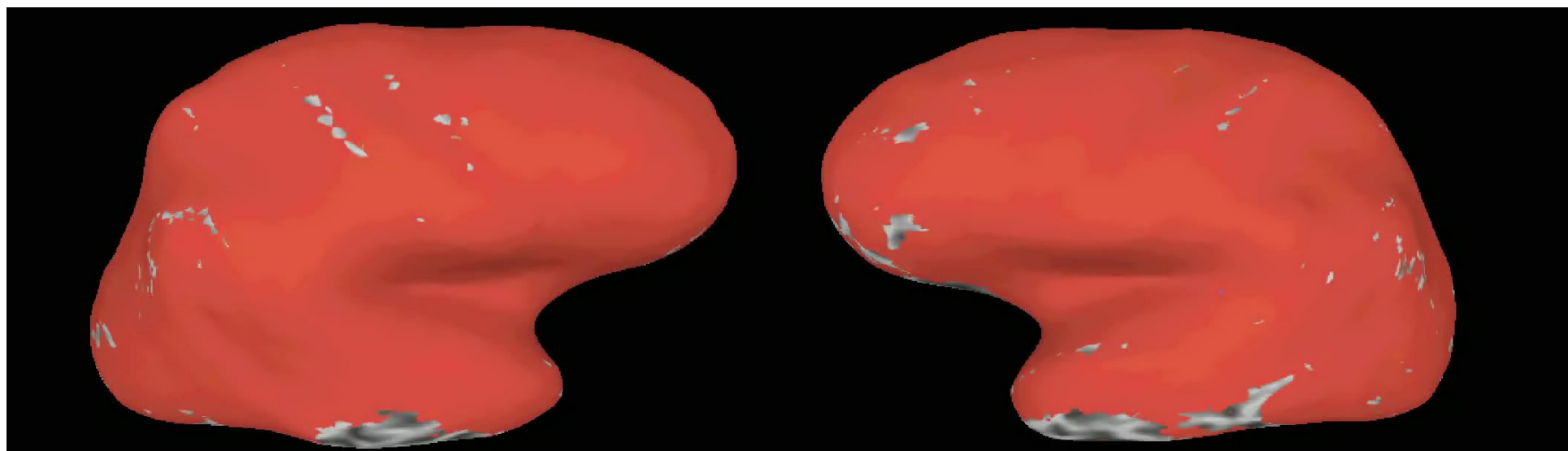
Run 1 - 150 clusters (Target)

Run 2 - 150 clusters

Brodmann's Cytoarchitectonic Map

(Joaquin Fuster; *The Prefrontal Cortex*, 22)





Right Hemi

Left Hemi

Fluctuations

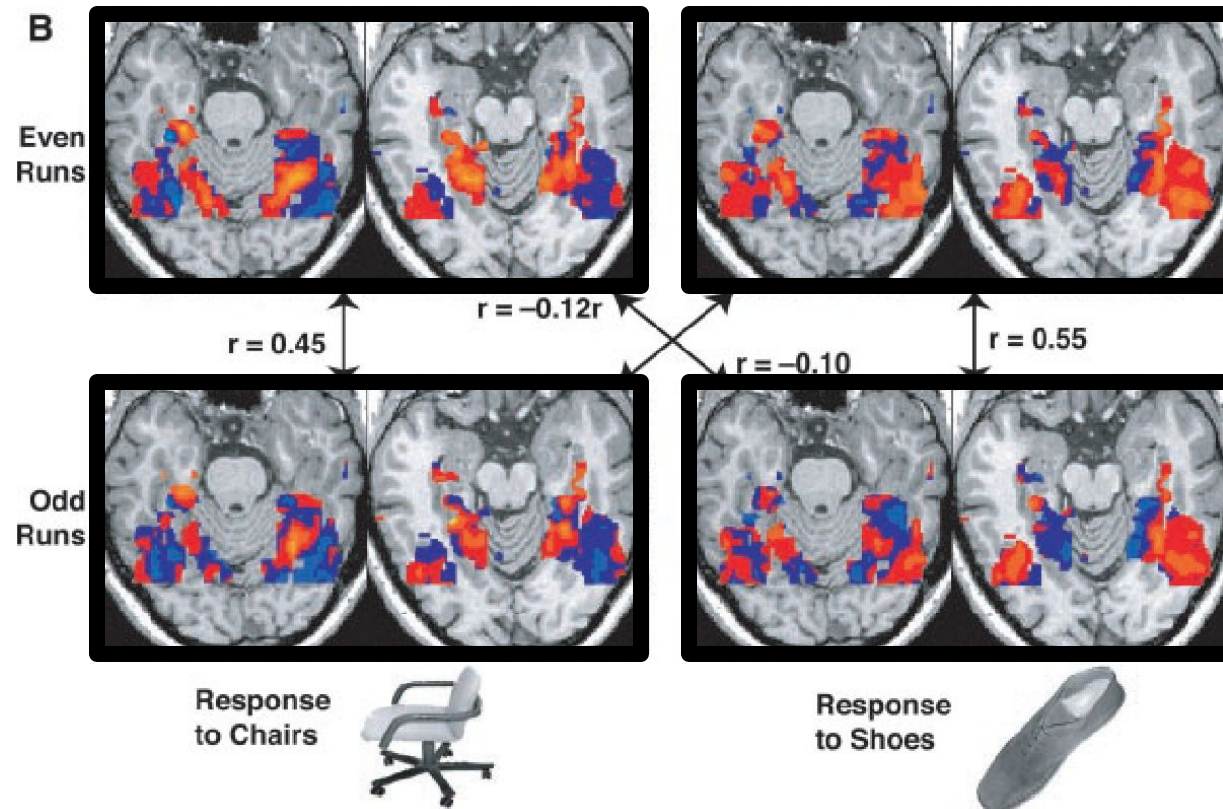
Patterns



1991

Ventral temporal category representations

Object categories are associated with distributed representations in ventral temporal cortex



Haxby et al. 2001

Pattern-recognition analysis of fMRI activity patterns

- Haxby et al. (2001)
- Cox & Savoy (2003)
- Carlson et al. (2003)
- Kamitani & Tong (2005)
- Haynes & Rees (2005)
- Kriegeskorte et al (2006)

Technology

Magnet
RF Coils
Pulse Sequences

Methodology

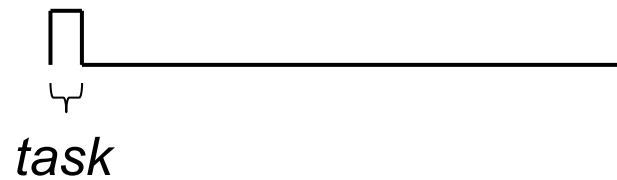
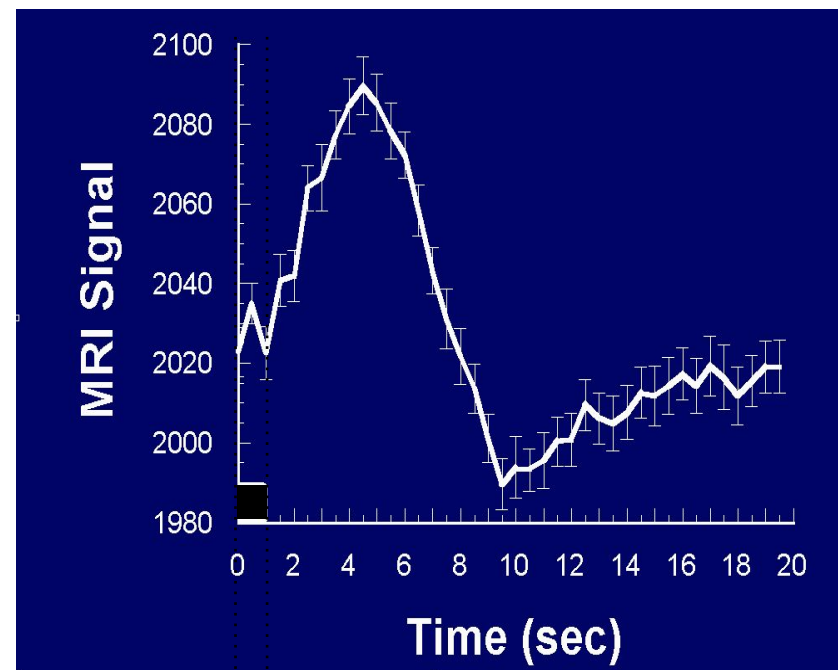
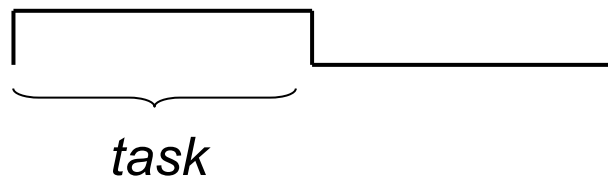
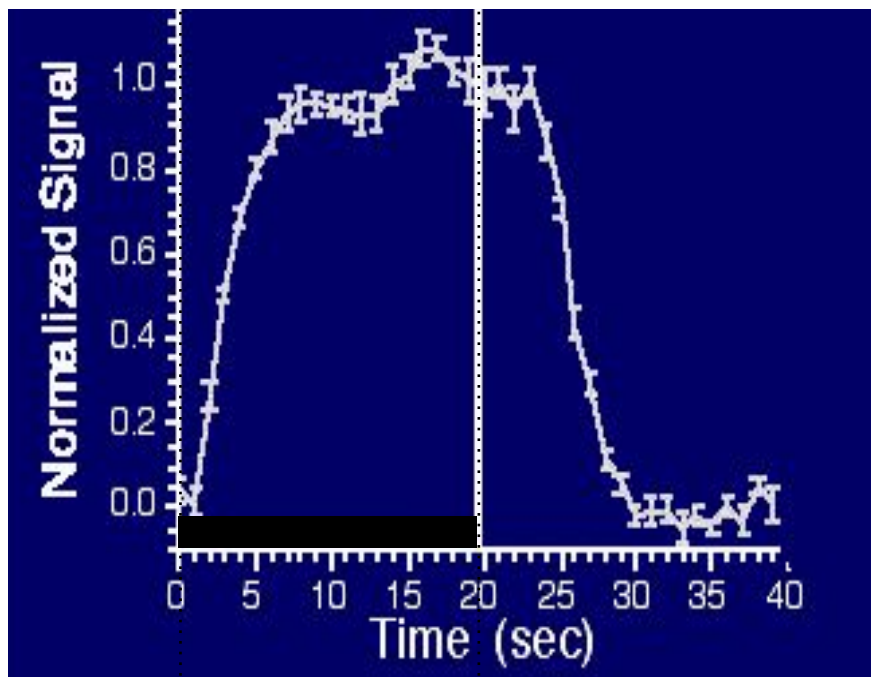
Paradigm Design
Pre and Post Processing
Subject Interface
Data Display and Comparison

Increases
Decreases
Dynamics
Locations

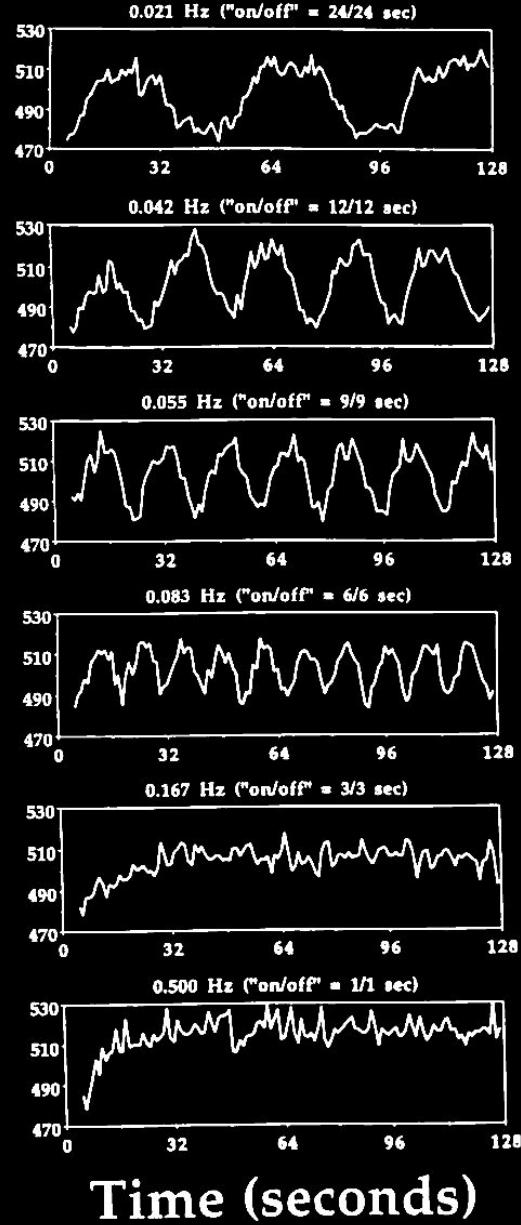
Interpretation

Neuroscience
Physiology
Genetics
Practical Clinical

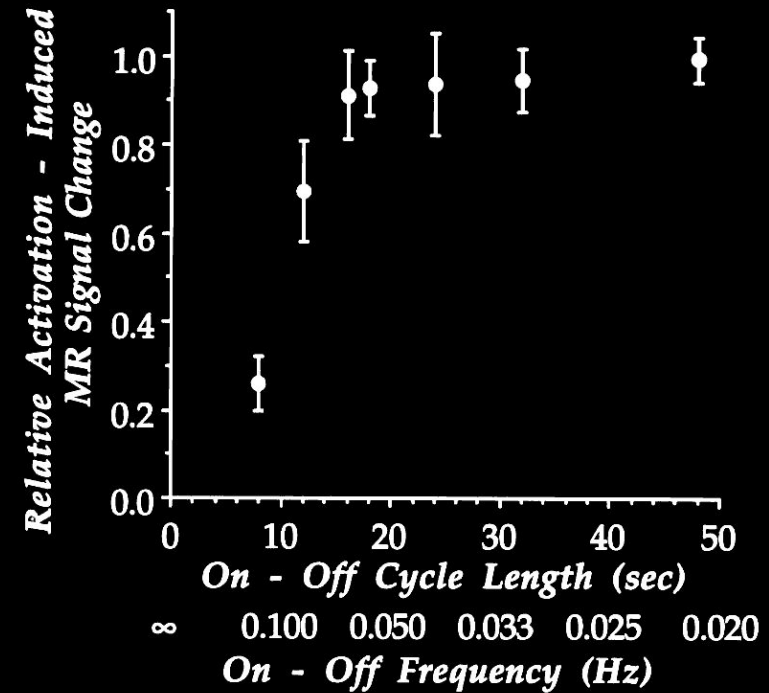
Applications



MRI Signal

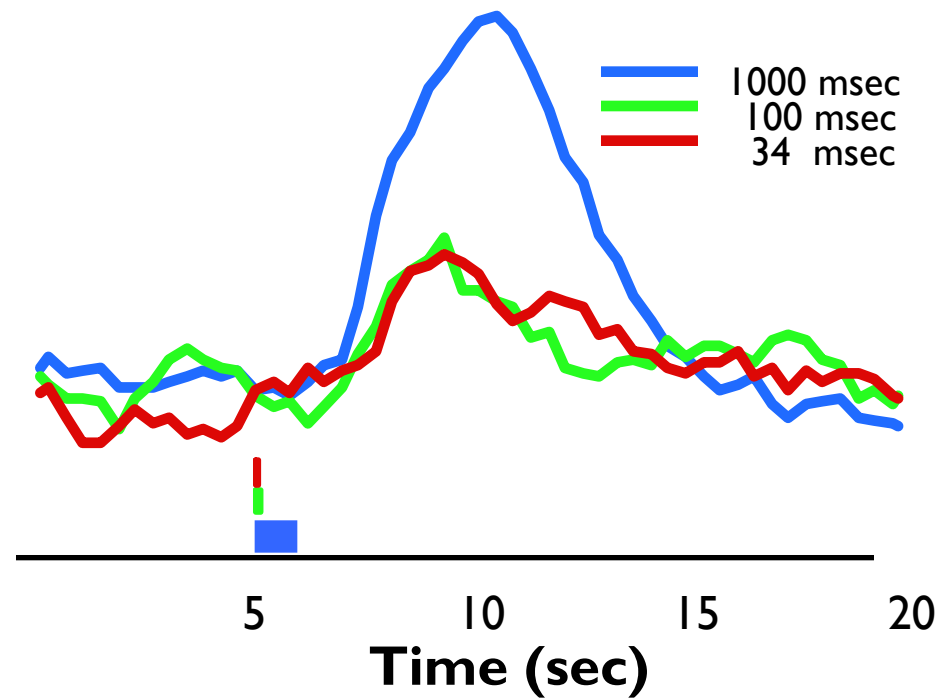


How rapidly can one switch on and off?



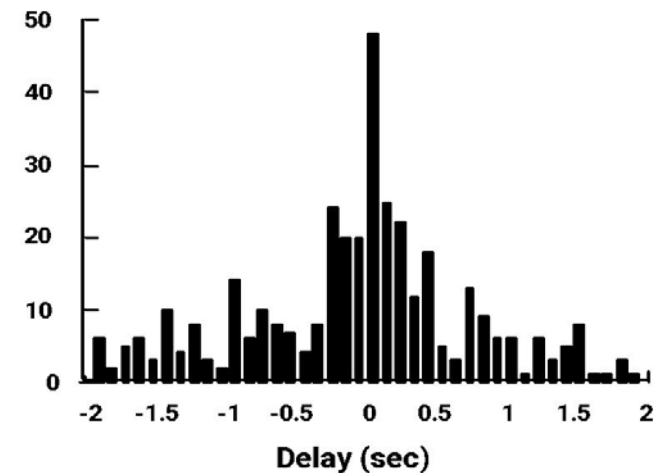
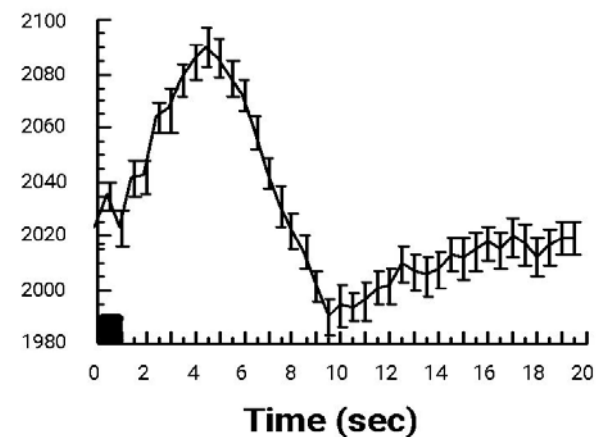
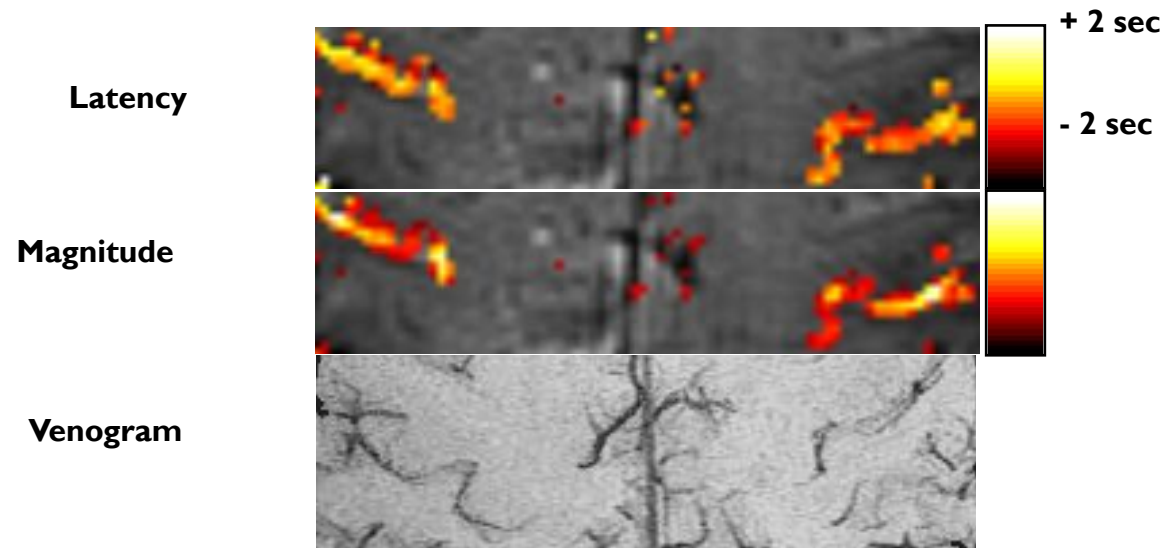
P.A. Bandettini, Functional MRI using the BOLD approach: dynamic characteristics and data analysis methods, in "Diffusion and Perfusion: Magnetic Resonance Imaging" (D. L. Bihan, Ed.), p.351-362, Raven Press, New York, 1995.

How brief of a stimulus can one give?

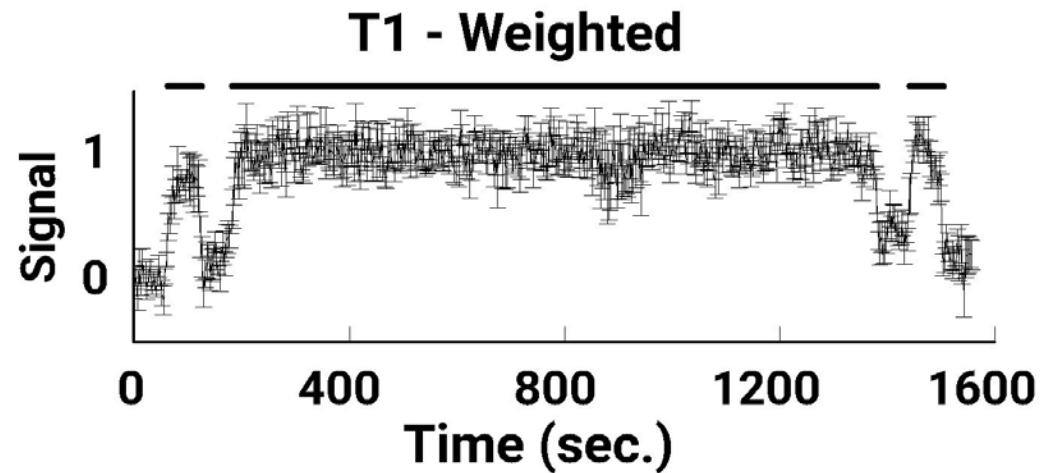
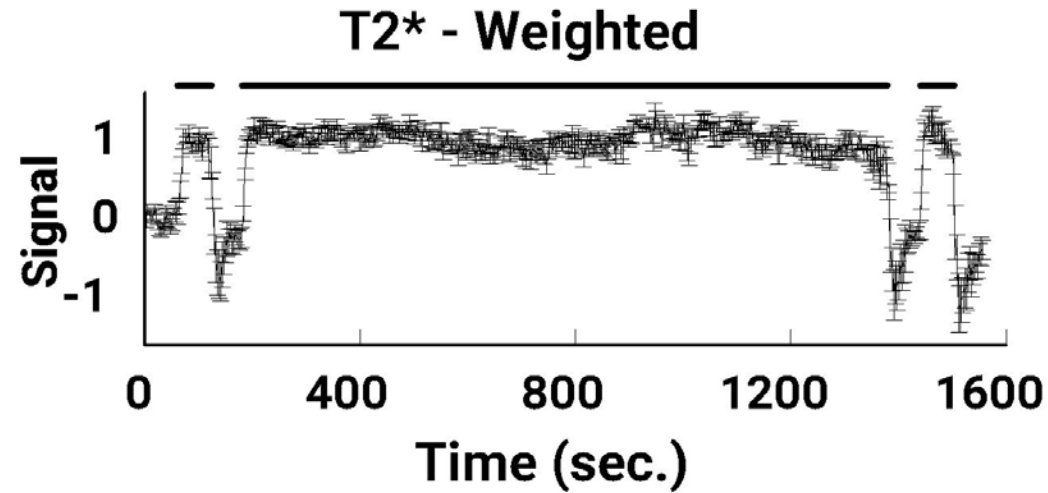


R. L. Savoy, et al., Pushing the temporal resolution of fMRI: studies of very brief visual stimuli, onset variability and asynchrony, and stimulus-correlated changes in noise, 3rd Proc. Soc. Magn. Reson., Nice, p. 450. (1995).

Latency Variation...

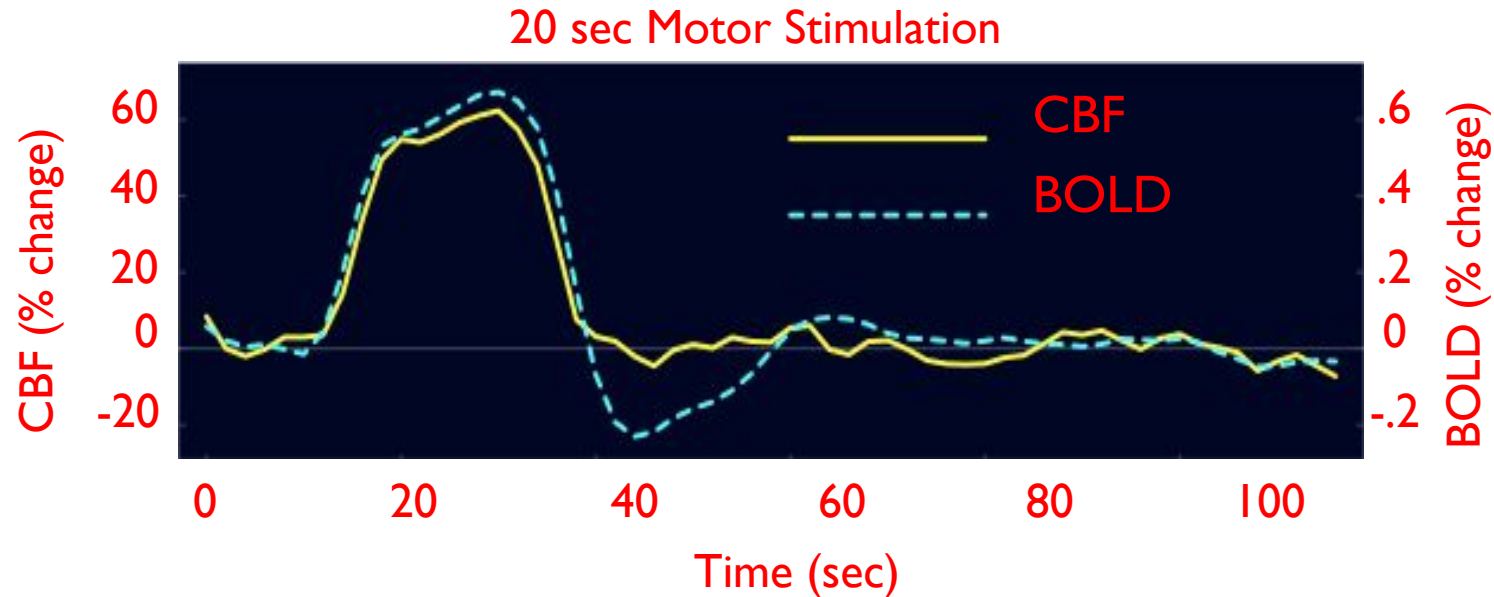


P.A. Bandettini, (1999) "Functional MRI" 205-220.



P. A. Bandettini, K. K. Kwong, T. L. Davis, R. B. H. Tootell, E. C. Wong, P. T. Fox, J. W. Belliveau, R. M. Weisskoff, B. R. Rosen, (1997). "Characterization of cerebral blood oxygenation and flow changes during prolonged brain activation." *Human Brain Mapping* 5, 93-109.

BOLD post-stimulus undershoot



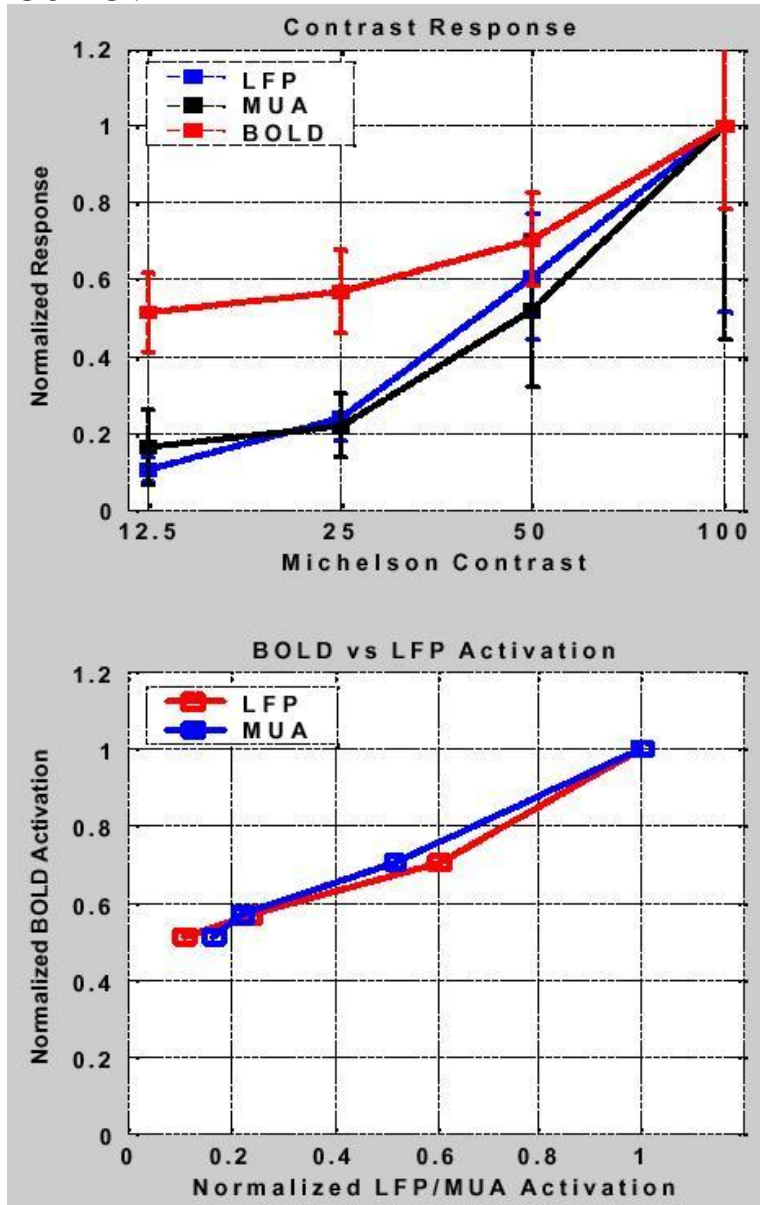
A BOLD undershoot without a CBF undershoot could be due to a slow return to baseline of either CBV or CMRO_2

Courtesy Rick Buxton

fMRI Contrast

- **Volume (gadolinium)**
- **BOLD (GE and SE)**
- **Perfusion (ASL)**
- **ΔCMRO_2**
- **ΔVolume (VASO)**
- **Neuronal Currents**
- **Diffusion coefficient**
- **Temperature**

Logothetis et al. (2001)
“Neurophysiological investigation of the basis of the fMRI signal” Nature, 412, 150-157



Technology

Magnet
RF Coils
Pulse Sequences

Methodology

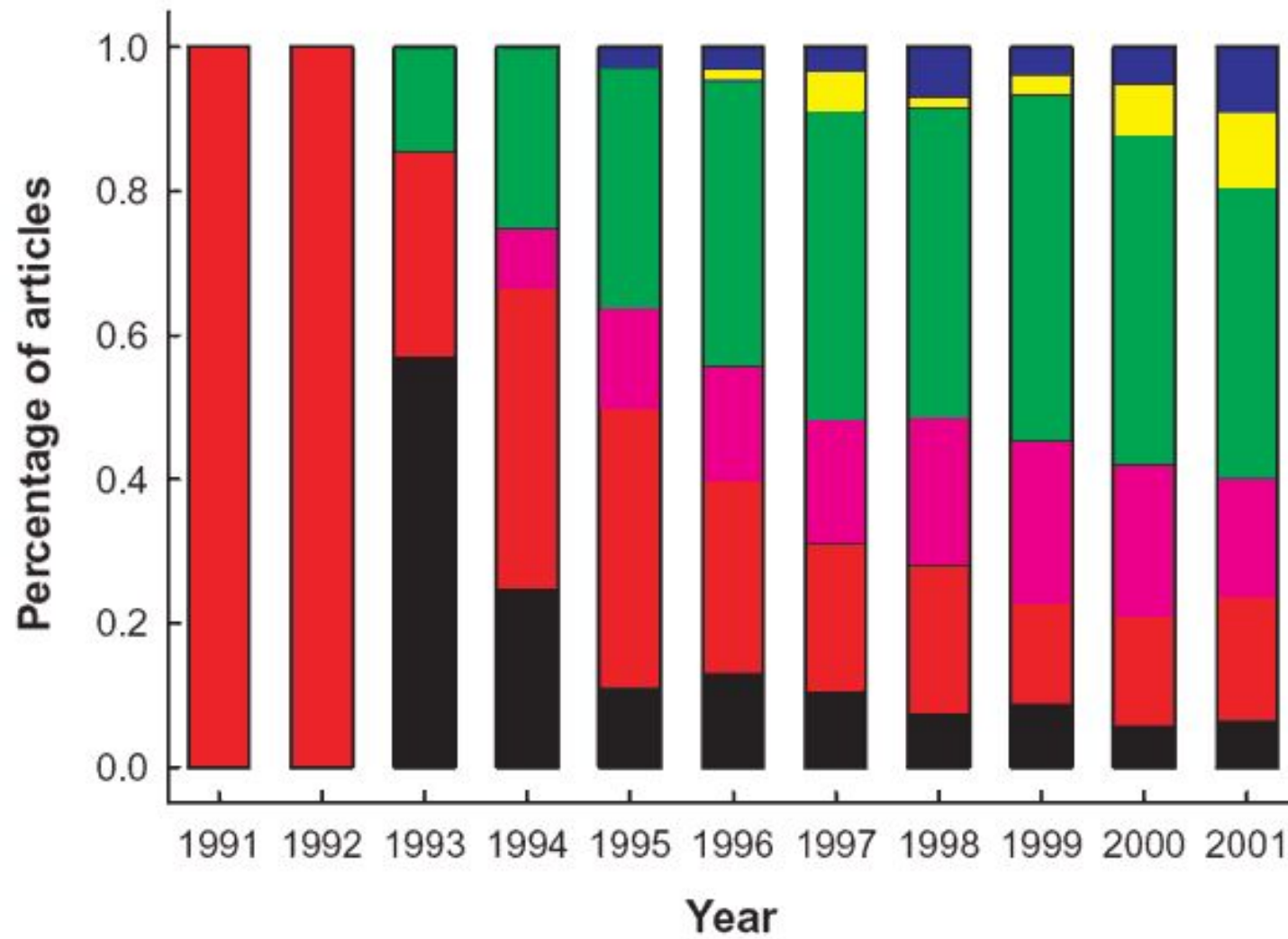
Paradigm Design
Pre and Post Processing
Subject Interface
Data Display and Comparison

Increases
Decreases
Dynamics
Locations

Interpretation

Neuroscience
Physiology
Genetics
Practical Clinical

Applications



Motor (black)
Primary Sensory (red)
Integrative Sensory (violet)
Basic Cognition (green)
High-Order Cognition (yellow)
Emotion (blue)

J. Illes, M. P. Kirschen, J. D. E. Gabrieli, Nature Neuroscience, 6 (3) p.205

How fMRI Is Currently Used

Research Applications

- map networks involved with specific behavior, stimulus, or performance
- characterize changes over time (seconds to years)
- determine correlates of behavior (response accuracy, etc...)
- characterization of groups or individuals

Clinical Research

- clinical population characterization (probe task or resting state)
- assessment of recovery and plasticity
- attempts to characterize (classify) individuals

Clinical Applications

- presurgical mapping (CPT code in place as of Jan, 2007)

Exciting Trends

- **FMRI Decoding**
- **Resting State Fluctuations (Connectivity)**
- **Quantitative fMRI (active and baseline)**
- **High Field / High Temporal & Spatial Resolution**
- **Real Time fMRI**
- **Longitudinal fMRI / MRI studies over multiple time scales**
- **Clinical inroads**